POPULATION GENETICS OF THE CALIFORNIA HORN SHARK (*HETERODONTUS FRANCISCI*)

A DISSERTATION SUBMITTED TO THE GRADUATE DIVISION OF THE UNIVERSITY OF HAWAIʻI AT MĀNOA IN PARTIAL FULFILLMENT OF THE REQUIREMENTS FOR THE DEGREE OF

DOCTOR OF PHILOSOPHY

IN

ZOOLOGY (ECOLOGY, EVOLUTION, AND CONSERVATION BIOLOGY)

DECEMBER 2021

By

Sean James Canfield

Dissertation Committee:

Brian Bowen, Chairperson
Floyd Reed
Robert Thomson
Mark Hixon
Daniel Rubinoff

ACKNOWLEDGEMENTS

This dissertation would have been an impossible accomplishment if not for the support, guidance, and love of many people. This is a journey that has taken a lifetime, and I fear that it is simply not possible to acknowledge every single person who set and guided me along this path. Still, I will try to include everyone, in some form or another.

To the surgeon who delivered me on that fateful, probably cold January day in 1987, I offer my sincerest (…just kidding; but really: good job!).

I'd like to begin by thanking my advisor, Brian Bowen, for taking me on as a graduate student during a period of great uncertainty. You have been a tremendous mentor, and I cannot express enough how much I have appreciated your guidance and support these last several years. Never once did I feel that your confidence in me wavered, and your always-constructive feedback has left me feeling fully capable of not just succeeding, but excelling as a scientist. Even before I was a graduate student, I remember reaching out via email for advice when I was developing project ideas and applying to graduate schools, all the way from Utah. I will always remember those conversations, and the time you took to help me. I'd also like to acknowledge Steve Karl, who did the same.

I would also like to offer my sincerest thanks to David Carlon, who is the person who first took me on as a graduate student in his lab. You took a chance on me, and without that leap of faith, I wouldn't be writing this dissertation now.

I'd like to thank my other committee members for their advice and support: Mark Hixon, my original ecology professor during my undergrad at Oregon State University, who tempered my genetics-lensed worldview with principles of marine ecology; Robert Thomson, who helped me think about and work through some of the more challenging technical aspects of my analyses; Floyd Reed, who was always willing to indulge me with long, navel-gazing conversations about population genetics (which routinely ended up providing useful insights); and Daniel Rubinoff, who has been a wonderful mentor and verbal sparring partner in equal measure.

It would be a crime of the highest order not to thank the ToBo Lab, which has been my academic family over the past several years. Your advice and guidance during my hundreds of

hours in the lab are directly responsible for my success today. I'd like to thank Robert Toonen, the "To" of the ToBo Lab, and the rest of the lab's members. The list of names is long so I will omit it here, but know that you are seen, appreciated, and loved.

Special thanks and acknowledgement go to the folks who have helped me wrangle a horn shark or two in the field for sampling, including Natalie Blea, Kelcie Chiquillo, Walker Gareri, Ethan Grossman, Jenny Hofmeister, Norbert Lee, Jessica Maxfield, Maddie Smith, and Hamdi Tevfik Kitapçı. I'd especially like to thank Luca Silva (and Enrique Silva) for facilitating several weeks of fieldwork and collections across the Baja Peninsula. Not only did you make a huge portion of this work possible, but you made the experience far more fun and educational than I could have ever hoped for. I'll always remember those trips, and will surely continue to tell those stories for years to come. I would also like to thank Mauricio Hoyos-Padilla and Felipe Galván-Magaña for providing critical assistance, continued support, and valuable tissue samples. Thanks to Sean Hoobler, who provided tissue samples from the northern portion of the range, including extremely valuable samples from Anacapa Island, Santa Cruz Island, and the Santa Barbara area in California, and to Maximilian Hirschfeld, who provided tissues from the Galapagos horn shark (*H. quoyi*) for my first data chapter (Chapter 2; Canfield and Bowen 2020). Finally, I cannot express enough gratitude to the fishers and fishing communities of Baja California and Baja California Sur, Mexico. I was able to spend a lot of time with these amazing folks while I was in Baja, and I learned so much about their lives and livelihoods, which has played a critical role in shaping my perspectives on fisheries and conservation. Many opened their doors to us, as well as their pangas, and I am humbled and forever grateful.

A number of people have provided critical support and services, both at UH and elsewhere. I'd like to thank Shaobin Hou, Jennifer Saito, and the University of Hawai‘i's Advanced Studies of Genomics, Proteomics, and Bioinformatics sequencing facility (ASGPB) for Sanger sequencing services. For next-generation sequencing services, I'd like to thank the QB3 Vincent J. Coates Sequencing Laboratory at the University of California Berkeley, as well as the Genomics and Cell Characterization Core Facility (GC3F) at the University of Oregon. I would also like to acknowledge Amy Eggers and Mindy Mizobe at the HIMB EPSCoR Core Genetics Facility for many conversations and advice regarding sequencing and library preparation. Special thanks for training and support go to the University of Hawai‘i Dive Safety Program. I would also like to give a heartfelt shout-out to the University of Southern California's

Wrigley Institute for Environmental Studies, who hosted me during the summer of 2014 on Santa Catalina Island and provided essential resources and support for my California sampling.

I am extremely grateful to the agencies that have funded this dissertation research, including the National Science Foundation (NSF; Award No. OCE-1558852 to Brian W. Bowen); the UH Mānoa Graduate Student Organization (Award No. 18-03-28); Sigma Xi (Grant ID: G2018031573884449); the Colonel W.E. Lord, DVM & S.L. Lord Endowed Scholarship; and the Watson T. Yoshimoto Foundation Endowed Fellowship in Animal Wildlife Conservation Biology.

Finally, I have to thank my friends and family for their continued love and support. I have had the privilege of meeting some absolutely amazing people over the past several years and developing sincere friendships with so many of you. I will not attempt to write all of your names individually, but know that you have all touched me profoundly. I will, however, acknowledge my closest friend, Áki. I cannot express how much your friendship has meant to me throughout this journey and I look forward to future adventures! Also: you're a fish. Deal with it. Now it's in writing, on official record, and I win. To my mom (Karen), my dad (Michael), and my sister (Lauren): thank you for believing in me. You are every bit the reason that I am where I am today. This is for you. And to my partner, Robyn: thank you for being supportive and generally amazing, and for helping to push me to the finish line. I couldn't have done it without you. I love you.

Cheers!

ABSTRACT

Sharks (superorder Selachimorpha) display a wide range of dispersal capabilities, with some species undertaking migrations that span ocean basins, and others undertaking comparatively short migrations limited to coastal margins. The spatial scale of population genetic structure among shark taxa is similarly variable, with some oceanic species showing little to no structure on a global scale, and other, more coastal species displaying structure over distances on the order of 150 km. The identification of discrete populations is critical to the development and implementation of conservation measures, allowing managers to determine appropriate spatial scales for management initiatives, identify populations in need of special protection, and maximize the genetic diversity and adaptive potential of a species. Additionally, understanding the mechanisms underlying population structure can shed light on evolutionary processes that generate and maintain biodiversity in the marine environment. To date, population genetic studies in sharks have focused on large-bodied, highly mobile species, while smaller, coastal species with limited dispersal have received little attention. Here, I utilized multiple genetic techniques to assess population genetic structure of the California horn shark (*Heterodontus francisci*), a small, benthic species inhabiting shallow coastal habitat from California, U.S.A. to the Gulf of California, Mexico. First, I present a Restriction Fragment Length Polymorphism (RFLP) method to quickly and cheaply distinguish between the three species of *Heterodontus* occupying eastern Pacific shorelines (Chapter 2). Then, I present analyses of population genetic structure across the range of *H. francisci* using the mitochondrial control region (mtCR; Chapter 3) and 9,063 neutral SNP loci (Chapter 4). Analyses of the mtCR and neutral SNP datasets both support the role of deep-water channels as barriers to dispersal among island and mainland populations over unprecedented small spatial scales. Analysis of SNP loci revealed a population break between northern and southern Channel Islands that was not detected with the mtCR, supporting the assumption of greater resolution with SNP technology. The published suggestion that a cryptic evolutionary lineage exists within the East Pacific was not supported by any of the three genetic approaches. These analyses indicate that barriers limiting the dispersal of demersal elasmobranchs can exist at spatial scales much smaller than previously detected, highlighting a need for further research on this understudied component of shark biodiversity.

TABLE OF CONTENTS

LIST OF TABLES

LIST OF FIGURES

CHAPTER 1. INTRODUCTION

Understanding dispersal, and the processes underlying population structure and the partitioning of genetic diversity in the marine environment, is crucial to the effective implementation of marine conservation initiatives (Palumbi 2003; Arenas et al. 2012; Selkoe et al. 2014). This knowledge allows for targeted management strategies which can be used to prevent overharvesting of local stocks, and to maximize the genetic diversity – and therefore the adaptive potential – of target species (Fogarty and Botsford 2007; Allendorf et al. 2010; Domingues et al. 2018). Additionally, an understanding of the mechanisms underlying population structure (e.g., barriers to dispersal) in the marine environment can lead to key insights into the processes that generate and maintain species diversity over macroevolutionary timescales (e.g., dispersal and vicariance; Bowen et al. 2016).

Sharks (superorder Selachimorpha) display a wide range of dispersal capabilities. Highly mobile, oceanic species such as the Blue shark (*Prionace glauca*), the Great white shark (*Carcharodon carcharias*), and the Whale shark (*Rhincodon typus*) can undertake migrations that span ocean basins, while coastal species such as the Nurse shark (*Ginglymostoma cirratum*) and the Bonnethead shark (*Sphyrna tiburo*) may exhibit strong site-fidelity or undertake comparatively short migrations restricted to coastal margins (Bonfil et al. 2005; Heupel et al. 2006; Vandeperre et al. 2014; Guzman et al. 2018; Pratt et al. 2018).

The spatial scale of population genetic structure among shark taxa is similarly variable, and dependent on life history as well as habitat preference. Truly oceanic species, such as the Basking shark (*Cetorhinus maximus*) and Blue shark (*Prionace glauca*) show little or no structure on a global scale (Hoelzel et al. 2006; Taguchi et al. 2015; Veríssimo et al. 2017; Bailleul et al. 2018). Large coastal species may exhibit structure on the scale of ocean basins, such as North versus South Atlantic for the Tiger shark (*Galeocerdo cuvier*; Bernard et al. 2016), East versus Central Pacific for the Scalloped hammerhead shark (*Sphyrna lewini*; Daly-Engel et al. 2012), and eastern versus western Australia in the Sandbar shark (*Carcharhinus plumbeus*; Portnoy et al. 2010). Smaller coastal sharks may display population structure within ocean basins, including the Spiny dogfish (*Squalus acanthias*; Veríssimo et al. 2010), Starspotted dogfish (*Mustelus manazo*; Chen et al. 2001), Blacknose shark (*Carcharhinus acronotus*;

Portnoy et al. 2014), and Spot-tail shark (*Carcharhinus sorrah*; Giles et al. 2014). At the smallest scale, significant population structure has been detected in the Pacific angel shark (*Squatina californica*) (Gaida 1997) and the Lemon shark (*Negaprion brevirostris*) (Ashe et al. 2015) over distances of roughly 150 kilometers.

This wide range in the spatial scale of population subdivision has important implications for the management of shark species, which have faced severe population declines over the past several decades due to overfishing, habitat loss, and climate change (Dulvy et al. 2014, 2021). For example, sharks with few to no population subdivisions and ranges extending across multiple regional fisheries jurisdictions may require a cooperative management approach. Veríssimo et al. (2017) suggest such a strategy for the panmictic Blue shark. On the other hand, sharks displaying complex metapopulation structure over small spatial scales would likely benefit from more localized strategies.

Despite strong conservation concerns, there is a paucity of studies describing genetic diversity and population structure in sharks (Domingues et al. 2018). To date, intraspecific genetic structure has only been examined in roughly 70 shark species, which collectively represent only 14% of the described species diversity (Hirschfeld et al. 2021). Furthermore, these studies have predominantly focused on large-bodied species (> 150 cm TL) with moderate to high dispersal potential, while much less attention has been paid to smaller, benthic taxa, such as members of the family Scyliorhinidae, sharks of the genus *Hemiscyllium*, and sharks of the genus *Heterodontus* (Hirschfeld et al. 2021, see supplemental information therein). This taxonomic bias could lead to a general underestimation of population genetic structure in sharks, and could simultaneously result in a general overestimation of the spatial scale of management units in this highly diverse group.

My work, presented in this dissertation, focused on the genetics of sharks in the genus *Heterodontus* (order Heterodontiformes, family Heterodontidae). This genus consists of nine species distributed tropically and subtropically along the coastal margins of the Pacific Ocean, the Indo-Pacific, and the Western Indian Ocean. These small-to-medium sized sharks are exclusively benthic, rarely venturing more than two meters above the substrate, and are typically restricted to a nearshore, shallow-water environment (Compagno 2002; Ebert et al. 2013).

In the Eastern Pacific, there are three species of *Heterodontus* with overlapping distributions: the California horn shark (*Heterodontus francisci*; Girard 1855), which ranges

from Point Conception, California south to the Sea of Cortez, Mexico; the Mexican horn shark (*Heterodontus mexicanus*; Taylor and Castro-Aguirre 1972), which ranges from the Sea of Cortez, Mexico, south to Guatemala, and possibly even further south to Peru; and the Galapagos horn shark (*Heterodontus quoyi*; Fréminville 1840), which can be found along the coast of Peru, as well as in the Galapagos Islands (Taylor 1972; Ebert 2003; Compagno et al. 2005; Garayzar 2006). However, there is uncertainty with respect to the geographic ranges of these species, because they can be difficult to tell apart both in the field and in museum collections (Compagno et al. 2005; Garayzar 2006; S.J.C. pers. obs). In Chapter 2 of this dissertation, I present a simple, rapid PCR-RFLP assay that can cheaply and reliably distinguish between the three eastern Pacific species of *Heterodontus* without the need for whole specimens or genetic sequencing. My hope is that this simple test will be used to elucidate species ranges, and the species composition in regional fisheries and markets.

In Chapters 3 and 4 of this dissertation, I examine population genetic structure across the range of the California horn shark (*Heterodontus francisci*) using two types of genetic marker: the mitochondrial control region (mtCR; Chapter 3), and a dataset comprised of 9,063 putatively neutral, nuclear SNP loci obtained using double-digest restriction site-associated DNA sequencing (ddRADseq; Chapter 4). The California horn shark is a small (max 122 cm TL), coastal species inhabiting shallow waters from Point Conception, California south to the Gulf of California, Mexico, including the offshore Channel Islands and Isla Guadalupe (Love 1996). The California Channel Islands are tens of kilometers off the coast of southern California, but Isla Guadalupe is truly oceanic, a small volcanic island located approximately 250 kilometers west of the Baja peninsula. Members of this species are strongly benthic, and are commonly found at depths ranging from 2-11 m, though they may occasionally be encountered as deep as 150 m (Compagno 2002). These nocturnally active reef predators are known to shelter during the day, maintaining relatively small home-ranges and demonstrating strong site-fidelity (Nelson and Johnson 1970; Strong 1989; Meese and Lowe 2020). Intriguingly, the horn sharks inhabiting the waters around Santa Catalina Island – a mere 32 kilometers from the California mainland – were hypothesized to be a distinct population based on differences in egg-case morphology (Taylor 1972). However, there have been no further inquiries about whether this species exhibits population genetic structure across their range, although at least two authors have proposed the existence of cryptic evolutionary partitions within *H. francisci* in the Gulf of California based on

differences in color, markings, and fin shape (Michael 1993; Castro 2010). Given that the IUCN Red List currently lists *H. francisci* as Data Deficient (Carlisle 2015) and at least one recent study has identified the species as vulnerable to overexploitation throughout portions of its range (Furlong-Estrada et al. 2017), these are questions with strong conservation implications.

Thus, the primary goals of Chapters 3 and 4 were to (*i*) determine whether population genetic structure pertinent to conservation occurs between island and mainland ranges; (*ii*) determine whether the deep-water channel separating the Channel Islands from the California mainland acts as a barrier to dispersal in horn sharks; (*iii*) determine whether population genetic structure exists along the contiguous coastline from Santa Barbara, CA to Las Animas in the Gulf of California; and (*iv*) test for proposed cryptic evolutionary lineages across the species range. My hope is that this information will provide a stronger foundation for management of *H. francisci*, and provide impetus to investigate the population structure and conservation genetics of the small demersal sharks that inhabit coastal waters. Increasing research effort on this neglected component of shark biodiversity has the potential to reshape our perspective on the pattern and scale of evolutionary processes in this group, providing key insights into their conservation, their evolutionary origins, and their future in a changing world.

CHAPTER 2. A RAPID PCR-RFLP METHOD FOR SPECIES IDENTIFICATION OF THE EASTERN PACIFIC HORN SHARKS (GENUS *HETERODONTUS*)

Citation: Canfield SJ, Bowen BW (2021) A rapid PCR-RFLP method for species identification of the eastern Pacific horn sharks (genus *Heterodontus*). *Conserv Genet Resour* 13:79–84. https://doi.org/10.1007/s12686-020-01172-6

ABSTRACT

Accurate species identification is essential for the successful implementation of species conservation strategies and research. East Pacific horn sharks (genus *Heterodontus*) may be subject to overfishing and depletion in some areas, mandating an assessment of risk and vulnerability to exploitation. Unfortunately, morphological identification of the three eastern Pacific species can be challenging, creating uncertainty about species identifications and the true extent of their respective ranges. To address this problem, we developed a PCR-RFLP method to quickly and accurately identify the three species of *Heterodontus* occupying the coastlines and islands of the eastern Pacific (*H. francisci*, *H. mexicanus*, and *H. quoyi*). The PCR-RFLP assay requires only a single amplification of the mitochondrial NADH2 locus (1,216 bp) and a single digestion step with restriction enzyme AluI. The assay was tested on 67 individuals representing all three species and resulted in unambiguous species identification for 100% of individuals tested.

INTRODUCTION

The sharks of the genus *Heterodontus* (Order Heterodontiformes) consist of nine species distributed tropically and subtropically along the coastal margins of the Pacific Ocean, the Indo-Pacific and the Western Indian Ocean (Compagno 2002). In the Eastern Pacific, there are three species with overlapping distributions: the California horn shark (*Heterodontus francisci*; Girard 1855), which ranges from Point Conception, California south to the Sea of Cortez, Mexico; the Mexican horn shark (*Heterodontus mexicanus*; Taylor and Castro-Aguirre 1972), which ranges from the Sea of Cortez, Mexico, south to Guatemala, and possibly even further south to Peru; and the Galapagos horn shark (*Heterodontus quoyi*; Fréminville 1840), which can be found along

the coast of Peru, as well as the Galapagos Islands (Taylor 1972; Ebert 2003; Compagno et al. 2005; Garayzar 2006).

There is uncertainty with respect to the geographic ranges of these species. For example, Compagno (2005) stated that the range of *H. francisci* may extend as far south as Peru, and that the same is "probably" true for *H. mexicanus*. Recently, both species were reported in the waters of Colombia (Mejía-Falla and Navia 2019). While this does indicate the presence of at least one species of *Heterodontus* in the region, the survey relied upon collection records and museum specimens for species identification, and the authors assumed that specimens were correctly identified upon collection. These species are often difficult to tell apart both in the field and in museum collections, as many of their distinguishing characteristics can be quite subtle (Compagno 2002; Garayzar 2006; S.J.C. pers. obs.).

This uncertainty surrounding species identification and range has the potential to confound conservation measures; all three species have been listed as Data Deficient in their respective IUCN Red List profiles, indicating a need for more data regarding catch rates, population status, and distribution (Kyne et al. 2004; Garayzar 2006; Carlisle 2015). Horn sharks are frequently caught as bycatch in gillnets, which are widely employed in Mexico and South America (Alfaro-Shigueto et al. 2010; Ramírez-Amaro and Galván-Magaña 2019). Furthermore, there have been reports of local population declines in California and Mexico (Carlisle 2015; S.J.C. pers. obs.). Without the ability to accurately distinguish species and determine true geographic ranges, assessing the impacts of these fisheries on horn shark populations will be difficult, if not impossible. Thus, there is a clear need for tools which allow for inexpensive and unambiguous identification of the eastern Pacific horn sharks.

Molecular techniques, such as DNA barcoding, provide means for accurate species identification even among morphologically cryptic species (Kress et al. 2015). However, the cost of sequencing associated with DNA barcoding may be prohibitive in large-scale applications or resource-limited management initiatives. PCR-RFLP analysis, on the other hand, allows for the identification of many individuals without direct DNA sequencing and at a fraction of the cost of DNA barcoding.

In the present study we develop and introduce a simple, rapid, PCR-RFLP method which will allow researchers and managers to quickly, cheaply, and reliably distinguish between *H. francisci*, *H. mexicanus*, and *H. quoyi*.

MATERIALS AND METHODS

Specimen Collection and DNA Extraction

Specimens of *Heterodontus francisci* and *Heterodontus mexicanus* were captured via gillnet, crab trap, or lobster trap by fishermen in Baja California and Baja California Sur, Mexico in 2018 and 2019 (Table 2.1; Figure 2.1). Fin-clips were collected from the posterior margin of the first dorsal fin and immediately preserved in salt-saturated 20% DMSO. Species identities were putatively assigned in the field by the lead author based on morphological characters (Compagno 2002), and later confirmed via sequencing for a subset of individuals (see "PCR, Sequencing, and Final Species Assignment" below). Fin-clips from *Heterodontus quoyi* (n = 10) were collected by researchers in the Galapagos Islands, Ecuador in 2015 and preserved in 70% ethanol. DNA was extracted from a total of 67 specimens using the Omega Bio-Tek E.Z.N.A. Tissue DNA Kit with minor adjustments to the manufacturer's protocol.

Primer Design

For this study we've chosen the mitochondrial NADH dehydrogenase subunit 2 (NADH2) gene as our target marker. NADH2 is commonly employed as a barcoding locus for elasmobranchs, providing greater resolution than cytochrome oxidase c subunit 1 (COI) with respect to species delineation (Naylor et al. 2012). Thus, we deemed it an appropriate choice for the current study.

The primers used in this study were designed to target the full mitochondrial NADH2 sequence, along with some flanking tRNA sequence, resulting in a total product length of 1,216 base-pairs, hereafter referred to as NADH2(+). Briefly, complete mitochondrial genomes of *Heterodontus francisci* (accession number AJ310141; Arnason et al. 2001) and the Indo-Pacific *Heterodontus zebra* (accession number NC_021615; Chen et al. 2014) were downloaded from GenBank (Clark et al. 2016) and aligned in GENEIOUS 6.1.8 (Biomatters Ltd, Auckland, NZ). The NADH2 gene was isolated, and flanking sequence greater than 200 base-pairs from either the 5' or 3' end of the NADH2 gene was removed. Primer pairs were generated using Primer3 v0.4.0 (Untergasser et al. 2012) and selected based on GC content, primer melting temperature (Tm) compatibility (< 1.5°C difference), and placement in flanking regions with no sequence variation between the two mitochondrial genomes. The primer sequences are provided in Table 2.2.

PCR, Sequencing, and Species Assignment

PCR was performed in 50 µL reactions with the following components: 1.0x GoTaq Green Master Mix (Promega, Madison, WI, USA), 0.4 pmol/µL of each oligonucleotide primer (HFND2F and HFND2R; see Table 2.2), ~ 50 ng (1.0 µL) DNA template, and HPLC H_20 to adjust to the final 50 µL volume. PCR was then carried out with the following parameters: one cycle at 95°C for 3 min; 39 cycles of 95°C for 30 s, 57°C for 30 s, 72°C for 1 min 15 s; and one cycle at 72°C for 5 min. To confirm successful PCR, products were run on a 1.5% agarose gel (using 1x TAE running buffer) at 100 V for 35 min and visualized using a Bio-Rad Gel Doc EZ Gel Imaging System (Bio-Rad, Hercules, CA, USA). PCR products were then cleaned at a 0.5x concentration using PCR-Clean DX bead solution (Aline Biosciences, Woburn, MA, USA), and a subset of products from each of the three species (n = 30; Table 2.1) was sent to the Advanced Studies in Genomics, Proteomics and Bioinformatics (University of Hawai‘i at Mānoa) to be sequenced in both directions on an Applied Biosystems 3730XL DNA Analyzer.

Forward and reverse sequences were aligned, edited, and assembled in GENEIOUS. In order to confirm species identifications, consensus sequences from each individual were subjected to an NCBI Nucleotide BLAST search.

Development of PCR-RFLP Assay

The PCR-RFLP assay was developed by exploring restriction sites of the NADH2(+) sequences in our three study species, as well as the full mitochondrial genome of *H. francisci* (to aid in predicting cut-sites immediately adjacent to priming sites), using the built-in Restriction Analysis function of GENEIOUS. The program was instructed to display cut-sites for "commonly used enzymes," and minimum recognition sequence length was set to four base-pairs. Enzymes that are methylation-sensitive were excluded from consideration, as were enzymes that either cut exclusively at non-polymorphic sites (*e.g.*, would produce identical restriction-fragment profiles across species), or cut at one or more sites displaying intraspecific variation (*e.g.*, would *not* produce identical restriction-fragment profiles *within* a given species in the dataset). AluI was the restriction enzyme selected, as it met all of the above requirements and produced simulated RFLP-profiles that most clearly distinguished between the three species of *Heterodontus*.

Testing the PCR-RFLP Assay

The PCR-RFLP assay was tested on 67 specimens (Table 2.1) by performing PCR (as described previously) and subjecting PCR products to an AluI restriction digest in a 25 µL total reaction volume (1x CutSmart® Buffer, 20 U AluI restriction enzyme (New England Biolabs, Ipswich, MA, USA), 200 – 400 ng PCR product, and HPLC H_20 to adjust to the final 25 µL reaction volume). Digest reactions were incubated for 3 hours at 37°C and subsequently stored at –20°C. Digested products were run on a 1.8% agarose gel (using 0.5x TBE running buffer) at 70V for 120 minutes. The gel was then stained with a 3x GelRed Nucleic Acid Gel Stain solution (Biotium, Fremont, CA, USA) – prepared according to the manufacturer's recommendations – for 90 minutes before it was visualized using the Bio-Rad Gel Doc EZ Gel Imaging System (Bio-Rad, Hercules, CA, USA).

RESULTS

Sequencing and Final Species Assignment

The primer pair employed in this study successfully amplified a single fragment (1,216 bp) for all 67 specimens. A subset of 30 specimens was selected for sequencing of NADH2(+), including representatives from each of the three species (Table 2.1; Genbank Accession numbers MN977334-63). Post-trimming sequence lengths ranged from 1,083 bp to 1,105 bp.

Species identities were confirmed for each of the 30 individuals following an NCBI Nucleotide BLAST search. Examination of sequences in GENEIOUS revealed low intraspecific variation (< 1%) and relatively high interspecific variation (7 – 8%) across all three species of *Heterodontus*. A thorough (multilocus) phylogenetic analysis will follow in a subsequent publication. NADH2 sequences from *H. quoyi* were not available in the NCBI Nucleotide BLAST database, but NADH2(+) sequences were sufficiently different from both *H. francisci* and *H. mexicanus* (7 – 8% divergence) to justify phylogenetic distinction. A BLAST search (NCBI) returned *H. francisci* and *H. mexicanus* as the closest available matches by sequence identity.

PCR-RFLP Assay

The PCR-RFLP assay performed as predicted by the *in-silico* analysis implemented in GENEIOUS, resulting in distinct restriction fragment profiles for each of the three species (*H.*

francisci, *H. mexicanus*, and *H. quoyi*) (Table 2.3; Figure 2.2). The PCR-RFLP assay allowed successful identification of all 67 specimens with only a single PCR product and a single AluI restriction digest per individual.

The number of fragments produced for each species ranges from 6 (*H. francisci*) to 7 (*H. mexicanus* and *H. quoyi*). Two fragments are shared across all three species (73 bp and 9 bp), and three fragments are shared among two species (423 bp; 164 bp; and 58 bp). Still, there are clear diagnostic patterns, notably: 1) two closely-spaced bands at 489 bp and 423 bp, indicating *H. francisci*; 2) two unique bands at 587 bp and at 239 bp, indicating *H. mexicanus*; and 3) a roughly even, ladder-like pattern of bands (including unique bands at 297 bp and 219 bp), indicating *H. quoyi* (Figure 2.2).

DISCUSSION

Selection of an appropriate marker-enzyme pair is essential to the development of a robust, reliable PCR-RFLP assay for species identification; an ideal marker should display little to no intraspecific variation and relatively high interspecific variation with respect to enzyme cut-sites. In this regard the combination of NADH2(+) and enzyme AluI performs quite well. The PCR-RFLP assay is able to clearly and unambiguously distinguish between *Heterodontus francisci*, *H. mexicanus*, and *H. quoyi* for all specimens tested, with each species displaying a unique and reproducible restriction fragment profile.

In addition, the custom primer pair designed in this study was able to produce a PCR product in all individuals regardless of species, indicating its potential utility and ease-of-use for future work.

It should be noted that fragments smaller than 100 base-pairs are not easily discerned in Figure 2.2, despite the fact that their presence was predicted based on our *in-silico* digest (indicated in Table 2.3). This is likely the result of our decision to stain the gel after it had been subjected to electrophoresis; gels run with stain already incorporated displayed these bands more clearly. Regardless, species can be definitively identified by banding patterns with DNA fragments greater than 100 base-pairs.

Accurate species identification is a critical first step for the development and implementation of conservation strategies. The PCR-RFLP assay introduced in the present study provides a rapid and low-cost method for distinguishing between the three Eastern Pacific

species of *Heterodontus*, and could prove especially useful for resolving standing questions about these species' ranges as well as their vulnerability to harvest and bycatch in Mexico, Central America, and South America.

Table 2.1. Sampling sites for horn sharks (*Heterodontus* spp.) in the eastern Pacific, species obtained per sampling site, number of individuals subjected to PCR-RFLP assay, and number of individuals for which NADH2(+) sequences were obtained.

Sampling Site	Species	Total No. Individuals	No. Sequenced
Laguna San Ignacio, BCS, MX	*Heterodontus francisci*	2	2
Bahia Magdalena, BCS, MX	*Heterodontus francisci*	15	5
	Heterodontus mexicanus	23	12
El Sargento, BCS, MX	*Heterodontus francisci*	3	0
	Heterodontus mexicanus	1	0
San Bruno, BCS, MX	*Heterodontus mexicanus*	1	1
Bahia de Los Angeles, BC, MX	*Heterodontus francisci*	12	0
Galapagos Islands, EC	*Heterodontus quoyi*	10	10
	Total	67	30

Table 2.2. PCR and sequencing primers for the NADH2(+) locus that was amplified from horn sharks (*Heterodontus* spp.) of the eastern Pacific.

Primer Name	Direction	Primer Sequence (5' - 3')
HFND2-F	Forward	AGG ACT CGA ACC TAC ACT CA
HFND2-R	Reverse	GCT TTG AAG GCT TTT GGT CT

Table 2.3. Restriction fragment profiles generated from an AluI digest of the 1,216 bp NADH2(+) PCR product from horn sharks (*Heterodontus* spp.) in the eastern Pacific; fragment sizes below 100 bp are from *in-silico* predictions based on sequence data and are not readily visible in the gel in Figure 2.2.

Species	Number of Fragments (Post-Digest)	Fragment Sizes (bp)
Heterodontus francisci	6	489*, 423, 164, 73, 58, 9
Heterodontus mexicanus	7	587*, 239*, 150*, 100*, 73, 58, 9
Heterodontus quoyi	7	423, 297*, 219*, 164, 73, 31*, 9

*Fragment is unique to respective species

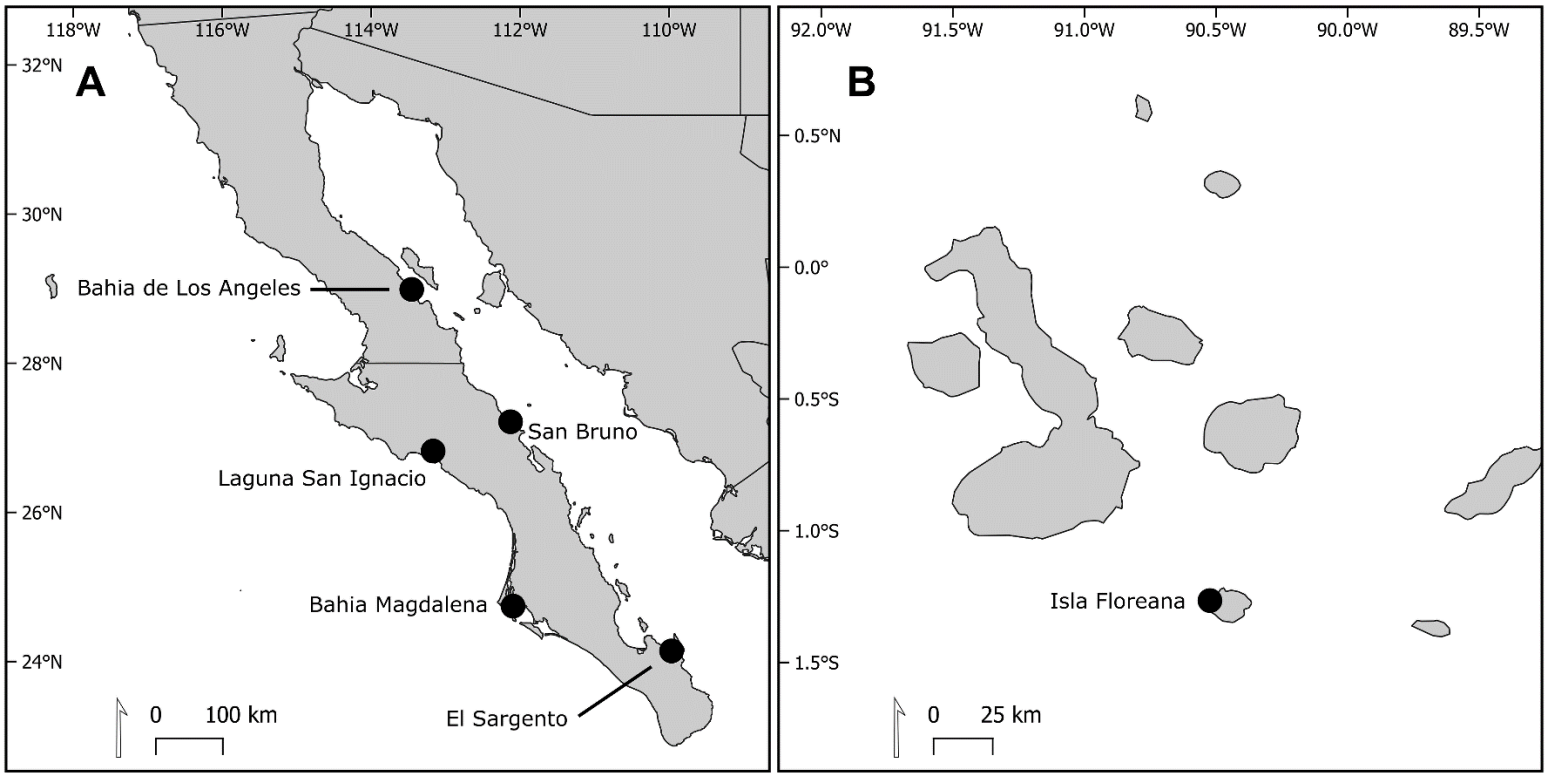

Figure 2.1. Sampling locations for horn sharks (*Heterodontus* spp.) of the eastern Pacific, in A) Baja California and Baja California Sur, Mexico and B) the Galapagos Islands, Ecuador.

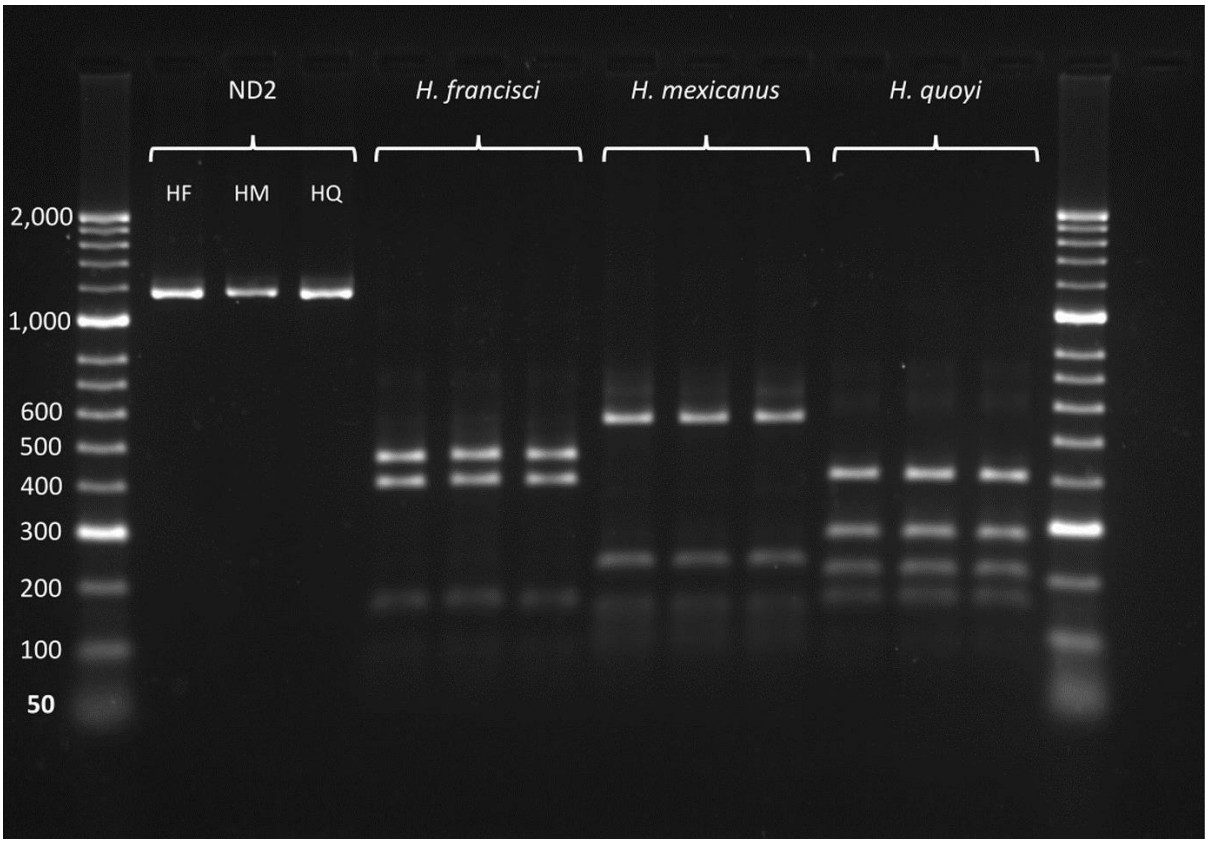

Figure 2.2. RFLP bands from horn sharks (*Heterodontus* spp.) in the eastern Pacific, after restriction digests of NADH2(+) with enzyme AluI; length of RFLP bands provided in Table 2.3. The three lanes denoted ND2 represent undigested PCR product for *H. francisci* (HF), *H. mexicanus* (HM), and *H. quoyi* (HQ).

CHAPTER 3. LITTLE SHARKS IN A BIG WORLD: MITOCHONDRIAL DNA REVEALS SMALL-SCALE POPULATION STRUCTURE IN THE CALIFORNIA HORN SHARK (*HETERODONTUS FRANCISCI*)

ABSTRACT

The California horn shark (*Heterodontus francisci*) is a small demersal species distributed from southern California and the Channel Islands to Baja California and the Gulf of California. These nocturnal reef predators maintain small home-ranges as adults, and lay auger-shaped egg cases that become wedged into the substrate. While population trends are not well documented, this species is subject to fishing pressure through portions of its range and has been identified as vulnerable to overexploitation. Here we present a survey of 318 specimens from across the range, using mtDNA control region sequences to provide the first genetic assessment of *H. francisci*. Overall population structure ($\Phi_{ST} = 0.266$, $P < 0.001$) is consistent with limited dispersal as indicated by life history, with two distinct features. Population structure along the continuous coastline is low, with no discernable breaks from Santa Barbara, CA to Bahia Tortugas (Baja California Sur, Mexico); however, there is a notable partition at Punta Eugenia (BCS), a well-known biogeographic break between tropical and subtropical marine faunas. In contrast, population structure is much higher (max $\Phi_{ST} = 0.601$, $P < 0.05$) between the coast and adjacent Channel Islands, a minimum distance of 19 km, indicating that horn sharks rarely disperse across deep habitat and open water. Population structure in most elasmobranchs is measured on a scale of hundreds to thousands of kilometers, but the California Horn Shark has population partitions on an unprecedented small scale, indicating a need for localized management strategies which ensure adequate protection of distinct stocks.

INTRODUCTION

Elasmobranchs, the group of cartilaginous fishes which includes sharks and rays, have experienced steep and widespread population declines over the past several decades due to overharvesting and bycatch (Baum et al. 2003; Dulvy et al. 2008). Sharks are particularly ill-suited to deal with such pressures due to their life histories, which often include slow growth, late age at maturity, and low fecundity (Musick et al. 2000; Dulvy et al. 2017). Dulvy et al. (2014) estimated that approximately one-quarter of Chondrichthyan species are threatened. The

IUCN Red List (2020) includes 199 species (19% of 1060 sharks and rays) classified as threatened or endangered, 41% as Data Deficient, and 29% as Least Concern. There is, therefore, a clear and urgent need for informed management of elasmobranch populations.

Population genetics has proven useful for informing conservation management strategies (Schwartz et al. 2007; Allendorf et al. 2010; Frankham 2010). In particular, the field of population genetics has provided managers with techniques for identifying population subdivision (or "population structure"), which in turn allows them to target management strategies towards independent populations. Such targeted strategies are useful because they can be used to prevent overharvesting of local stocks, identify populations in need of special protection, and maximize the genetic diversity and adaptive potential of a given species (Domingues et al. 2018).

Crucial to these efforts is an understanding of the processes underlying population structure and the partitioning of genetic diversity (Arenas et al. 2012; Selkoe et al. 2014). This knowledge can enhance conservation efforts in two ways: (*i*) informing the delineation of appropriate spatial scales for management, and (*ii*) allowing the identification of subareas in need of protection within broader management units (Fogarty and Botsford 2007; Hilário et al. 2015).

Previous genetic studies in sharks have demonstrated that the spatial scale of population structure can vary widely among taxa. For example, multiple studies on the Blue shark (*Prionace glauca*) – a highly migratory, large-bodied shark with a circumglobal distribution – detected little to no significant population structure on a global scale (Taguchi et al. 2015; Veríssimo et al. 2017; Bailleul et al. 2018). Consequently, Veríssimo et al. (2017) suggest a cooperative management approach among regional fisheries management organizations. At the opposite end of the spectrum, significant population structure has been detected in the Pacific angel shark (*Squatina californica*) (Gaida 1997) and the Lemon shark (*Negaprion brevirostris*) (Ashe et al. 2015) over a scale of roughly 150 kilometers. This implies the existence of multiple stocks which may warrant independent consideration and local-scale management.

The large variation in the spatial scale of population structure in sharks is attributable to fundamental differences in life history and ecology in an evolutionary lineage that dates back at least 400 million years (Musick et al. 2004; Dudgeon et al. 2012). In the Blue shark, high migration rates across ocean basins can explain a lack of genetic structuring. For the Lemon shark, population structure (detected using mtDNA) appears to be driven by female reproductive

philopatry; Feldheim et al. (2014) found that females would faithfully return to the same site to give birth over the course of nearly two decades. The Pacific angel shark, a benthic ambush predator, revealed population genetic structure between the northern Channel Islands (Santa Rosa Island and Santa Cruz Island, California) and those residing in the waters around San Clemente Island, separated by only 140 kilometers of open water (Gaida 1997). Hence the deep, open waters separating these islands may act as a barrier to dispersal in the Pacific angel shark.

The California horn shark (*Heterodontus francisci*) is a small (max 122 cm TL), coastal species inhabiting shallow waters from Point Conception, California south to the Gulf of California, Mexico (Love 1996). This species is almost exclusively benthic, rarely venturing more than two meters above the substrate, and is commonly found at depths ranging from 2-11 meters (though they may occasionally be encountered as deep as 150 meters) (Compagno 2002). Furthermore, these nocturnally active reef predators are known to shelter during the day, maintaining relatively small home-ranges and demonstrating strong site-fidelity (Nelson and Johnson 1970; Strong 1989; Meese and Lowe 2020).

Like the Pacific angel shark, *H. francisci* can be found in the waters surrounding the California Channel Islands. They are also frequently encountered by divers and fishers in the islands off the coast of the Baja Peninsula, including Isla Guadalupe, approximately 250 kilometers from the continental mainland. Intriguingly, the horn sharks inhabiting the waters around Santa Catalina Island – a mere 32 kilometers from the California mainland – were hypothesized to be a distinct population based on differences in egg-case morphology (Taylor 1972; Strong 1989). However, there have been no further inquiries about whether H. francisci exhibits population structure across the range. Moreover, at least two authors have proposed the existence of cryptic evolutionary partitions within H. francisci in the Gulf of California based on differences in color, markings, and fin shape (Michael 1993; Castro 2010). Given that the IUCN Red List currently lists *H. francisci* as Data Deficient (Carlisle 2015) and at least one recent study has identified the species as vulnerable to overexploitation throughout portions of its range (Furlong-Estrada et al. 2017), these are questions with strong conservation implications.

In this study, we examine population genetic structure in *H. francisci* across its range using a 724-basepair fragment of the mitochondrial control region (mtCR). The mtCR is a useful genetic marker for resolving population genetic structure in sharks because it lacks a protein-coding function, allowing it to accumulate more variation than protein-coding markers (Avise

1994). This is especially useful because sharks tend to have relatively low mutation rates (Martin et al. 1992; Martin 1999); as a result, it has become one of the most widely used markers in studies of shark population genetics (Dudgeon et al. 2012; Domingues et al. 2018). Specifically, we used the mtCR to: (*i*) determine whether population genetic structure pertinent to conservation occurs between island and mainland ranges; (*ii*) determine whether the deep-water channel separating the Channel Islands from the California mainland acts as a barrier to dispersal in horn sharks; (*iii*) determine whether population genetic structure exists along the contiguous coastline from Santa Barbara, CA to Las Animas in the Gulf of California; and (*iv*) test for proposed cryptic evolutionary lineages across the species range.

MATERIALS AND METHODS

Sample Collection and DNA Extraction

Tissue samples (N = 318) from California horn sharks (*H. francisci*) were obtained from 14 locations throughout their range, from Santa Barbara, CA to Las Animas, Baja California, Mexico between 2004 and 2019 (Figure 3.1a, 3.1b). Where possible specimens were collected from spatially distinct sites within the collection area, to reduce the possibility of sampling closely related individuals. Tissue samples consisted of either fin clips or muscle tissue plugs, and were preserved in either 70% ethanol, 20% salt-saturated DMSO, or RNAlater (Sigma Aldrich, St. Louis, MO, USA). When possible, tissues were immediately stored at -20°C. Total genomic DNA was extracted from tissues using the E.Z.N.A. Tissue DNA Kit (Omega Bio-Tek, Norcross GA, USA) with minor adjustments to the manufacturer's protocol. Extracted DNA was visually inspected for quality via agarose gel electrophoresis.

mtDNA Amplification and Sequencing

The complete mitochondrial control region (mtCR) was amplified via polymerase chain reaction (PCR) using custom-designed forward and reverse primers (HFCR2-F: 5'-ACA TGG CCC ACA TTC CTT AA-3' and HFCR2-R: 5'-TTG ATC AGG GCA TTC TCA CG-3'). PCR was carried out in 40 µL reactions containing 20 µL GoTaq Green 2x Master Mix (Promega, Madison, WI, USA), 0.4 pmol/µL of each oligonucleotide primer (forward and reverse), 1-2 µL DNA template, and HPLC water to adjust to a final volume of 40 µL. PCR cycling conditions consisted of one cycle at 95°C for 3 min; 39 cycles of 95°C for 30 s, 57°C for 30 s, 72°C for 1

min 15 s; and one cycle at 72°C for 5 min. Amplified PCR products were then cleaned using PCRCLEAN DX™ bead solution (Aline Biosciences, Woburn, MA, USA) and sent to the Advanced Studies in Genomics, Proteomics and Bioinformatics (ASGPB) facility at the University of Hawai‘i at Mānoa to be sequenced in the forward and reverse directions on an Applied Biosystems 3730XL DNA Analyzer (Thermo Fisher Scientific, Waltham, MA, USA).

Genetic Diversity and Population Structure

Forward and reverse sequences were assembled into contigs, trimmed, aligned, and edited in GENEIOUS v6.1.8 (Biomatters Ltd, Auckland, NZ). Basic statistics, including the number of unique haplotypes (*H*), haplotype diversity (*h*) and nucleotide diversity (π), were calculated using ARLEQUIN v3.5 (Excoffier and Lischer 2010). To analyze the relationships among haplotypes and their geographic distribution, a haplotype network was assembled using a minimum-spanning algorithm (Bandelt et al. 1999) and visualized using the program PopART (Leigh and Bryant 2015).

To examine population genetic structure among sampling sites, Φ_{ST} – an F_{ST} analog that incorporates DNA sequence divergence between haplotypes (Excoffier et al. 1992) – was calculated for each pair of populations (excluding La Ventana, Baja California Sur, due to small sample size). To estimate overall population structure, an Analysis of Molecular Variance (AMOVA) (Excoffier et al. 1992) was performed. Mantel tests were conducted on the total dataset as well as subsets of populations in order to test for patterns of isolation by distance (IBD). For Mantel tests, shortest overwater distances among sampling sites were estimated using Google Earth (http://earth.google.com), and analyses were performed on Φ_{ST} and estimated geographic distances. Pairwise Φ_{ST} estimates, AMOVA, and Mantel tests were all conducted in ARLEQUIN, and statistical significance of all three analyses was determined via non-parametric permutation tests, each consisting of 20,000 permutations. In the case of pairwise Φ_{ST} estimates and Mantel tests, a false discovery rate (FDR) correction for multiple comparisons was implemented in R v4.0.2 (R Core Team 2020) using the method proposed by Benjamini and Hochberg (1995).

Coalescent Estimation of Migration

Genetic diversity (θ_1, θ_2, and ancestral θ_A), mutation scaled migration rates ($m_{1\rightarrow2}$, $m_{2\rightarrow1}$), number of migrants per generation ($Nm_{1\rightarrow2}$, $Nm_{2\rightarrow1}$), and time since population divergence (t_0) were estimated for pairs of populations spanning putative biogeographic barriers using the program IMa3 (Hey et al. 2018). IMa3 implements an Isolation with Migration (IM) model that does not assume drift-migration equilibrium, and is therefore ideally suited for estimating migration in recently diverged populations that share haplotypes due to both migration and ancestral polymorphism (Nielsen and Wakeley 2001). Additionally, unlike its predecessor IMa2 which requires a user-defined topology as an input (Hey 2010), IMa3 can estimate a phylogenetic topology before implementing the IM model across multiple populations simultaneously. However, since our single-locus dataset did not yield well-resolved phylogenies during preliminary testing, population pairs were analyzed independently. In total, four pairwise IMa analyses were performed on five population units (CAT, NCI, MLCA, BT, and LSIBM, defined below) spanning putative biogeographic barriers. Based on the results of pairwise Φ_{ST} estimates, the five mainland California sites (Santa Barbara, Malibu, Palos Verdes, Laguna, and San Diego) were combined into a single mainland California population (MLCA). Similarly, to allow for migration rate estimates between the Northern Channel Islands (Anacapa Island and Santa Cruz Island) and the southern Santa Catalina Island (CAT), the two northern islands were also combined into a single population (NCI). Finally, Laguna San Ignacio and Bahia Magdalena were combined to form a single population (LSIBM) on the basis of non-significant pairwise ΦST estimates and were analyzed against the population in Bahia Tortugas (BT) to the north.

The HKY mutation model (Hasegawa et al. 1985) was determined to be the best fit to our data based on analyses in jModelTest v2.1.4 (Guindon and Gascuel 2003; Darriba et al. 2012) and was used for all analyses. Preliminary runs in IMa3 were used to determine appropriate MCMC burn-in durations as well as an optimal maximum value of the uniform prior for the divergence time parameter (t = 0.5). Hyperprior distributions (option -j3) were invoked in preliminary runs for each pairwise analysis to determine optimal prior values for θ and m; an exponential prior distribution was specified for the migration rate parameter (m) for all analyses. Once optimal priors were estimated, simulations were run for each population pair in triplicate to assess whether sample distributions could be considered reasonable estimates of the true posterior distribution. Specifically, effective sample size (ESS) and autocorrelation values were

examined to ensure proper chain mixing (per the program manual), and posterior distributions were compared among runs to assess convergence. Each analysis utilized 40 metropolis-coupled chains for 30 million total steps (300,000 sampled genealogies) after a burn-in period of 60 hours. All simulations were run using the CIPRES Science Gateway (Miller et al. 2010).

For each pairwise estimation of *m*, posterior probability distributions were divided by the prior distribution and plotted to assess the prior distribution's effect on the posterior. If the exponential prior distribution has a large effect on the posterior, then this procedure should result in a large rightward shift in the peak of the new distribution relative to the posterior (towards larger values of *m*).

Estimates of parameters t_0 and θ were converted to demographic units (lineage age in years and effective population size N_e, respectively) based on an estimated generation time for *H. francisci* and mutation rates derived from the literature. The California horn shark has an age at maturity of 3 – 7 years for both males and females, with a maximum age of approximately 16 years for males and 22 years for females (Strong 1989; Ebert et al. 2013; Castellanos-Vidal 2017; Domínguez-Reza 2017). Based on these values, a generation time of 10 years was provisionally applied to *H. francisci*. A literature search revealed a number of estimates for mutation rates in the shark mtCR, with values ranging from 0.43% per million years (MY^{-1}) for the blacktip shark (*Carcharhinus limbatus*; Keeney and Heist 2006) to 1.2% MY^{-1} in the scalloped hammerhead (*Sphyrna lewini*; Nance et al. 2011). These values were converted to a per locus per year mutation rate – resulting in values of 1.56×10^{-6} and 4.37×10^{-6} substitutions per locus per year, respectively – and each was applied in calculations to obtain a range of estimates for splitting times and N_e. Because our value for generation time represents a rough estimate, and because of the reliance on data from other species with respect to mutation rates, all resulting values should be interpreted with caution, useful only for qualitative comparisons.

Demographic Analyses

To gain insight into how past demographic processes may have shaped contemporary patterns of genetic diversity, the population demographic history of the California horn shark was inferred using multiple approaches. A mismatch distribution analysis was conducted in ARLEQUIN to test two demographic scenarios: sudden demographic expansion (Rogers and Harpending 1992) and spatial expansion (Ray et al. 2003). ARLEQUIN assesses the goodness of

fit between the observed data and the expected mismatch distribution under each demographic scenario by calculating Harpending's raggedness (*r*) index (Harpending 1994) and the sum of squared deviations (SSD). For each demographic scenario, statistical significance was determined using 10,000 bootstrap replicates. In addition, two neutrality tests – Fu's F_s (Fu 1997) and Ramos-Onsis and Roza's R_2 (Ramos-Onsins and Rozas 2002) – were performed, and the statistical significance for each was determined via 10,000 simulations under coalescent processes as implemented in DNAsp v6.12 (Rozas et al. 2017). In each case, the data were compared to null distributions generated under the standard neutral model (SNM). While R_2 and Fu's F_s are each able to detect signatures of demographic expansions and deviations from neutrality, R_2 performs better when sample sizes are small, and Fu's F_s performs better with large sample sizes (Ramos-Onsins and Rozas 2002). Extended Bayesian skyline plots were constructed using BEAST v2.6.2 (Bouckaert et al. 2019) and visualized in R, but were uniformly uninformative with no evidence of population expansion or contraction.

RESULTS

Genetic Diversity

After trimming and editing, 724 bp of the mtCR were retained for 318 horn sharks, covering roughly 68% of the total mtCR for this species as reported by Arnason et al. (2001). The final sequences consisted of 20 unique haplotypes (H1-H20; GenBank Accession Numbers MZ442361-MZ442380), with 12 polymorphic sites (Table S3.1). Overall haplotype and nucleotide diversities were $h = 0.811$ (± 0.011) and $\pi = 0.00334$ (± 0.00007), respectively. Haplotype diversity values ranged between a low of 0.227 ± 0.106 (Anacapa Island) and highs of 0.894 ± 0.063 (Las Animas) and 1.000 (La Ventana; n = 3), while nucleotide diversity values ranged between a low of 0.00104 ± 0.00075 (Isla Guadalupe) and a high of 0.00327 ± 0.00022 (Malibu) (Table 3.1).

A median-joining haplotype network revealed shallow coalescence among haplotypes (Figure 3.1c), a common outcome in marine fishes (Grant and Bowen 1998). Haplotypes H1 (n = 92), H2 (n = 77), and H3 (n = 61) collectively represented more than 73% of individuals in the entire dataset. Haplotypes H1 and H3 were also the most geographically widespread, each represented in all but one population (Anacapa and Guadalupe, respectively). Haplotype H2 was detected at elevated frequency in the California Channel Islands (SCI, ANA, and CAT in Figure

3.1), and was absent in samples south of San Diego, California. Of the 20 unique haplotypes recorded, 10 were singletons (observed in single individuals); of these 10 singleton haplotypes, eight were exclusive to populations of Baja California, and four were exclusive to Las Animas (LA in Figure 3.1). In total, six haplotypes were exclusive to populations of California and the Channel Islands, and 10 were exclusive to populations of Baja California and the Gulf of California (Table S3.1).

Population Structure

An analysis of molecular variance (AMOVA) revealed significant population genetic structure across the range of *H. francisci* (overall $\Phi_{ST} = 0.266$, $P < 0.001$). Pairwise Φ_{ST} comparisons indicated strong matrilineal population structure between the California Channel Islands and all other sampled sites, with values ranging from $\Phi_{ST} = 0.131 - 0.810$, $P < 0.05$; Table 3.2). No comparisons between the three Channel Island sites resulted in statistically significant Φ_{ST} values after FDR correction. Comparisons among mainland sites – from Santa Barbara, CA to Las Animas, BC, MX – revealed no population structure among sites along the California mainland, but indicate a break between Bahia Tortugas and the two sites immediately to the south, Laguna San Ignacio and Bahia Magdalena ($\Phi_{ST} = 0.198 - 0.266$, $P < 0.01$). Except for the California Channel Islands, only Bahia Tortugas demonstrated significant population genetic structure when compared with Las Animas ($\Phi_{ST} = 0.119$, $P < 0.05$). Similarly, only Malibu, Laguna San Ignacio, and Bahia Magdalena demonstrated significant population genetic structure when compared to offshore Isla Guadalupe ($\Phi_{ST} = 0.206 - 0.343$, $P < 0.05$).

A Mantel test with all 13 populations (excluding La Ventana) did not reveal a statistically significant relationship between genetic distance and geographic distance ($r_m = 0.053$, $P = 0.356$; Table 3.3). To test for a pattern of isolation-by-distance among mainland populations, a Mantel test was conducted with island populations excluded, and likewise did not result in statistical support for IBD ($r_m = 0.315$, $P = 0.137$). Las Animas in the Gulf of California was excluded for the next analysis, because it is located in a biogeographic province distinct from the Pacific coastline (Briggs and Bowen 2012).When Las Animas was excluded along with island populations, the Mantel test indicated a relationship between genetic distance and geographic distance for Pacific coast populations that tended towards significance, approaching the significance threshold of $\alpha = 0.05$ after FDR correction ($r_m = 0.541$, $P = 0.058$). Single-locus

mtDNA estimates of the relationship between genetic and geographic distance should be interpreted with caution (see Teske et al. 2018), but may nonetheless be useful for a generalized interpretation of the processes underlying the distribution of genetic diversity. A plot of genetic distance versus geographic distance is provided in Figure 3.2.

Coalescent Estimation of Migration

Estimates of the effective number of migrants per generation (*Nm*) were low for all pairwise comparisons, ranging from 0.55 (NCI to CAT) to a maximum of 2.53 (CAT to MLCA) (Table 3.4). Estimates of mutation-scaled migration rates (*m*) were similarly low, with a maximum value of 2.27 (CAT to MLCA). Migration rates for each population pair were roughly equal in each direction, displaying considerable overlap in the posterior distributions (Figure 3.3a, 3.3b). Posterior distributions for all pairwise estimates of migration included zero; while the peaks of many of these distributions hint at non-zero migration rates, a zero-migration model could not be rejected for any population pair. Dividing the posterior distribution by the prior resulted in relatively modest peak shifts to higher values of *m* except in the case of the comparison between CAT and NCI, which resulted in new peaks at values that were 7.67 to 550 times the original estimate and a much flatter overall distribution (Figure 3.3c).

Channel Island populations (CAT and NCI) had smaller estimated values of θ than MLCA, though there was considerable overlap in their posterior distributions (95% Highest Posterior Density (HPD); Table 3.4). Estimates of θ for MLCA were relatively consistent across both comparisons (3.74 vs. 4.26). All four pairwise analyses indicated values of θ for ancestral populations (θ_A) that were larger than contemporary population estimates. Unfortunately, because the right tails of the posterior distributions of all θ_A estimates did not reach a probability of zero within the bounds of the prior distribution, a reliable 95% HPD could not be reported, precluding statistically meaningful comparisons. Converting peak estimates of θ to effective population size (N_e) resulted in values ranging from 6,751 to 82,051 for contemporary populations and values ranging from 37,071 to 126,282 for theoretical ancestral populations (Table 3.5).

Reliable estimates of splitting times (t_0) for each population pair could not be obtained, as the right tails of the posterior distributions tended to plateau and extend rightward indefinitely (Figure S3.1). This pattern is expected in situations where the data do not contain enough

information to clearly identify the full model under the specified prior (per the IMa3 user manual). Despite this uncertainty, converting the most recent peak value of t_0 to time since divergence in years yielded estimates ranging from 21,281 - 75,000 years for the split between the populations of the Channel Islands (CAT, NCI) and MLCA, and an earlier split between the populations of BT and LSIBM (31,808 - 89,103 years; Table 3.5).

Demographic Analyses

Of the 13 populations included in the mismatch distribution analysis, only Laguna San Ignacio deviated significantly from the expectations of the sudden demographic expansion model, and none deviated significantly from the expectations of the spatial expansion model (Table S3.2). Simulations involving Anacapa Island, San Diego, and Isla Guadalupe failed to converge after 2,000 steps, and therefore did not yield estimates of θ, Harpending's raggedness (*r*) index, or SSD. The number of pairwise differences among sequences ranged from zero to six for each sampling site (Figure S3.2).

None of the 13 populations yielded Fu's F_s statistics significantly different from zero, with values ranging from -2.245 to 1.415 ($P > 0.05$). Three populations – Malibu, Palos Verdes, and Isla Guadalupe – yielded significant positive values of R_2 ($P < 0.05$) (Table S3.2).

DISCUSSION

This study is the first to examine population genetic structure in the California horn shark (*Heterodontus francisci*) and the third to examine population genetic structure in the genus *Heterodontus* (O'Gower and Nash 1978; Day et al. 2019). The California horn shark shows no population partitions along hundreds of kilometers of relatively continuous coastal habitat, a modest genetic partition at Punta Eugenia (BCS), a known biogeographic boundary, and strong population separations between coastline and adjacent islands (Φ_{ST} = 0.131-0.601) separated by as little as 19 km of deep water. Thus, our results indicate strong matrilineal population structure over spatial scales much smaller than those reported for any other elasmobranch species to date. Furthermore, these findings carry strong implications for elasmobranch conservation.

Our results show no evidence of cryptic evolutionary lineages in the Gulf of California. These cryptic lineages were originally proposed by Michael (1993) and Castro (2010) for the Gulf of California population based on higher, more falcate dorsal fins, a lack of dark spots, a

lighter abdomen, and low supraorbital ridges. Notably, none the specimens we obtained from the Gulf of California met this description. It is therefore possible that more extensive sampling could yet reveal the presence of cryptic diversity within the genus *Heterodontus*.

Genetic Diversity

The overall values for genetic diversity detected in this study ($h = 0.811 \pm 0.011$, $\pi = 0.00334 \pm 0.00007$) are consistent with values obtained in other mtDNA studies on sharks (Domingues et al. 2018). However, the values we report here are generally higher than those reported for other benthic, coastal species, including *Heterodontus portusjacksoni* (Day et al. 2019), *Stegostoma tigrinum* (formerly *S. fasciatum*; Dudgeon et al. 2009), *Ginglymostoma cirratum* (Karl et al. 2012a), and *Orectolobus spp.* (Corrigan et al. 2016). Among mainland sites, both Bahia Tortugas and Laguna San Ignacio had the lowest genetic diversity, with > 50% of individuals in each population possessing a sinsgle mitochondrial haplotype (H1 and H3, respectively) (Figure 3.1). While the haplotypic composition of Bahia Tortugas closely resembles that of the California mainland, however, there is a significant shift in haplotype composition between Bahia Tortugas and Laguna San Ignacio (corresponding to Punta Eugenia), the latter of which most closely resembles Bahia Magdalena to the south.

We observed a general trend towards lower genetic diversity in island populations (Table 3.1). Guadalupe Island – the most geographically isolated island in our dataset – was represented by only two haplotypes. Interestingly, Anacapa Island – the closest to the mainland – had similarly low haplotype and nucleotide diversity. Lower genetic diversity in island populations (compared to their mainland counterparts) is a well-documented phenomenon, particularly for terrestrial species, and is often correlated with distance, dispersal capability, and population size (Frankham 1997). Lower genetic diversity in the Channel Island populations, coupled with the prevalence of the haplotype H2, hints strongly at island founder effects with rare migration events between island and mainland populations.

Population Genetic Structure

The California horn shark displays significant population genetic structure across its range (overall $\Phi_{ST} = 0.266$), with the strongest partitioning of genetic diversity appearing between island and mainland populations. We also report a strong genetic break corresponding to

Punta Eugenia (Baja, California), and weak evidence for a pattern of isolation by distance (IBD) among mainland sites along the Pacific coast.

The Channel Islands off the California coast have been the subject of numerous studies in island biology, but they are not a homogenous geographic unit. The four Southern Channel Islands are part of the Peninsular Ranges geologic province, and the four Northern Channel Islands are part of the Transverse Ranges province, with the two regions separated by about 100 km of deep water. The northern islands are separated by shallow seas, whereas the southern islands have deeper separations. Our sampling regime includes two northern islands (Santa Cruz Island and Anacapa Island) and one southern island (Santa Catalina Island).

Our results support the long-standing hypothesis, first proposed by Taylor (1972), that the horn sharks of Santa Catalina Island comprise a distinct population separate from the California mainland (Φ_{ST} = 0.193 - 0.387). These two landmasses are separated by approximately 30 km of open water, most of which is deeper than 200 meters. This level of population subdivision is remarkable for a shark; however, at least one other elasmobranch, the round stingray (*Urobatis halleri*), has been shown to exhibit population genetic structure between the California mainland and Santa Catalina Island (Plank et al. 2010). Like the horn shark, the round stingray is a shallow, benthic elasmobranch, possibly limited in both depth and distribution by a preference for warmer water (Ebert 2003; Jirik and Lowe 2012). Morphometric evidence from adult swell sharks (*Cephaloscyllium ventriosum*), as well as their egg cases, also suggests genetic differentiation between populations inhabiting Santa Catalina Island and the California mainland (Grover 1970). Apparently the deep, cold waters separating Santa Catalina Island and the California mainland act as a barrier to dispersal for other benthic elasmobranchs in the region, in addition to the California horn shark.

The structure detected between the California mainland and the Northern Channel Islands – Santa Cruz Island and Anacapa Island – is unprecedented in its scale (Φ_{ST} = 0.131 - 0.601). Anacapa Island is separated from the California mainland by only 19 km of open water and is the nearest of the Channel Islands. Regardless, it consistently yielded the highest Φ_{ST} values of any of the Channel Islands in pairwise comparisons (Table 3.2). To our knowledge, this represents the smallest distance over which significant population genetic structure has been detected in any elasmobranch to date. Paradoxically, the most remote island in our sampling, Isla Guadalupe (GI), approximately 250 km from shore, does not present a consistent signal of population

genetic structure when compared to mainland populations. This is likely due to two factors: small sample size (n = 8) and the high frequency of haplotype H1, which is also present at high frequency in both our mainland California sites as well as Bahia Tortugas (BT). Better resolution may be achieved with either a higher sample size or with additional genetic markers (see Outstanding Questions and Future Directions, below).

Despite evidence that deep, open water acts as a barrier to dispersal among populations of *H. francisci* at the northern end of their range, no population structure is detected between the three Channel Islands included in our study. However, higher sample sizes might change this conclusion; Santa Cruz (SCI) and Anacapa (ANA) in the Northern Channel Islands have a pairwise Φ_{ST} value of 0.095, verging on significance (P = 0.068). This is somewhat surprising as these sites are linked by shallow channels of the Transverse Ranges province, whereas Catalina (CAT) in the Southern Channel Islands is separated from the northern islands by approximately 100 km of deep water. Clearly deep water is guiding population structure in *H. francisci*, but other factors are shaping genetic architecture as well.

While we report strong genetic structuring between island and mainland populations, there is little evidence of population structure along contiguous coastlines, with one notable exception: a distinct genetic break between Bahia Tortugas (BT) and the two sample sites to the south, Laguna San Ignacio (LSI; Φ_{ST} = 0.266) and Bahia Magdalena (BM; Φ_{ST} = 0.198; Table 3.2). This corresponds to Punta Eugenia, the prominent point of land extending seaward from the middle of Baja California. Punta Eugenia is the southern limit of many fish distributions and is recognized as the transition zone between Californian and Panamic Biogeographic Provinces (Briggs and Bowen 2012). Furthermore, many fishes that extend south into the Gulf of California show a phylogeographic partition at Punta Eugenia (Bernardi et al. 2003). This biogeographic partition is attributed to different water masses north and south of the break that may entrain the larvae of pelagic and benthic fish species (Aceves-Medina et al. 2018). Hence it is an interesting outcome that the break defined with bony fishes extends to a shark that lacks a pelagic larval stage. Additionally, it is worth noting that our results do not support the existence of population genetic structure between Pacific coast and Gulf of California populations of *H. francisci*, despite the apparent genetic break at Punta Eugenia and previous work indicating that genetic partitions between these regions are common in shorefishes (Bernardi et al. 2003; see also Robertson and Cramer 2009) as well as the Pacific angel shark (Ramírez-Amaro et al. 2017). As

with our Isla Guadalupe (GI) dataset, this too may be the result of low sample sizes and may be better resolved in the future with more individuals and/or more genetic markers (see Outstanding Questions and Future Directions, below).

Mantel tests did not demonstrate a statistically significant association between geographic distance and Φ_{ST} for the full dataset after a correction for multiple comparisons ($P > 0.05$; Table 3.3). But when island populations and Las Animas were excluded from the analysis, placing focus solely on populations occupying the continuous Pacific coastline, the result approached significance ($r_m = 0.541$, $P = 0.058$). It is reasonable to expect a pattern of IBD among mainland populations of *H. francisci*, which lacks a pelagic larval stage and maintains relatively small home-ranges as an adult – both of which are characteristics likely to result in low dispersal capability (Strong 1989; Bernardi 2000). While the results from our current analysis do not support this conclusion in a strict statistical sense, we do not rule it out entirely.

Coalescent Estimation of Migration

Isolation with Migration analyses (IMa) revealed low migration rates among island-mainland population pairs and among populations north and south of Punta Eugenia on the Pacific coast of the Baja peninsula, in keeping with patterns observed via pairwise Φ_{ST} estimates (Table 3.4). Estimates of the effective number of migrants per generation (*Nm*) ranged from 0.64 to 2.53 for these population pairs, which is certainly low enough to facilitate genetic divergence. The choice of an exponential prior had a noticeable effect on the posterior distribution, likely resulting in an underestimate of the mutation scaled migration rate (*m*), and, consequently, *Nm*. This effect was especially strong for the comparison between the Northern Channel Islands (NCI) and Santa Catalina Island (CAT), whereas the effect on the other pairwise comparisons was relatively modest (Figure 3.3c). Still, even after correcting for the effect of the exponential prior, distributions still included migration rates of zero for all pairwise comparisons.

Converting estimates of θ and time since divergence (t_0) to demographic units revealed large effective population sizes and suggested relatively recent splits between pairs of populations, even after accounting for a range of possible mutation rates (Table 3.5). Assuming a mutation rate of 4.37×10^{-6} substitutions per year for the mtCR of *H. francisci*, the initial divergence between the Channel Islands and the California mainland appears to occur between 27,000 and 21,000 years before present (YBP). This roughly coincides with the Last Glacial

Maximum (LGM), approximately 27,000-19,000 YBP (Clark et al. 2009). On the other hand, if we assume a lower mutation rate of $1.56x10^{-6}$ substitutions per year, the date of initial divergence jumps to approximately 75,000-59,000 years ago, predating the LGM by a large margin. In reality, these divergences could have occurred even deeper in the past than indicated by these values, as IMa3 was not able to resolve clearly defined peaks in the posterior distributions for t_0 (Figure S3.1).

Estimates of effective population size (N_e) also varied widely depending on the mutation rate considered, with values ranging from 6,751 individuals (NCI) to 82,051 individuals (LSIBM). Estimates of N_e were overall lower for island populations than for mainland populations, which is perhaps unsurprising given the islands' small size and apparent demographic isolation. This suggests that genetic drift may act more strongly on the island populations, accelerating genetic divergence from mainland stocks. It has been proposed that an N_e of at least 500 (Frankham et al. 2010) to 5,000 breeding individuals (Lande 1995) may be required for populations to maintain adaptive potential in the face of environmental changes. In that regard these estimates are encouraging, as the California Channel Islands are likely to experience increasingly frequent and severe impacts from marine heatwaves (Holbrook et al. 2019; Oliver et al. 2019).

Demographic History

The results of our demographic analyses were minimally informative. While non-significant values for Harpending's raggedness index (r) and SSD appear to suggest recent spatial expansions for all populations tested and demographic expansions for all populations except for Laguna San Ignacio, neutrality tests (Fu's F_s and Ramos-Onsis and Rozas' R_2) seem to suggest the opposite for most populations (Table S3.2). In populations where R_2 had significant positive values (Malibu, Palos Verdes, and Isla Guadalupe), Fu's F_s had non-significant, sometimes positive values. Under a scenario of demographic expansion, Fu's F_s is expected to take on highly negative values.

Comparative Phylogeography

Sharks tend to have large ranges with few population divisions. At the scale of truly oceanic species, the Basking shark (*Cetorhinus maximus*) and Blue shark (*Prionace glauca*)

show little or no structure on a global scale (Hoelzel et al. 2006; Veríssimo et al. 2017). The Whale shark (*Rhincodon typus*) shows population structure only on the scale of Atlantic versus Indo-Pacific (Castro et al. 2007). Large coastal sharks may show structure on the scale of ocean basins, such as North versus South Atlantic for the Tiger shark (*Galeocerdo cuvier*; Bernard et al. 2016), East versus Central Pacific for the Scalloped hammerhead shark (*Sphyrna lewini*; Daly-Engel et al. 2012), eastern versus western Australia in the Sandbar shark (*Carcharhinus plumbeus*; Portnoy et al. 2010), and Indian versus Pacific Oceans in the Whitetip reef shark (*Triaenodon obesus*; Whitney et al. 2012). Smaller coastal sharks may have population structure within ocean basins, including the Spiny dogfish (*Squalus acanthias*; Veríssimo et al. 2010), Starspotted dogfish (*Mustelus manazo*; Chen et al. 2001), Blacknose shark (*Carcharhinus acronotus*; Portnoy et al. 2014), and Spot-tail shark (*Carcharhinus sorrah*; Giles et al. 2014).

Among sharks, the population structure of the California horn shark is exceptional. In some respects, the population structure of *H. francisci* may be more similar to that of terrestrial occupants of the Channel Islands. Eggert et al. (2004) found that the loggerhead shrike *Lanius ludovicianus* (a songbird) is divided into two lineages in the South Channel Islands and one lineage in the North Channel Islands that is closely affiliated with nearby mainland populations. California Channel Island foxes (*Urocyon littoralis*) are even more isolated, as might be expected in a truly terrestrial vertebrate (Gilbert et al. 1990). Where the Channel Island sharks differ from their terrestrial counterparts is in genetic diversity, which was low in some horn shark sample locations but extremely low in the endemic shrike and fox. Bowen et al. (2020) suggested that when marine animals lack a pelagic larval stage, their population structure might resemble that of terrestrial species, and that appears to be the case for the horn shark.

Conservation Implications

At least one recent study has indicated that *H. francisci* may be vulnerable to overexploitation in Mexican waters (Furlong-Estrada et al. 2017). The species is listed by the IUCN as Data Deficient, and the current assessment specifically notes a lack of information pertaining to metapopulation structure (Carlisle 2015). Our study is the first to evaluate the population genetic structure of this species across its range, and demonstrates that deep-water channels may act as a barrier to dispersal in benthic elasmobranchs over scales much smaller than previously reported. Thus, wildlife managers should ensure adequate protection of distinct

stocks which likely have independent demographic trajectories. More generally, these results highlight the need for further study of population genetic structure in shallow, benthic elasmobranchs, which are underrepresented in the population genetic literature (Domingues et al. 2018).

Outstanding Questions and Future Directions

While it is clear that California horn shark populations are structured across their range, key questions remain. For example, the marker used in our study – the mitochondrial control region – is a maternally inherited marker and can only be used to infer the degree of female-mediated gene flow among populations. Female reproductive philopatry is a frequently reported phenomenon in sharks, including the congeneric Port Jackson shark, *Heterodontus portusjacksoni* (Hueter et al. 2005; Dudgeon et al. 2012; Day et al. 2019). Therefore, we cannot rule out the possibility that female reproductive philopatry drives the patterns of population structure observed in this study. Secondly, a key interpretation of our research is that deep-water channels separating the Channel Islands from the California mainland act as a barrier to dispersal for *H. francisci*. The apparent lack of genetic structure among the three Channel Islands in our study challenges this conclusion. It is possible that this is due to the prevalence of haplotype H2 at all three island sites, which may obscure a signal of population structure among the islands. Finally, low sample sizes at Isla Guadalupe (n = 8) and Las Animas (n = 12) limit our power to detect population structure with a single mitochondrial marker.

Single marker mtDNA studies continue to provide useful insights into marine population structure (Bowen et al. 2014). However, the questions and limitations highlighted above could potentially be resolved with the use of next-generation sequencing techniques such as restriction site-associated DNA sequencing (RADseq). RADseq methods can provide thousands of markers in the form of single nucleotide polymorphisms (SNPs), resulting in greater power to detect population structure on fine scales with sample sizes much smaller than those necessary for single-marker population genetics (Miller et al. 2007; Baird et al. 2008; Puritz et al. 2014; Li et al. 2020).

Conclusion

The California horn shark displays strong population genetic structure over remarkably small spatial scales. We have implicated the deep-water channel between the California mainland and the Channel Islands as a potential barrier to dispersal in this small, demersal elasmobranch, and suggest that this may be a common pattern for other demersal elasmobranchs in the region, including the Pacific angel shark (*S. californica*) and the swell shark (*C. ventriosum*). We also detected a significant genetic break corresponding to Punta Eugenia, a well-known biogeographic barrier in coastal marine fauna. Further discoveries are likely in this sedentary shark with high population structure across distances demonstrably shorter than a human (and possibly a fox) can swim.

Table 3.1. Genetic diversity indices for *Heterodontus francisci* for each sampling locality and for all individuals pooled.

Sample Site	*n*	S	H	*h* ± SD	π ± SD
SCI	26	5	5	0.600 ± 0.098	0.00283 ± 0.00042
ANA	25	5	3	0.227 ± 0.106	0.00114 ± 0.00054
CAT	29	6	5	0.616 ± 0.083	0.00259 ± 0.00053
SB	17	5	6	0.757 ± 0.091	0.00278 ± 0.00050
MAL	28	5	6	0.817 ± 0.035	0.00327 ± 0.00022
PV	30	5	7	0.816 ± 0.041	0.00303 ± 0.00032
LAG	28	5	6	0.712 ± 0.074	0.00271 ± 0.00040
SD	28	5	7	0.794 ± 0.055	0.00262 ± 0.00040
BT	30	5	7	0.586 ± 0.098	0.00157 ± 0.00033
LSI	30	7	5	0.584 ± 0.066	0.00255 ± 0.00036
BM	24	5	6	0.801 ± 0.044	0.00271 ± 0.00022
LV	3	3	3	1.000 ± 0.272	0.00276 ± 0.00097
LA	12	8	7	0.894 ± 0.063	0.00306 ± 0.00049
GI	8	3	2	0.250 ± 0.180	0.00104 ± 0.00075
Total	318	12	20	0.811 ± 0.011	0.00334 ± 0.00007

n = number of individuals, S = polymorphic sites, H = number of haplotypes, *h* = haplotype diversity, π = nucleotide diversity, SD = standard deviation; Site Abbreviations: **ANA** = Anacapa Island, **SCI** = Santa Cruz Island, **CAT** = Santa Catalina Island, **SB** = Santa Barbara, **MAL** = Malibu, **PV** = Palos Verdes, **LAG** = Laguna, **SD** = San Diego, **GI** = Isla Guadalupe, **BT** = Bahia Tortugas, **LSI** = Laguna San Ignacio, **BM** = Bahia Magdalena, **LV** = La Ventana, **LA** = Las Animas

Table 3.2. Pairwise Φ_{ST} values (below diagonal) and FDR-corrected *P* values (above diagonal) based on the partial mitochondrial control region (mtCR) of *Heterodontus francisci*. Significant values ($P < 0.05$) are bolded. Location abbreviations are defined in Table 3.1.

Sample Site	SCI	ANA	CAT	SB	MAL	PV	LAG	SD	BT	LSI	BM	LA	GI
SCI	-	0.0684	0.6559	**0.0031**	**0.0253**	**0.0024**	**0.0003**	**0.0003**	**<0.0001**	**<0.0001**	**0.0003**	**0.0024**	**0.0003**
ANA	0.095	-	0.1367	**<0.0001**	**<0.0001**	**<0.0001**	**<0.0001**	**<0.0001**	**<0.0001**	**<0.0001**	**<0.0001**	**<0.0001**	**<0.0001**
CAT	-0.019	0.051	-	**0.0009**	**0.0076**	**0.0003**	**<0.0001**	**<0.0001**	**<0.0001**	**<0.0001**	**<0.0001**	**0.0003**	**0.0003**
SB	**0.295**	**0.601**	**0.366**	-	0.2496	0.6729	0.7511	0.7809	0.0752	**0.0051**	**0.0308**	0.2305	0.2470
MAL	**0.131**	**0.407**	**0.193**	0.022	-	0.5991	0.2293	0.1991	**0.0024**	**0.0125**	0.0707	0.2156	**0.0427**
PV	**0.225**	**0.502**	**0.294**	-0.023	-0.013	-	0.8430	0.7511	**0.0228**	**0.0054**	**0.0498**	0.2591	0.1113
LAG	**0.303**	**0.578**	**0.370**	-0.029	0.022	-0.026	-	1.0000	0.1008	**0.0024**	**0.0326**	0.2305	0.1991
SD	**0.321**	**0.595**	**0.387**	-0.031	0.030	-0.021	-0.036	-	0.1351	**0.0012**	**0.0308**	0.2470	0.2257
BT	**0.519**	**0.754**	**0.573**	0.073	**0.191**	**0.102**	0.051	0.038	-	**0.0003**	**0.0017**	**0.0407**	0.5575
LSI	**0.337**	**0.589**	**0.403**	**0.183**	**0.122**	**0.141**	**0.169**	**0.169**	**0.266**	-	0.5059	0.2141	**0.0039**
BM	**0.306**	**0.579**	**0.371**	**0.118**	0.066	**0.073**	**0.093**	**0.094**	**0.198**	-0.008	-	0.2470	**0.0132**
LA	**0.311**	**0.624**	**0.390**	0.035	0.039	0.021	0.029	0.027	**0.119**	0.045	0.027	-	0.0832
GI	**0.520**	**0.810**	**0.579**	0.048	**0.206**	0.113	0.063	0.051	-0.010	**0.343**	**0.277**	0.172	-

Table 3.3. Mantel test results (with FDR-corrected *P* values) for the mtCR of *Heterodontus francisci*, with sequential exclusion of island sites (No Islands) and Las Animas (Pacific Coast).

Populations	**Mantel's r_m**	***P***
All Populations	0.053	0.356
No Islands	0.315	0.137
Pacific Coast	0.541	0.058

Table 3.4. IMa3 parameter estimates for four population pairs of *Heterodontus francisci*. Estimates of migration are given forward in time (i.e., $m_{1>2}$ denotes the rate at which population 2 receives immigrants from population 1). 95% Highest Posterior Densities (HPD) are reported in parentheses where appropriate, but are not reported in cases where the right tail of the posterior distribution never reached a probability of zero (*) or when the 95% HPD interval included values of zero for θ, *m*, or *Nm* (**). Population abbreviations are defined in Figure 3.3.

Populations	**θ_1**	**θ_2**	**θ_A**	***$m_{1>2}$***	***$m_{2>1}$***	***$Nm_{1>2}$***	***$Nm_{2>1}$***	***t_0***
NCI-MLCA	1.18 (0.17 - 5.26)	3.74 (0.95 - 11.70)	7.88*	1.27**	2.22**	1.34**	1.21**	0.093*
CAT-MLCA	1.64 (0.21 - 8.64)	4.26 (1.08 - 14.57)	7.63*	2.27**	0.70**	2.53**	0.64**	0.117*
CAT-NCI	2.67*	2.41*	6.48*	0.50**	0.02**	1.27**	0.55**	0.041*
BT-LSIBM	3.16*	5.12*	7.54*	0.54**	1.60**	1.40**	2.34**	0.139*

$\theta = 4N_e\mu$ for population 1 (θ_1), population 2 (θ_2), and the hypothetical ancestral population for both (θ_A); *m* = the per gene, per generation migration rate; *Nm* = the effective number of migrants per generation; t_0 = time since population divergence scaled by the mutation rate ($t\mu$, where *t* is the time since splitting in years). For each pair of populations, population 1 is listed first

Table 3.5. IMa3 parameter estimates converted to demographic values. Lower values of each range were calculated using a mutation rate of 4.37×10^{-6} mutations per locus per year, and larger values were calculated using a mutation rate of 1.56×10^{-6} mutations per locus per year.

Populations	N_e1	N_e2	N_eA	t (Years)
NCI-MLCA	6,751 - 18,910	21,396 - 59,936	43,650 - 122,276	21,281 - 59,615
CAT-MLCA	9,382 - 26,282	24,371 - 68,269	45,080 - 126,282	26,773 - 75,000
CAT-NCI	15,275 - 42,788	13,787 - 38,622	37,071 - 103,846	9,382 - 26,282
BT-LSIBM	18,078 - 50,641	29,291 - 82,051	43,135 - 120,833	31,808 - 89,103

N_e represents the effective population size for population 1 (N_e1), population 2 (N_e2), and the hypothetical ancestral population for both (N_eA); t is the time since population divergence. For each pair of populations, population 1 is listed first

Table S3.1. Position (in base pairs) of polymorphic sites from a 724 base pair fragment of the mitochondrial control region (mtCR) of *Heterodontus francisci* and the distribution of haplotypes per sampling location. Letters represent nucleotides and points represent no change relative to the reference haplotype (H1). Location abbreviations are defined in Table 3.1 of the main text.

	Polymorphic Sites (1-724)												**Haplotype Counts by Sampling Site**												
Hap	012	016	037	089	189	489	490	611	614	669	687	696	SCI	ANA	CAT	SB	MAL	PV	LAG	SD	GI	BT	LSI	BM	LV	LA
H1	C	A	A	T	T	T	C	C	G	T	C	C	2	-	5	8	8	10	14	11	7	19	1	4	1	3
H2	.	.	.	.	C	.	T	T	.	C	.	T	16	22	17	2	7	6	4	3	-	-	-	-	-	-
H3	.	.	.	.	.	.	.	.	.	C	.	.	4	2	1	2	6	6	2	6	-	4	17	8	1	3
H4	.	.	.	.	.	C	T	T	.	C	.	.	-	-	-	-	-	-	-	-	-	1	10	6	-	-
H5	.	.	.	.	.	.	T	.	.	C	.	.	-	-	-	-	2	2	5	1	-	3	-	-	-	-
H6	.	.	.	.	.	.	T	T	.	.	.	.	3	1	-	3	2	3	2	2	-	-	-	-	-	-
H7	.	.	.	.	.	.	T	T	.	C	.	T	-	-	5	1	3	1	1	2	-	-	-	-	-	-
H8	.	.	.	.	.	.	T	.	.	.	.	.	-	-	-	-	-	2	-	3	-	-	-	-	-	-
H9	.	.	.	.	.	.	T	.	.	C	.	T	-	-	-	-	-	-	-	-	-	1	-	4	1	-
H10	.	.	.	.	.	.	T	T	.	C	.	.	1	-	-	-	-	-	-	-	1	1	-	1	-	2
H11	.	.	.	.	C	.	T	T	A	C	.	T	-	-	1	-	-	-	-	-	-	-	-	-	-	-
H12	.	.	.	.	.	.	.	T	.	C	.	.	-	-	-	1	-	-	-	-	-	-	-	-	-	-
H13	.	.	.	.	.	C	.	.	.	C	.	.	-	-	-	-	-	-	-	-	-	1	-	-	-	-
H14	.	.	.	.	.	.	T	T	.	C	T	T	-	-	-	-	-	-	-	-	-	-	1	-	-	-
H15	.	.	.	.	C	.	T	T	.	C	T	T	-	-	-	-	-	-	-	-	-	-	1	-	-	-
H16	.	.	.	.	.	C	T	.	.	C	.	.	-	-	-	-	-	-	-	-	-	-	-	1	-	-
H17	.	G	.	.	.	.	T	T	.	C	.	.	-	-	-	-	-	-	-	-	-	-	-	-	-	1
H18	.	.	.	.	C	.	.	.	.	C	.	.	-	-	-	-	-	-	-	-	-	-	-	-	-	1
H19	T	.	.	.	.	.	T	T	.	C	.	.	-	-	-	-	-	-	-	-	-	-	-	-	-	1
H20	.	.	G	C	.	.	.	.	.	C	.	.	-	-	-	-	-	-	-	-	-	-	-	-	-	1
										Total Count			**26**	**25**	**29**	**17**	**28**	**30**	**28**	**28**	**8**	**30**	**30**	**24**	**3**	**12**

Table S3.2. Mismatch distribution analysis parameters and neutrality test results for *Heterodontus francisci.*

Sample Site	Sudden-expansion model						Spatial-expansion model				Neutrality tests			
	θ_0	θ_1	SSD	*P* (SSD)	*r*	*P* (*r*)	SSD	*P* (SSD)	*r*	*P* (*r*)	Fu's F_s	*P* F_s	R_2	*P* R_2
ANA	*NC*	*NC*	*NC*	*NC*	*NC*	*NC*	0.013	0.356	0.630	0.844	0.989	0.508	0.084	0.126
SCI	0.002	2.720	0.068	0.158	0.168	0.253	0.010	0.784	0.168	0.791	1.175	0.489	0.205	0.069
CAT	0.000	1.675	0.058	0.390	0.138	0.487	0.044	0.312	0.138	0.714	1.067	0.524	0.153	0.465
SB	0.037	3.962	0.018	0.516	0.073	0.514	0.014	0.643	0.073	0.687	-0.550	0.743	0.202	0.196
MAL	0.000	4.990	0.009	0.631	0.032	0.838	0.013	0.469	0.032	0.887	0.811	0.624	**0.237**	**0.005**
PV	0.204	4.250	0.009	0.653	0.031	0.849	0.008	0.404	0.031	0.768	-0.159	0.997	**0.219**	**0.025**
LAG	0.032	3.064	0.039	0.294	0.146	0.240	0.030	0.431	0.146	0.498	0.233	0.854	0.196	0.104
SD	*NC*	*NC*	*NC*	*NC*	*NC*	*NC*	0.010	0.397	0.051	0.509	-0.735	0.719	0.189	0.147
BT	0.002	1.589	0.003	0.865	0.052	0.797	0.000	0.910	0.052	0.895	-2.290	0.139	0.113	0.730
LSI	0.000	2.392	**0.158**	**0.029**	**0.425**	**0.036**	0.097	0.179	0.425	0.337	1.069	0.523	0.127	0.878
BM	0.000	8.350	0.032	0.071	0.099	0.168	0.026	0.215	0.099	0.386	-0.011	0.947	0.196	0.136
LA	0.004	30.937	0.01	0.373	0.057	0.365	0.010	0.364	0.057	0.396	-2.245	0.111	0.118	0.116
GI	*NC*	*NC*	*NC*	*NC*	*NC*	*NC*	0.040	0.258	0.688	0.875	1.415	0.283	**0.331**	**<0.001**
Total	0.000	5.100	0.010	0.505	0.025	0.745	0.011	0.542	0.025	0.875	-4.255	0.244	0.100	0.410

Significant test values ($P < 0.05$) are bolded

NC denotes non-convergence after 2,000 steps

θ_0 = theta at time 0; θ_1 = theta at present time; SSD = sum of square deviations; *P* (SSD) = *P* value of SSD; *r* = Harpending's raggedness index; *P* (*r*) = *P* value of *r*; *P* F_s = *P* value of F_s; *P* R_2 = *P* value of R_2

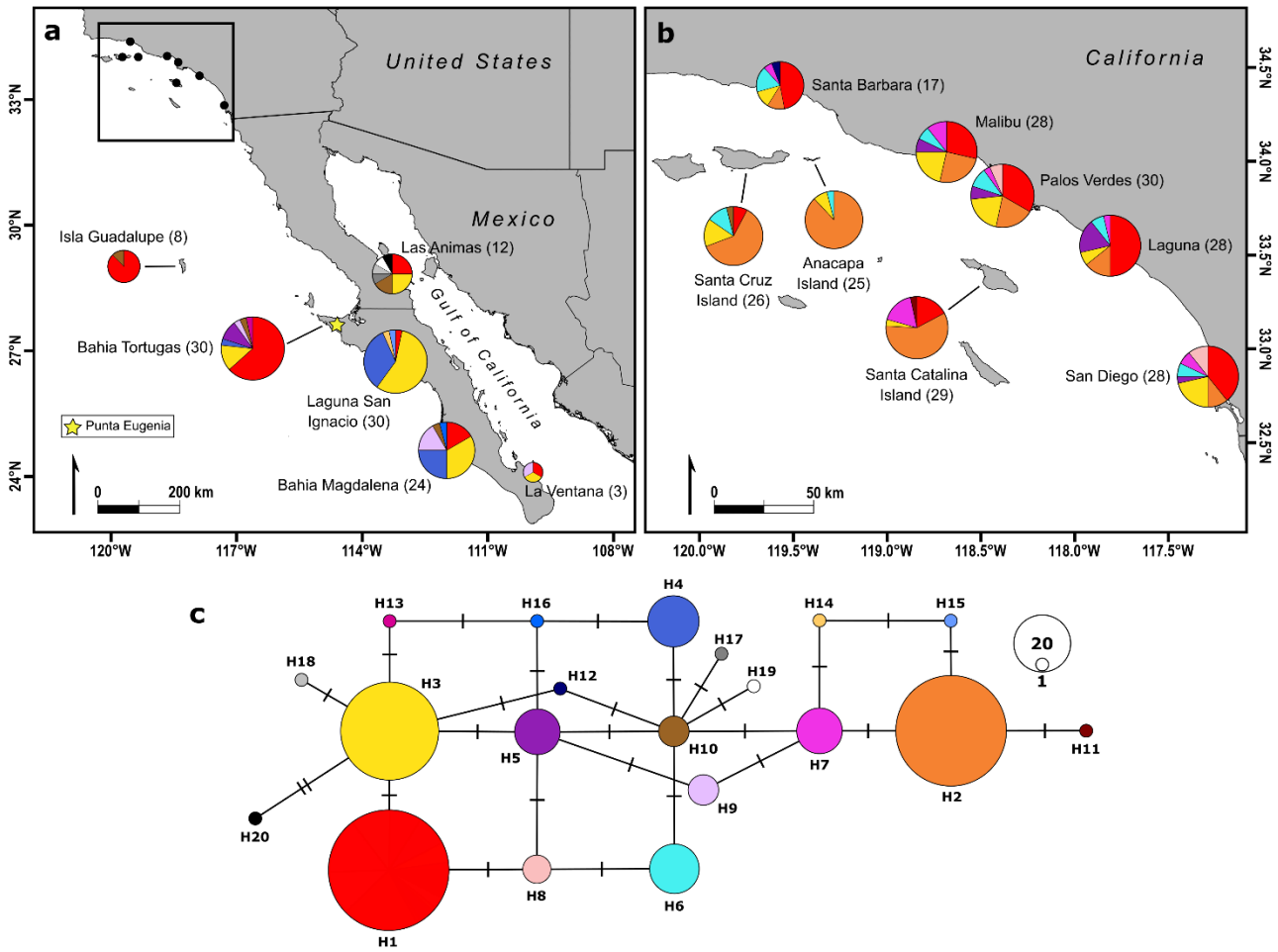

Figure 3.1. (**a**,**b**) Geographic distribution of haplotypes for the mtCR of *Heterodontus francisci*. Circle size is proportional to sample size; colors represent individual haplotypes. Sample sizes for each site are indicated in parentheses. (**a**) A large-scale view of sampling locations along the Baja California peninsula (along with Isla Guadalupe). (**b**) Expanded view of the inset box in (**a**) showing sampling locations along the California mainland and the California Channel Islands. (**c**) Median-joining haplotype network for the mitochondrial control region (mtCR) of *H. francisci*. Circles represent observed haplotypes (H = 20), and circle size is proportional to overall haplotype frequency. Tick marks represent the number of mutational steps between haplotypes. Colors correspond with those in (**a**) and (**b**).

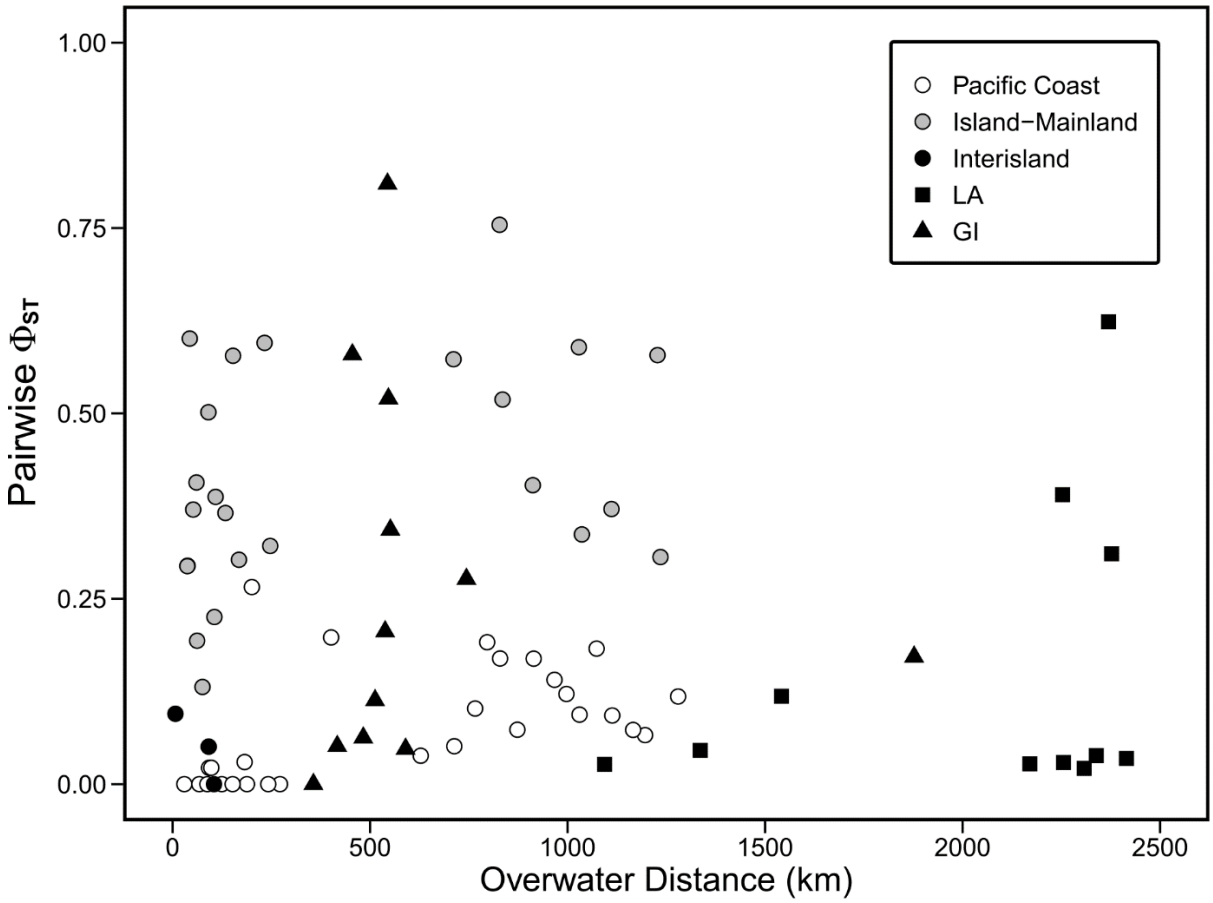

Figure 3.2. A plot of pairwise genetic distance (Φ_{ST}) vs overwater distance (km) among sampling sites for *Heterodontus francisci*. Symbols represent the type of pairwise comparison: between mainland sites along the Pacific Coast (open circles), between the California Channel Islands and mainland sites along the Pacific Coast (gray circles), between the three California Channel Islands (black circles), all pairwise comparisons involving Las Animas (black squares), and all pairwise comparisons involving Isla Guadalupe (black triangles).

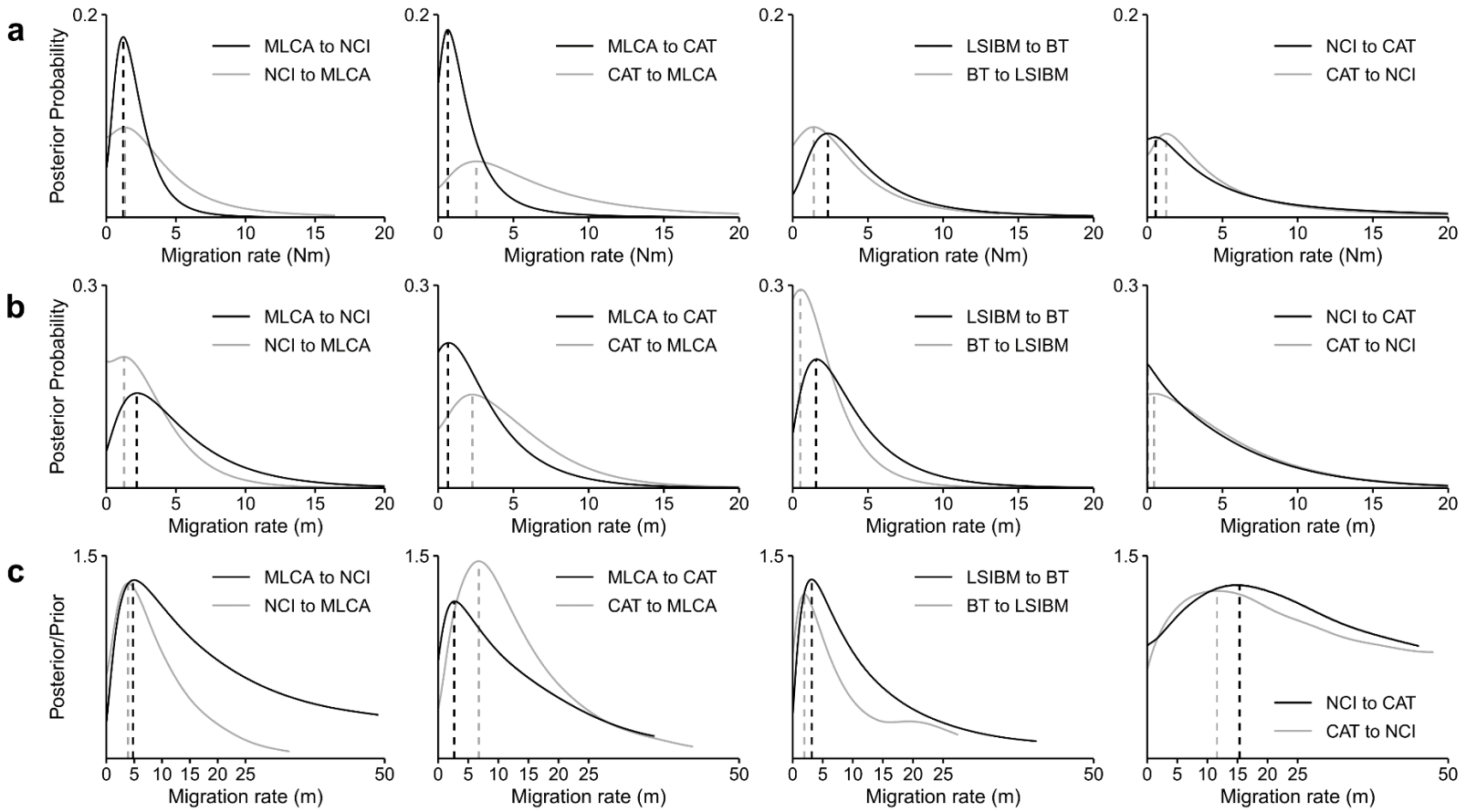

Figure 3.3. IMa3 results for four population pairs of *Heterodontus francisci* spanning putative biogeographic barriers. Solid lines represent posterior distributions (or the posterior divided by the prior distribution, as in row **c**), while dashed vertical lines indicate peak locations for each curve. Curves are color-coded by the direction of migrant exchange forward in time (black or gray). Note that scales on x and y axes vary by row. (**a**) Posterior probability curves for estimates of the effective number of migrants per generation (*Nm*). (**b**) Posterior probability curves for estimates of the per locus mutation scaled migration rate (*m*). (**c**) The posterior distribution divided by the prior distribution (Posterior/Prior) for estimates of the per locus mutation scaled migration rate (*m*). **MLCA** = Mainland California, **NCI** = Northern Channel Islands, **CAT** = Santa Catalina Island, **BT** = Bahia Tortugas, **LSIBM** = Laguna San Ignacio and Bahia Magdalena (combined).

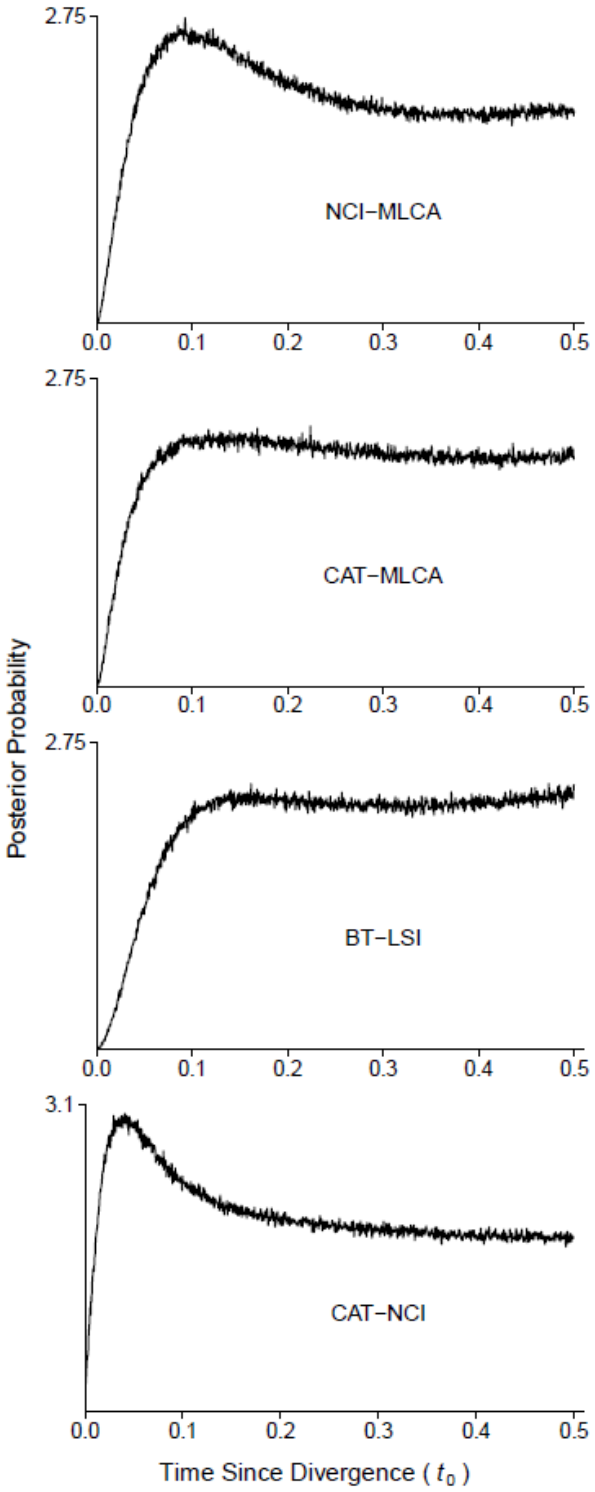

Figure S3.1. *Heterodontus francisci* posterior probability distributions of divergence time (t_0) for each pair of populations analyzed in IMa3. Divergence time (t_0) is not represented in demographic units (i.e., years), but rather as the product of time since divergence (in years) and the per locus mutation rate (μ). Population abbreviations are defined in Figure 3.3.

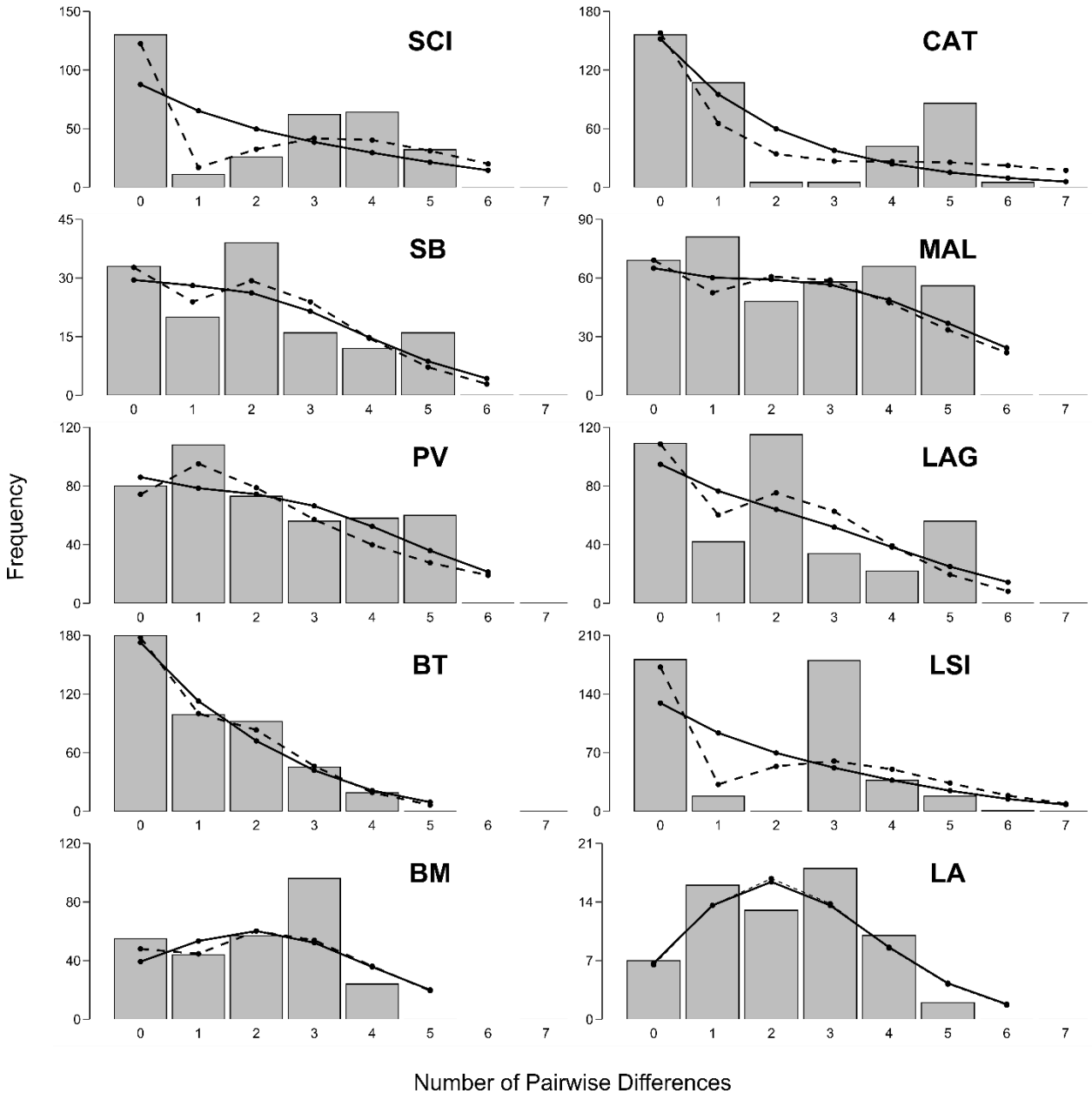

Figure S3.2. Mismatch distributions for the mtCR of *Heterodontus francisci*. Gray bars represent observed mismatch distributions, solid lines represent the expected distribution under a model of sudden demographic expansion, and dashed lines represent the expected distribution under a model of spatial expansion. Location abbreviations are defined in Table 3.1.

CHAPTER 4. NEXT-GENERATION SEQUENCING (DDRADSEQ) RESOLVES FINE-SCALE PATTERNS OF POPULATION STRUCTURE IN THE CALIFORNIA HORN SHARK (*HETERODONTUS FRANCISCI*)

ABSTRACT

The California horn shark (*Heterodontus francisci*) is a small, demersal species occupying shallow coastal habitat from southern California to the Gulf of California, Mexico. Previous research using the mitochondrial control region (mtCR) of *H. francisci* revealed strong matrilineal population structure across the species range, including a genetic break between the California coast and the nearby Channel Islands, indicating that deep-water channels may limit dispersal across extremely small scales (< 25 km). However, analyses failed to detect population structure between the Northern and Southern Channel Islands, separated by nearly 100 km of deep water. Furthermore, mitochondrial population structure may result from female reproductive philopatry and male-mediated dispersal (common in sharks). To address these issues, we used double-digest RADseq (ddRADseq) to analyze 9,063 neutral SNP loci from 173 specimens from across the range of *H. francisci*. Our results confirm that significant population structure exists among island and mainland populations separated by a minimum distance of 19 km ($F_{ST} \geq 0.023$), and resolved the Northern and Southern Channel Islands as distinct population units ($F_{ST} = 0.041$). Clustering analyses identified horn sharks in the Gulf of California as genetically distinct from their Pacific coast counterparts, but sampling gaps and a weak (but significant) pattern of isolation-by-distance among mainland populations preclude firm conclusions about the nature of this separation. Overall, our results support the role of deep-water channels as strong drivers of population structure in *H. francisci* across remarkably small spatial scales, and indicate genetic cohesiveness across more than 1,500 km of continental coastline.

INTRODUCTION

Sharks (superorder Selachimorpha) display a wide range of dispersal capabilities. Highly migratory species such as the Blue shark (*Prionace glauca*) and the Great white shark (*Carcharodon carcharias*) can undertake migrations that span ocean basins, while coastal species such as the Nurse shark (*Ginglymostoma cirratum*) and the Bonnethead shark (*Sphyrna*

tiburo) may exhibit strong site-fidelity or undertake comparatively short migrations limited to coastal margins (Bonfil et al. 2005; Heupel et al. 2006; Vandeperre et al. 2014; Pratt et al. 2018). The spatial scale of population genetic structure among shark taxa is similarly variable, with some oceanic species showing little to no structure on a global scale (e.g., Hoelzel et al. 2006; Veríssimo et al. 2017), and coastal bottom-dwellers displaying population genetic structure over distances smaller than 150 km (e.g., Gaida 1997).

The sharks of the genus *Heterodontus* (family Heterodontidae) consist of nine species distributed tropically and subtropically along the margins of the Pacific Ocean (absent in the Central Pacific), the Indo-Pacific, and the Western Indian Ocean. These small sharks are exclusively benthic, rarely venturing more than two meters above the substrate; are confined to near-shore, shallow-water environments; and are often strongly associated with complex benthic habitats, such as kelp beds and rocky reef (Compagno et al. 2005). These sharks lay distinct, auger-shaped eggs that sink and become wedged into the substrate (or attached via string-like tendrils in some species). This combination of traits indicates that dispersal may be limited across stretches of deep, open ocean separating shallow coastal environments. Indeed, this pattern has been observed in population genetic studies of other small coastal shark species such as the Spot-tail shark (*Carcharhinus sorrah*; Giles et al. 2014), the Small-spotted catshark (*Scyliorhinus canicula*; Gubili et al. 2014; Kousteni et al. 2015), and the Brown banded bamboo shark (*Chiloscyllium punctatum*; Lim et al. 2021).

The California horn shark (*Heterodontus francisci*) inhabits shallow coastal waters from Point Conception in California, around the peninsula of Baja California, and into the Gulf of California, Mexico (Love 1996; Compagno 2002). The species occurs at adjacent nearshore islands, such as the California Channel Islands, but can also be found at Isla Guadalupe, a small volcanic island located approximately 250 kilometers west of the Baja peninsula. In a previous study (Chapter 3 of this dissertation), we examined population genetic structure across the range of *H. francisci* using the mitochondrial control region (mtCR) and found strong population structure and low rates of migration between the populations of the California mainland and the California Channel Islands, separated by as little as 19 km of open ocean. In addition, we found a population genetic break among mainland populations corresponding to Punta Eugenia on the Pacific coast of the Baja peninsula, a known biogeographic barrier (Bernardi et al. 2003; Briggs and Bowen 2012). This study demonstrated genetic isolation on an unprecedented scale for

sharks, shorter than an athletic human can swim, yet key questions remained unresolved. First, since mitochondrial markers are maternally inherited, it remained unclear whether the observed population genetic structure could be the result of female reproductive philopatry. This is a common phenomenon in sharks, including the congeneric Port Jackson shark, *H. portusjacksoni* (Hueter et al. 2005; Dudgeon et al. 2012; Day et al. 2019). Secondly, a lack of detectable population structure between the northern Channel Islands (Anacapa Island and Santa Cruz Island) and Santa Catalina Island to the south – due in large part to the shared prevalence of a single mitochondrial haplotype – challenged the conclusion that the deep, cold waters separating the Channel Islands from the California mainland are the primary drivers of divergence. Finally, small sample sizes at two key sites (Isla Guadalupe and Las Animas, Baja California, Mexico) limited our power to detect population structure with a single mitochondrial marker.

In the present study, we explored patterns of population genetic structure in *H. francisci* by using next-generation sequencing (NGS) based on double-digest restriction site-associated DNA (ddRAD) libraries (Peterson et al. 2012). While traditional DNA sequencing methods necessarily limit studies to a small number of genetic loci, NGS technologies have made it feasible to produce datasets with orders of magnitude more loci in non-model organisms. Reduced representation approaches such as ddRAD allow researchers to cast a wide net over the genomes of study organisms, dramatically increasing the power to detect signatures of selection, adaptation, and subtle population genetic structure arising from neutral evolutionary processes (Allendorf et al. 2010; Funk et al. 2012; Narum et al. 2013).

The California horn shark is subject to artisanal fisheries and may be vulnerable to overexploitation in Mexican waters (Furlong-Estrada et al. 2017). Furthermore, the IUCN lists this species as 'data deficient,' a common status for small sharks with restricted distributions (Carlisle 2015). In these circumstances ddRAD data can serve the dual purposes of revealing dispersal behavior in an extremely sedentary shark, as well as documenting the isolated management units that may include small, single-island populations.

MATERIALS AND METHODS

Sample Collection and DNA Extraction

Tissue samples (N = 177) from California horn sharks (*H. francisci*) were obtained from 12 locations throughout their range, from Malibu, CA to Las Animas, Baja California, Mexico

between 2005 and 2019 (Figure 4.1). Tissue specimens consisted of either fin clips or muscle tissue plugs, and were preserved in either 70% ethanol, 20% salt-saturated DMSO, or RNAlater (Sigma Aldrich, St. Louis, MO, USA). When possible, tissues were immediately stored at -20°C. Total genomic DNA was extracted from tissues using the E.Z.N.A. Tissue DNA Kit (Omega Bio-Tek, Norcross, GA, USA) with minor adjustments to the manufacturer's protocol. Extracted DNA was visually inspected for quality via agarose gel electrophoresis, then quantified using the AccuClear® Ultra High Sensitivity dsDNA Quantitation Kit (Biotium, Fremont, CA, USA) and measured with a SpectraMax M2 microplate reader (Molecular Devices, San Jose, CA, USA).

ddRADseq Library Preparation and Sequencing

Double-digest RADseq (ddRADseq) libraries were prepared following the protocol described by Peterson et al. (2012) with minor modifications. Up to 1,000 ng of genomic DNA from each specimen was digested with the restriction enzymes BamHI and PstI in a single reaction with the manufacturer's recommended buffer (Thermo Fisher Scientific, Waltham, MA, USA) for 4-8 hours at 37°C. This restriction enzyme pair was selected based on the results of *in silico* digests of the draft whale shark (*Rhincodon typus*) genome published by Read et al. (2017), which were performed using the package SimRAD v0.95 (Lepais and Weir 2014) implemented in R v3.1 (R Core Team 2015). Following digestion of genomic DNA, barcoded adapters were ligated to restriction fragments. Libraries were then pooled in equimolar amounts and purified with PCRCLEAN DX™ magnetic beads (Aline Biosciences, Woburn, MA, USA) before size-selection on a Pippin Prep DNA Size Selection System (Sage Science, Beverley, MA, USA), targeting fragments between 325 and 395 bp. Amplification was carried out on each library using Kapa HiFi DNA Polymerase (Sigma-Aldrich, St. Louis, MO, USA) and primers to append indexed Illumina adapters. Amplified libraries were purified using magnetic beads and eluted in HPLC water, and then re-quantified before being pooled into a final sequencing library.

Libraries were prepared according to the above protocol in three batches: Batch 1 (June 2017; n = 69 individuals), Batch 2 (March 2020; n = 54), and Batch 3 (July 2020; n = 55). Batch 1 was sequenced on a single lane on the Illumina HiSeq 4000 sequencing platform (150-bp paired-end reads) at the QB3 Vincent J. Coates Genomics Sequencing Laboratory at UC Berkeley; Batch 2 and Batch 3 were sequenced on separate lanes on the Illumina HiSeq 4000 sequencing platform (100-bp single-end reads) at the Genomics and Cell Characterization Core

Facility (GC3F) at the University of Oregon. When possible, individuals from a single sampling location were split across two or more sequencing runs.

Data Processing, Locus Assembly, and Genotyping

The quality of raw Illumina sequencing reads was assessed using the program FastQC v0.11.5 (Andrews 2017). The program Kraken v2.0.9 (Wood and Salzberg 2014; Wood et al. 2019) was used to identify and remove reads matching bacterial and viral sequences in the 'MiniKraken2_v1' database. Sequences were then trimmed, filtered, and demultiplexed using the '*process_radtags*' command in the program STACKS v2.42 (Catchen et al. 2011; Rochette et al. 2019). Sequences were trimmed to 95 base pairs (-*t* 95) and demultiplexed into individual sharks based on a unique 6-bp barcode sequence (--*inline_null*). Quality filtering consisted of detecting and removing reads with adapter sequence, removing any sequences with an uncalled base (-*c* option), removing sequences with >1 mismatch in either the restriction enzyme site or the 6-bp barcode (sequences with a single mismatch were corrected using the -*r* option), and removing sequences with an average Phred33 quality score below 20 within a sliding window of 15% of the read length (-*s* 20, -*w* 0.15, -*q*).

Loci were assembled and individuals were genotyped using the '*denovo_map.pl'* pipeline implemented in STACKS. Parameters of the pipeline were optimized for *de novo* assembly in *H. francisci* using the method outlined in Paris et al. (2017). The optimized parameters were as follows: a minimum of five identical sequences were required to form a stack (-*m* 5), a maximum of one mismatch was allowed between stacks within individuals (-*M* 1), and a maximum of one mismatch was allowed between sample loci when building the catalog (-*n* 1). Stacks with a number of reads more than three standard deviations above the mean were excluded from the final dataset, as these are assumed to represent repetitive elements. Genotypes were determined using a Bayesian genotype caller implemented in STACKS, which is described in Rochette et al. (2019).

SNP Filtering

Using the '*populations'* command in STACKS, loci were filtered so that the final dataset consisted only of loci that were present in all 12 populations (-*p* 12), were present in at least 75% of individuals within each population (-*r* 0.75), had an observed heterozygosity lower than 0.6 (--

max-obs-het 0.6), and had a minimum minor allele count of 3 (ensuring that the minor allele was present in two or more individuals; --*min-mac* 3). An output VCF file was generated with the '--*write_single_snp'* option, which outputs only the first SNP of each locus. Individuals with fewer than 250,000 reads or missing more than 30% of loci were removed from the dataset using VCFtools v0.1.17 (Danecek et al. 2011). Based on these criteria two individuals were removed from the final dataset, resulting in a final sample size of 175 individuals.

To detect paralogous sequence variants (PSVs), the SNP dataset was analyzed using HDplot (McKinney et al. 2017) implemented in R v4.0.2 (R Core Team 2020). HDplot identifies potential PSVs by looking for loci that (*i*) greatly exceed levels of heterozygosity expected in non-PSV loci (this is the same rationale behind using the '--*max-obs-het*' filter in STACKS) and (*ii*) deviate significantly from the approximate 1:1 read-depth ratio expected within heterozygous individuals. Loci were regarded as PSVs and excluded from further analysis if $|z| \geq 5$. Loci in linkage disequilibrium (LD) were detected using the program PLINK v2.0 (Purcell et al. 2007; Chang et al. 2015). Pairs of loci with an $r^2 > 0.8$ were identified, and the locus with the lower minor allele frequency was excluded from further analysis. Lastly, the program BayeScan v2.1 (Foll and Gaggiotti 2008; Foll et al. 2010; Fischer et al. 2011) was used to detect loci under selection with the following settings: prior odds of 100 (-*pr_odds* 100), 10 pilot runs with 5,000 iterations (-*nbp* 10 -*pilot* 5000), a burn-in period of 50,000 generations (-*burn* 50000), and 50,000 iterations with a thinning interval of 10 (-*n* 50000 -*thin* 10). SNPs with a q-value < 0.05 were considered statistically significant – and therefore likely under selection – and were separated from the final neutral SNP dataset. Consensus sequences of loci under presumed selection were obtained and subjected to an NCBI Nucleotide BLAST search. When necessary, conversions from VCF to other input file formats were performed using PGDSpider v2.1.1.5 (Lischer and Excoffier 2012) or using the *vcf_to_depth.py* Python script provided by McKinney et al. (2017). A total of 589 SNPs (572 flagged as PSVs and/or under LD, 17 under putative selection) were removed from the final SNP dataset.

To check for the presence of mitochondrial sequences in the final dataset, loci that passed filtering were added to a whitelist, and a fasta file of full consensus sequences was produced with the '*populations*' command in STACKS using the '--*fasta-loci*' option. Consensus sequences were then mapped to the full mitochondrial genome of *H. francisci* (GenBank Accession Number AJ310141; Arnason et al. 2001) in GENEIOUS v6.1.8 (Biomatters Ltd, Auckland, NZ)

using default parameters. None of the loci that passed filtering were successfully mapped to the mitochondrial genome of *H. francisci*, indicating that only nuclear loci were included in the final SNP dataset. Examination of the mitochondrial genome of *H. francisci* in GENEIOUS revealed the presence of a single cut-site for the enzyme BamHI near the origin of replication, and none for the enzyme PstI.

Population Genomic Analysis

Genetic diversity metrics (observed heterozygosity H_O, expected heterozygosity H_E, inbreeding coefficient F_{IS}, and allelic richness A_R) and the average number of individuals per locus (here denoted N_{perloc}) were calculated for the total set of samples, individual sampling locations, and putative populations using the '*basicStats*' command in the R package diveRsity (Keenan et al. 2013). The number of private alleles for each sampling location and each putative population was identified using the *populations* module implemented in STACKS.

Population structure was identified using multiple approaches. First, putative populations were identified using two clustering methods: Discriminant Analysis of Principal Components (DAPC), and the Bayesian clustering program STRUCTURE v2.3.4 (Pritchard et al. 2000). DAPC was performed using the R package ADEGENET v2.1.3 (Jombart 2008). For DAPC, the '*find.clusters*' function was used to generate clusters, and the Bayesian Information Criterion (BIC) was used to find the most likely number of clusters (*K*). An *a*-score optimization (*optim.a.score*) was then used to determine the optimal number of principal components to retain; 15 principal components and four discriminant functions were retained for the final analysis. To check for lane effects (*i.e.*, false signals of population structure caused by sequencing across multiple lanes), an additional DAPC was performed with individuals identified by "batch" (see ddRADseq Library Preparation and Sequencing). Results of this DAPC indicated no significant lane effects (Figure S4.1). Analyses in STRUCTURE were carried out on values of *K* ranging from 1-8 with 10 independent replicates for each value of *K*, using the correlated allele frequency, admixture ancestry, and LOCPRIOR models. Each replicate consisted of a burn-in period of 100,000 generations, followed by 500,000 Markov chain Monte Carlo (MCMC) generations. If likelihood estimates for a given value of *K* did not converge across replicates, the burn-in period and MCMC sampling durations were increased to 250,000 and 750,000 generations, respectively. Results were combined and assessed using the

web-based tool STRUCTURE HARVESTER v0.6.94 (Earl and vonHoldt 2012), and visualized using the Cluster Markov Packager Across *K*s (CLUMPAK) online tool (Kopelman et al. 2015). The most likely values of *K* were identified based on the following criteria: maximum likelihood or likelihood "plateau" behavior (suggested by Pritchard et al. (2010)), the Δ*K* method described by Evanno et al. (2005), concordance with DAPC and other analytical results, and biological plausibility.

To test for hierarchical population structure, Analysis of Molecular Variance (AMOVA) was performed in ARLEQUIN v3.5 (Excoffier et al. 1992; Excoffier and Lischer 2010). AMOVA was performed both in the absence of defined population groups (to calculate global F_{ST}) and using the population groupings suggested by clustering analyses (DAPC and STRUCTURE). Statistical significance for both AMOVAs was determined using 20,000 permutations. Pairwise F_{ST} (Weir and Cockerham 1984) comparisons among sampling sites and among putative populations were carried out in the R package diveRsity using the '*diffCalc*' command. Rather than provide a *P*-value for each pairwise comparison, '*diffCalc*' instead provides a confidence interval corresponding to a specified significance threshold (i.e., to obtain a 95% confidence interval, $\alpha = 0.05$). To correct for multiple comparisons, a Bonferroni adjustment was applied to the α parameter supplied to '*diffCalc*,' and confidence intervals were calculated using 1,000 permutations. A heatmap and a UPGMA dendrogram were generated for site-by-site pairwise F_{ST} comparisons using the R packages corrplot and ggdendro (Wei and Simko 2017; de Vries and Ripley 2020).

Isolation-by-Distance (IBD)

Mantel tests and canonical redundancy analyses (RDA) were conducted on the total dataset and on subsets of sampling sites in order to test for patterns of IBD. Mantel tests were conducted in ARLEQUIN using matrices of pairwise F_{ST} and the shortest overwater distances among sampling sites (estimated using Google Earth), and statistical significance was assessed using 20,000 permutations.

RDA was performed using an adapted version of the R script provided in the supplemental materials of Meirmans (2015). This method uses a combination of principal component analysis (PCA) and multiple regression to assess the influence of a matrix of independent variables (in this case, a spatial component calculated from geographic coordinates)

on a matrix of dependent variables (population allele frequencies) (Orsini et al. 2013; Wang et al. 2013; Meirmans 2015). One notable advantage of the RDA output over Mantel's *r* is that it directly indicates the proportion of among-population genetic variation (F_{ST}) that is explained by a spatial component, making its interpretation comparatively straightforward.

Because the spatial component is calculated directly from geographic coordinates, and because Las Animas is separated from the other 11 sampling sites by the Baja peninsula, Las Animas was assigned an alternative latitude and longitude that preserved its overwater/coastal distance from other sites in the RDA. Statistical significance of each RDA was assessed via an ANOVA-like permutation test with 1,000 permutations per step. A false discovery rate (FDR) correction for multiple comparisons was implemented in R using the method of Benjamini and Hochberg (1995) and applied to both sets of analyses.

RESULTS

Genotyping and SNP Filtering

The final dataset consisted of 9,063 neutral SNPs across 175 individuals. As noted above, two individuals did not meet quality filtering thresholds and were removed from the dataset: one individual with fewer than 250,000 reads, and one individual with more than 30% missing data, both from Bahia Tortugas. Individuals had a mean coverage of 47.39 reads per SNP, and the total data matrix was 97.2% complete.

Population Genomic Analysis

Genetic diversity metrics based on 9,063 putatively neutral SNP loci show an overall observed heterozygosity $H_o = 0.169$, expected heterozygosity $H_e = 0.175$, inbreeding coefficient $F_{IS} = 0.038$, and allelic richness $A_R = 1.853$ (Table 4.1). Island populations displayed slightly lower observed heterozygosity, expected heterozygosity, and allelic richness than their mainland counterparts, with sharks from Isla Guadalupe displaying the lowest values in all three categories. Individual sampling sites always displayed an observed heterozygosity that was somewhat higher than expected under HWE, but this pattern was reversed when sampling sites were condensed into putative populations based on the results of clustering analyses and pairwise F_{ST} comparisons (see below). Each sampling site in the study contained private alleles; when sampling sites were considered separately, Las Animas had the largest number of private alleles

(n = 45), followed by Isla Guadalupe (n = 17). When sampling sites were condensed into putative populations, the Mainland Pacific Coast (MLPC) had the largest number of private alleles (n = 767), followed by the Northern Channel Islands (NCI; n = 47) (Table 4.1).

The results of the DAPC indicated five genetic clusters (K = 5; Figure 4.2). The horn sharks occupying the Mainland Pacific Coast (MLPC) comprised a single cluster, island populations formed distinct clusters, regardless of distance from the mainland. Santa Cruz Island (SCI) and Anacapa Island (ANA) clustered strongly together, representing a Northern Channel Island (NCI) population, while Santa Catalina Island (CAT) and Isla Guadalupe (GI) each formed their own independent clusters. Sharks from Las Animas (LA) in the Gulf of California comprised the fifth cluster. Despite the resolution of discrete clusters, one shark from the California mainland (PV) was assigned to the CAT cluster rather than to the MLPC cluster (specimen ID = PV_154).

Results from STRUCTURE HARVESTER (Figure S4.2) showed strong support for five genetic clusters (K = 5) based on likelihood estimates and Evanno's ΔK, though ΔK showed stronger support for K = 2 – a common outcome of STRUCTURE analysis (Janes et al. 2017). The result for K = 5 (Figure 4.3) is largely congruent with the results from DAPC, with the Northern Channel Islands, CAT, GI, and LA each forming distinct clusters with varying levels of admixture. In contrast, the plot for K = 4 groups LA with the other mainland populations, with a continuous increase in the signal from Channel Island clusters with sampling sites located further north along the Pacific coast. While all California mainland individuals show some level of admixture with Channel Island populations, one shark (specimen ID = PV_154) exhibited a much higher proportion of Channel Island ancestry (approximately 50%). Admixture proportions indicate that this individual may be a first- or second-generation hybrid offspring of a mainland shark and a recent migrant from Santa Catalina Island.

An AMOVA revealed significant population genetic structure across the range of *H. francisci* (overall F_{ST} = 0.031, $P < 0.0001$). When sampling sites were grouped into putative populations (as indicated by DAPC and STRUCTURE analyses), the proportion of genetic variation partitioned among groups was significant (F_{CT} = 0.039, $P < 0.0001$), while the proportion of genetic variation partitioned among sampling sites within groups was not significant (F_{SC} = 0.005, $P > 0.05$) (Table 4.2). Pairwise F_{ST} comparisons among sampling sites showed no indication of population genetic structure along the mainland Pacific coast or between

the two northern Channel Islands (95% confidence intervals included zero after Bonferroni correction), but demonstrated significant population structure among all other pairs of sites in agreement with the results from clustering analyses (Figure 4.4). When sampling sites were grouped into putative populations, all pairwise F_{ST} comparisons were statistically significant, with a value range of F_{ST} = 0.023-0.128 (Table 4.3). All Bonferroni-corrected confidence intervals for pairwise F_{ST} comparisons are reported in Tables S4.1 and S4.2.

Isolation-by-Distance (IBD)

A plot of F_{ST} versus overwater distance for all population pairs is provided in Figure 4.5a. The plot shows a roughly linear relationship between F_{ST} and overwater distance across most pairwise comparisons, with the notable exception of comparisons involving the furthest offshore GI, which exhibit the highest values of F_{ST} and are primarily distributed across a narrow range of overwater distances (357 km to 744 km). Pairwise comparisons involving the Channel Islands frequently resulted in higher values of F_{ST} than other comparisons across similar distances. This pattern is highlighted in Figure 4.5a for pairwise comparisons involving GI and LA. Figure 5b shows a similar pattern, with consistently higher values of F_{ST} for comparisons involving Channel Island and MLPC sites than for comparisons only among MLPC sites. This pattern is further stratified when CAT is considered separately from the two northern Channel Islands (NCI), which are closer to the California mainland.

A Mantel test on the total dataset (all 12 sampling sites) did not indicate a statistically significant relationship between pairwise F_{ST} and overwater distance (r = 0.212, P = 0.156; Table 4.4). In subsequent analyses, specific sites (or groups of sites) were excluded to examine whether they might obscure signals of IBD acting among subsets of populations. The strongest signal of IBD was recovered when all island sites were removed from the analysis (MLPC + LA: r = 0.903, P = 0.001). When LA in the Gulf was also removed, leaving only sites along the mainland Pacific coast, a slightly weaker but statistically significant signal of IBD was recovered (MLPC: r = 0.832, P = 0.011). Interestingly, excluding only GI resulted in a statistically significant Mantel test result (No GI: r = 0.595, P = 0.016), while the exclusion of both GI and LA did not (No LA or GI: r = 0.071, P = 0.311).

An RDA conducted on the total dataset yielded no constrained RDA axes and was unable to detect a significant effect of spatial variation on genetic variation, in agreement with the

Mantel test (Table 4.4). However, RDA analyses indicated a significant effect for all four reduced datasets ($P < 0.01$), indicating a pattern of IBD. The proportion of among-population genetic variation (F_{ST}) explained by spatial variance, denoted as %RDA in Table 4.4, ranged from 23.0% among mainland Pacific coast populations (MLPC) to 46.0% among all mainland populations (MLPC + LA). Multiplying these values by the overall F_{ST} for each subsampled dataset provides an estimate of the total genetic variation explained by spatial variance; these estimates ranged from 0.1% to 0.8%.

DISCUSSION

In the following sections, we provide a general overview of population genetic structure and diversity in *Heterodontus francisci*, and then discuss the roles of barriers to dispersal and isolation-by-distance in shaping the distribution of genetic diversity across the species range. We then briefly touch on the utility of next-generation sequencing and its implementation in population genetic studies on sharks before offering concluding remarks.

An overview of population genetic structure across the range of H. francisci

Our analysis of 9,063 putatively neutral, nuclear SNP loci demonstrates that the California horn shark exhibits significant population genetic structure across its range (overall $F_{ST} = 0.031$; Table 4.2). Based on the results of clustering analyses, we were able to identify five distinct genetic groups: the Mainland Pacific Coast (MLPC), which stretches from Malibu, CA down the entire west coast to Bahia Magdalena, BCS, Mexico; the Northern Channel Islands (NCI), comprised of Santa Cruz Island and Anacapa Island; Santa Catalina Island (CAT) in the Southern Channel Islands; Isla Guadalupe (GI); and Las Animas (LA), located in the northern Gulf of California (Figures 4.2 and 4.3). In addition to the pairwise F_{ST} comparisons, the AMOVA supports these population groupings, with no significant population structure detected among sampling sites within the larger groups (Table 4.2; Figure 4.4).

Despite their small size, sedentary lifestyle, and strong site fidelity, *H. francisci* appears capable of maintaining high levels of genetic connectivity along coastal margins (Ebert 2003). We found no evidence of population structure along the continuous coastal margin from Malibu, CA to Bahia Magdalena, BCS, a range which spans more than 1,500 km of coastline. This stands in contrast with the results of our previous mtCR study, which indicated a distinct genetic break

between Bahia Tortugas and the two sample sites to the south, Laguna San Ignacio and Bahia Magdalena (Φ_{ST} = 0.198-0.266; Chapter 3 of this dissertation). Significant population structure at mitochondrial loci, coupled with a lack of detectable genetic structure at nuclear loci, may be explained by female reproductive philopatry and male-biased dispersal. This is a frequent outcome of mixed-marker analysis in sharks, including the congeneric Port Jackson shark, *H. portusjacksoni* (Hueter et al. 2005; Dudgeon et al. 2012; Day et al. 2019). However, if female reproductive philopatry is a feature in the life history of *H. francisci*, then we struggle to explain the lack of mtDNA structure in the long (1000+ km) mainland coastline between Bahia Tortugas and Malibu. Alternatively, differing patterns of F_{ST} in mtDNA and nuclear DNA may be observed even in the absence of sex-biased dispersal, as mtDNA is more sensitive to the effects of genetic drift, selection, and demographic processes due to its smaller effective population size (Ballard and Whitlock 2004; Phillips et al. 2021). Thus, the mito-nuclear discordance observed in *H. francisci* warrants further investigation.

While horn sharks appear to demonstrate widespread connectivity along shallow coastal margins, significant structure exists between island and mainland populations (Table 4.3; Figure 4.4). Isla Guadalupe, a small volcanic island located 250 km to the west of the Baja peninsula, exhibited the highest values of F_{ST} among all pairwise comparisons (F_{ST} = 0.090-0.128). But island-mainland population structure was apparent at much smaller scales as well, and the horn sharks of the California Channel Islands also appear to be genetically isolated from their mainland counterparts (F_{ST} = 0.023-0.032). Our previous analyses using the mtCR indicated a similar pattern, but were unable to detect significant population structure between the Northern and Southern Channel Islands, which are separated by nearly 100 km of deep water (Chapter 3 of this dissertation). That finding challenged the conclusion that deep, cold-water channels were the primary driver of genetic structure among island and mainland populations. The present analysis based on neutral SNP loci not only found clear evidence of genetic divergence between the Northern and Southern Channel Island ranges, but also found that the level of divergence exceeds that observed among island-mainland population pairs (F_{ST} = 0.041). This finding supports the inference that deep, open water acts as a barrier to dispersal in *H. francisci*, and indicates that there may be an inverse relationship between overwater distance and genetic connectivity. This finding also reveals that the Northern and Southern Channel Islands are more

closely related to the mainland than to each other, indicating independent colonizations from the mainland.

Lower genetic diversity in island populations (when compared to their mainland counterparts) is a well-documented phenomenon, and is often correlated with distance, dispersal capability, and population size (Frankham 1997). Our previous analysis of the mtCR found reduced genetic diversity and smaller effective population sizes in Channel Island populations of *H. francisci* compared to the mainland (Chapter 3 of this dissertation). Analysis of neutral SNP loci likewise indicates that island populations exhibit slightly lower genetic diversity compared to the sharks of the mainland Pacific coast: observed heterozygosity (H_o), expected heterozygosity (H_e), and allelic richness (A_R) were all lower in island populations (Table 4.1). This finding was consistent whether the sites comprising the MLPC were considered separately or were combined into a single group. The lowest diversity values were observed in sharks from Isla Guadalupe, the most isolated island in our dataset. Furthermore, island populations possess unique genetic diversity, collectively harboring 77 private alleles. This has potential implications for conservation management initiatives, which often seek to maximize the genetic diversity and adaptive potential of managed stocks (Frankham 2010; Domingues et al. 2018).

Las Animas, a small bay located just to the south of Bahia de Los Angeles in the northern Gulf of California, represents the fifth genetic cluster recognized in our analysis. Genetic partitions on either side of the Baja peninsula are common in shorefishes (Bernardi et al. 2003; see also Robertson and Cramer 2009), and have been observed in the Pacific angel shark, another benthic elasmobranch (Ramírez-Amaro et al. 2017). Though the California horn shark exhibits a similar pattern of population structure, we are cautious in our interpretation due to the distance between Las Animas and the sampling sites along the mainland Pacific coast – approximately 1,100 km. Large sampling gaps make it difficult to distinguish between patterns of isolation-by-distance (IBD) and hierarchical population structure caused by barriers to dispersal (Meirmans 2012). Furthermore, clustering methods such as STRUCTURE are highly sensitive to IBD, leading to the detection of artificial genetic clusters and the overestimation of genetic structure (Frantz et al. 2009; Perez et al. 2018). Our own STRUCTURE analysis hints at such an effect of IBD: at K=4, there is an apparent gradient from north to south of increasing "mainland" coancestry up to and including Las Animas (Figure 4.3, in blue), and at K=5 there is a gradual trend of decreasing Las Animas coancestry from Bahia Magdalena north to Bahia Tortugas

(Figure 4.3, in magenta). Therefore, more sampling along the eastern shore of the Baja peninsula is necessary to determine whether distinct genetic partitions exist on either side of this prominent land barrier.

Depth barriers drive divergence across small geographic scales in H. francisci *and other shallow benthic elasmobranchs in the Southern California Bight*

The most common pattern of population structure revealed by our analyses was a break between island and mainland populations separated by as little as 19 km of open water, with F_{ST} ranging from 0.023 to 0.090 (Table 4.3; Figure 4.4). Given the high level of connectivity among mainland sites across much larger distances (> 1,000 km), this points to the deep, cold waters separating these landmasses acting as a barrier to dispersal in *H. francisci*. This conclusion is further supported by significant differentiation between the Northern Channel Islands and Santa Catalina Island in the Southern Channel Islands, separated by nearly 100 km of deep ocean. This result contrasts with those of our earlier mtDNA study, which failed to detect population structure among these geographically distinct island groups (Chapter 3 of this dissertation).

A recent meta-analysis of population genetic studies on elasmobranchs identified ocean depth as the most common dispersal barrier at intermediate to small spatial scales (Hirschfeld et al. 2021). The authors reported that the probability of significant genetic differentiation across depth barriers was negatively correlated with maximum body size and maximum depth of occurrence, and that benthopelagic species were more likely to demonstrate genetic differentiation across depth barriers. It may therefore be unsurprising that the diminutive, shallow, benthic California horn shark follows the described pattern. The Southern California Bight (SCB), characterized by its steep bathymetry, is home to two other elasmobranch species exhibiting population structure across depth barriers at exceptionally small geographic scales (< 100 km): the California angel shark (*Squatina californica*), with a genetic partition between the northern and southern Channel Islands (Gaida 1997); and the round stingray (*Urobatis halleri*), whose Santa Catalina Island residents are genetically distinct from their mainland counterparts (Plank et al. 2010). All three species – including *H. francisci* – are strongly affiliated with benthic habitat, and occupy depths less than 200 meters (Compagno et al. 2005; Weigmann 2016). In the case of *U. halleri*, this shallow depth distribution may be driven by thermal tolerances and a preference for warmer water (Ebert 2003; Vaudo and Lowe 2006; Jirik and

Lowe 2012). Distribution data suggest that the depth limit of *H. francisci* may be similarly limited by thermal tolerances: the northern limit of the species distribution corresponds with Point Conception, which is part of the California Transition Zone linking the cooler waters of the Oregon Province and the warmer waters of the California Province (Compagno 2002; Briggs and Bowen 2012; Toonen et al. 2016).

While the scale of population subdivision in *S. californica* and *U. halleri* is exceptional among elasmobranchs, the population structure exhibited by *H. francisci* between Anacapa Island and the California mainland – supported by both mtDNA and nuclear SNP datasets – occurs over an unprecedented small scale. The effectiveness of the deep, cold waters as a barrier to dispersal becomes even more impressive when considering the bathymetry of the area. The California horn shark is most commonly encountered at depths ranging from 2-11 meters, with an observed depth range of up to 152 meters (Weigmann 2016). While Anacapa Island lies a mere 19 km from the California mainland at sea level, the distance between the two landmasses becomes considerably smaller at depth: less than ten kilometers at 150 meters depth, and less than five kilometers at 200 meters depth (Figure 4.1). Thus, it is clear that depth is a potent driver of divergence among populations of shallow, benthic elasmobranchs over extremely small distances. As noted in Chapter 3 of this dissertation, this fish has population structure on a scale smaller than a healthy human can swim.

Isolation-by-distance (IBD) acts weakly but significantly across the range of H. francisci

Isolation-by-distance (IBD), a pattern of decreasing genetic relatedness as a function of increasing geographic distance, is an expected outcome in organisms with limited dispersal capability (Wright 1943; Meirmans 2012). Unlike most teleost fishes, sharks lack a pelagic larval stage, and dispersal is accomplished primarily by the active movements of fully formed juveniles and adults. The California horn shark, in addition to lacking a pelagic larval stage, is known to demonstrate a high level of site fidelity, maintaining relatively small home-ranges as adults (Strong 1989; Ebert 2003; Meese and Lowe 2020). Both of these traits are likely to result in limited dispersal.

Our results indicate that geographic distance has little to no explanatory power for the distribution of genetic diversity when all populations are considered simultaneously (Table 4.4). However, the removal of certain sites from the dataset resulted in significant associations,

indicating that IBD acts across subsets of populations. For example, Mantel tests for IBD detected a significant association between geographic distance and F_{ST} when the oceanic Isla Guadalupe sample was removed from the dataset ($r = 0.595$, $P = 0.016$). When Las Animas (Gulf of California) was further removed, no significant signal of IBD was detected ($r = 0.071$, $P = 0.311$), indicating that this sample exerts considerable leverage on the analysis. When all island sites were removed from the analysis, leaving only the mainland Pacific coast (MLPC) and Las Animas, Mantel's r increased to $r = 0.903$ ($P = 0.001$). Taken together, these results indicate that island populations have a disruptive effect on patterns of IBD, which is strongest when considering only mainland samples. This is consistent with the observation of deep-water channels as barriers to dispersal over short distances. The effect is represented visually in Figure 4.5a, with comparisons involving Isla Guadalupe exhibiting conspicuously large values of F_{ST} across a narrow range of geographic distances (approximately 500 km); and in Figure 4.5b, with comparisons involving Channel Island populations significantly expanding the range of F_{ST} values, thereby weakening the apparent relationship between geographic distance and genetic distance. Interestingly, the three sets of pairwise comparisons represented in Figure 4.5b – MLPC-MLPC, NCI-MLPC, and CAT-MLPC – each display linear relationships between F_{ST} and geographic distance that are distinctly stratified and roughly parallel to one another. Comparisons among CAT and MLPC sites reveal the highest values of F_{ST} for a given geographic distance, followed by comparisons among NCI and MLPC sites, likely reflecting the relative strengths of the deep-water barriers separating island and mainland populations.

Canonical redundancy analysis (RDA) on the full dataset likewise detected no significant association between geographic distance and allele frequency distributions (Table 4.4). However, every RDA on the reduced datasets (as above) indicated a significant association between the two factors, although the proportion of among-population genetic variation explained by spatial components (%RDA; Meirmans 2015) varied considerably depending on the subsets of populations included in the analysis. Removal of the island populations resulted in the highest %RDA value (46.0%; Table 4.4), reaffirming the results of the Mantel test and the islands' disruptive effect on patterns of IBD. The subsequent removal of Las Animas – leaving only the mainland Pacific coast – resulted in the lowest %RDA value (23.0%), affirming that Las Animas exerts a strong influence on signatures of IBD in the present dataset.

An attractive feature of RDA is the ability to multiply the proportion of among-population genetic variation explained by spatial components (%RDA) by F_{ST} in order to estimate the proportion of *total* genetic variation explained by spatial variables (Meirmans 2015). When this calculation was performed, the values ranged from 0.1% to 0.8%, indicating that while spatial variables explain significant proportions of among-population genetic variation, they explain very little of the overall genetic variance observed in *H. francisci*. In other words, while IBD is a significant explanatory factor when considering population genetic structure in the California horn shark, it does not strongly influence the distribution of genetic diversity across the species range overall.

SNPs provide improved resolution of population structure in H. francisci

Next-generation sequencing (NGS) technologies have dramatically increased our power to detect signatures of selection, adaptation, and population genetic structure in non-model organisms (Allendorf et al. 2010; Funk et al. 2012; Narum et al. 2013). Population genomic methods leveraging hundreds or thousands of single-nucleotide polymorphism (SNP) loci are able to detect fine-scale population structure that may be missed when examining a small number of traditional markers (Malenfant et al. 2015; Benestan et al. 2016; Jeffries et al. 2016; Vendrami et al. 2017; Younger et al. 2017; Hohenlohe et al. 2018). This was demonstrated in a recent study of population genetic structure of the Silky shark (*Carcharhinus falciformis*) in the western Atlantic Ocean (Kraft et al. 2020). Despite these advantages, population genomic studies on sharks are still relatively rare, though they are becoming increasingly common (Domingues et al. 2018; Hirschfeld et al. 2021).

In the present study, our dataset of 9,063 putatively neutral, nuclear SNP loci resolved population structure that went undetected in our previous study of the mtCR of *H. francisci*. Notably, analyses of SNP data indicate strong population genetic structure between the Northern Channel Islands and Santa Catalina Island, whereas no significant population structure could be detected among Anacapa Island, Santa Cruz Island, and Santa Catalina Island using the mtCR. This was largely due to the prevalence of a single mitochondrial haplotype among island populations, which may be the result of founder effects rather than ongoing genetic migration (Chapter 3 of this dissertation). The dominance of a single haplotype will also reduce the power to detect population structure (Ryman and Jorde 2001; Karl et al. 2012b). Analyses of SNP data

clearly distinguishes Isla Guadalupe and Las Animas from all other sampling sites, while analyses of the mtCR only indicated significant population structure between these sites and the Channel Islands, along with a seemingly random subset of mainland Pacific coast sites. Low sample sizes at Isla Guadalupe (n = 8) and Las Animas (n = 12) likewise limited our power to detect population structure with a single mitochondrial maker. On the other hand, the use of thousands of SNP loci to detect population structure can allow for the accurate estimation of F_{ST} with as few as two to six individuals per population (Willing et al. 2012; Nazareno et al. 2017; Li et al. 2020). This is an especially important consideration in studies of sharks, where sampling is usually difficult and may often be opportunistic.

CONCLUSIONS

Our analysis of 9,063 putatively neutral, nuclear SNP loci demonstrates that deep-water channels act as barriers to dispersal in *H. francisci* over remarkably small spatial scales, in agreement with our previous genetic assessment of the mitochondrial control region. Contrary to expectations based on life history, the California horn shark exhibits high levels of connectivity along continuous coastal habitat, displaying no significant population structure along the mainland Pacific coast from Malibu, California to Bahia Magdalena, Baja California Sur, Mexico. Furthermore, while isolation-by-distance does appear to influence the distribution of genetic diversity across the range of the California horn shark, its overall effect is small, accounting for less than 1% of genetic variance across hundreds of kilometers – a surprising outcome for a shark with supposedly limited dispersal capability. Given that *H. francisci* is currently classified as “Data Deficient” by the IUCN (Carlisle 2015), and at least one recent study has indicated that the species may be vulnerable to overexploitation in the southern portion of its range (Furlong-Estrada et al. 2017), this information may prove particularly valuable in informing conservation and management strategies.

Table 4.1. Genetic diversity metrics based on 9,063 neutral SNP loci from *Heterodontus francisci*. Populations reflect clusters identified with DAPC and STRUCTURE analyses.

Populations	Sampling Sites	N	N_{perloc}	H_o	H_e	F_{IS}	A_R	Priv
Northern Channel Islands (NCI)	Anacapa Island (ANA)	19	18.672	0.164	0.163	-0.013	1.526	1
	Santa Cruz Island (SCI)	16	14.612	0.162	0.161	-0.010	1.529	7
	Total (NCI)	35	33.284	0.163	0.164	0.006	1.528	47
Catalina (CAT)	Santa Catalina Island (CAT)	19	18.156	0.167	0.158	-0.048	1.503	13
Mainland Pacific Coast (MLPC)	Malibu (MAL)	16	15.692	0.173	0.168	-0.030	1.571	2
	Palos Verdes (PV)	14	13.613	0.172	0.166	-0.036	1.564	0
	Laguna (LAG)	14	13.530	0.174	0.167	-0.033	1.571	3
	San Diego (SD)	15	14.659	0.175	0.169	-0.032	1.570	4
	Bahia Tortugas (BT)	14	13.641	0.178	0.169	-0.047	1.577	1
	Laguna San Ignacio (LSI)	16	15.894	0.171	0.171	-0.007	1.581	5
	Bahia Magdalena (BM)	13	12.736	0.174	0.170	-0.026	1.580	10
	Total (MLPC)	121	99.765	0.174	0.175	0.012	1.581	767
Las Animas (LA)	Las Animas (LA)	12	11.919	0.168	0.165	-0.023	1.551	45
Isla Guadalupe (GI)	Isla Guadalupe (GI)	7	6.909	0.145	0.134	-0.087	1.409	17
All Samples		175	170.033	0.169	0.175	0.038	1.853	-

N = total sample size; N_{perloc} = average number of individuals per locus; H_o = average observed heterozygosity; H_e = average expected heterozygosity; F_{IS} = inbreeding coefficient; A_R = allelic richness; Priv = total number of private alleles for a given site or population

Table 4.2. AMOVA results for 9,063 neutral SNP loci from *Heterodontus francisci*. The top ANOVA ("All Sites") was run without any specified hierarchical structure; the bottom ANOVA ("5 Groups") was run with sampling sites assigned to groups (populations) according to the results from DAPC and STRUCTURE analysis. Significant fixation indices ($P < 0.05$) are denoted in bold. Group abbreviations are defined in Table 4.1.

Source of Variation	df	SS	% Variation	Fixation Indices
All Sites				
Among populations	11	12038.04	3.13	**F_{ST} = 0.031 (P < 0.01)**
Within populations	338	190943.53	96.87	
Total	349	202981.57		
5 Groups (NCI, CAT, MLPC, LA, GI)				
Among groups	4	7435.57	3.88	**F_{CT} = 0.039 (P < 0.01)**
Among populations within groups	7	4602.48	0.52	F_{SC} = 0.005 (P > 0.05)
Within populations	338	190943.53	95.59	**F_{ST} = 0.044 (P < 0.01)**
Total	349	202981.96		

Table 4.3. Pairwise F_{ST} among putative populations identified with DAPC and STRUCTURE analyses for *Heterodontus francisci*. All pairwise F_{ST} estimates were statistically significant (95% confidence intervals did not include zero after Bonferroni correction). Population abbreviations are defined in Table 4.1.

	NCI	**CAT**	**MLPC**	**LA**
CAT	**0.041**			
MLPC	**0.023**	**0.032**		
LA	**0.067**	**0.079**	**0.034**	
GI	**0.119**	**0.131**	**0.090**	**0.128**

Table 4.4. Mantel test and RDA results for *Heterodontus francisci*. Variable exclusion of the offshore Isla Guadalupe (GI), Las Animas (LA) in the Gulf of California, and the California Channel Islands allowed for tests of isolation-by-distance among subsets of populations, including the Mainland Pacific Coast (MLPC). Significant values ($P < 0.05$) are bolded.

	Mantel Test		**RDA**		
Populations	*r*	*P*	*%RDA*	*%RDA*F_{ST}*	*P*
All Populations	0.212	0.156	*NA*	*NA*	*NA*
No GI	**0.595**	**0.016**	**0.362**	**0.008**	**0.002**
No LA or GI	0.071	0.311	**0.330**	**0.006**	**0.008**
MLPC + LA	**0.903**	**0.001**	**0.460**	**0.006**	**0.002**
MLPC	**0.832**	**0.011**	**0.230**	**0.001**	**0.008**

r = Mantel's *r*; %RDA = the proportion of genetic variation explained by all constrained RDA axes (*i.e.*, the spatial component of the among-population genetic variation); *P* = the FDR-corrected *P* value

Table S4.1. Pairwise F_{ST} (below diagonal) and Bonferroni-corrected confidence intervals ($\alpha = 7.6x10^{-4}$; above diagonal) based on 9,063 putatively neutral SNP loci from *Heterodontus francisci*. Significant values and intervals excluding zero are bolded. Location abbreviations are defined in Table 3.1.

	SCI	**ANA**	**CAT**	**MAL**	**PV**	**LAG**	**SD**	**BT**	**LSI**	**BM**	**LA**	**GI**
SCI		(-0.013, 0.018)	**(0.029, 0.059)**	**(0.008, 0.041)**	**(0.007, 0.044)**	**(0.009, 0.047)**	**(0.012, 0.048)**	**(0.012, 0.050)**	**(0.017, 0.049)**	**(0.017, 0.056)**	**(0.049, 0.090)**	**(0.100, 0.158)**
ANA	0.000		**(0.032, 0.056)**	**(0.010, 0.038)**	**(0.009, 0.041)**	**(0.009, 0.043)**	**(0.014, 0.043)**	**(0.016, 0.047)**	**(0.019, 0.047)**	**(0.018, 0.049)**	**(0.051, 0.088)**	**(0.100, 0.153)**
CAT	**0.042**	**0.042**		**(0.022, 0.050)**	**(0.018, 0.050)**	**(0.021, 0.053)**	**(0.024, 0.054)**	**(0.028, 0.059)**	**(0.032, 0.060)**	**(0.031, 0.064)**	**(0.064, 0.100)**	**(0.108, 0.163)**
MAL	**0.022**	**0.022**	**0.033**		(-0.013, 0.021)	(-0.013, 0.025)	(-0.006, 0.028)	(-0.009, 0.025)	(-0.005, 0.028)	(-0.006, 0.030)	**(0.028, 0.068)**	**(0.077, 0.134)**
PV	**0.023**	**0.022**	**0.031**	0.001		(-0.014, 0.025)	(-0.009, 0.028)	(-0.012, 0.026)	(-0.006, 0.029)	(-0.006, 0.036)	**(0.027, 0.070)**	**(0.075, 0.137)**
LAG	**0.025**	**0.023**	**0.034**	0.003	0.003		(-0.014, 0.024)	(-0.010, 0.030)	(-0.007, 0.029)	(-0.008, 0.034)	**(0.027, 0.071)**	**(0.076, 0.138)**
SD	**0.027**	**0.027**	**0.037**	0.007	0.006	0.002		(-0.009, 0.029)	(-0.003, 0.032)	(-0.003, 0.035)	**(0.027, 0.067)**	**(0.080, 0.138)**
BT	**0.028**	**0.028**	**0.041**	0.005	0.004	0.006	0.007		(-0.011, 0.024)	(-0.012, 0.027)	**(0.019, 0.061)**	**(0.073, 0.132)**
LSI	**0.031**	**0.031**	**0.044**	0.008	0.009	0.008	0.011	0.003		(-0.014, 0.021)	**(0.017, 0.057)**	**(0.071, 0.128)**
BM	**0.033**	**0.032**	**0.045**	0.010	0.011	0.010	0.013	0.005	0.002		**(0.013, 0.056)**	**(0.074, 0.134)**
LA	**0.066**	**0.066**	**0.079**	**0.043**	**0.044**	**0.046**	**0.045**	**0.036**	**0.033**	**0.032**		**(0.102, 0.166)**
GI	**0.124**	**0.120**	**0.131**	**0.099**	**0.099**	**0.102**	**0.104**	**0.097**	**0.094**	**0.099**	**0.128**	

Table S4.2. Pairwise F_{ST} (below diagonal) and Bonferroni-corrected confidence intervals (α = 0.005; above diagonal) among putative populations identified with DAPC and STRUCTURE analyses for *Heterodontus francisci*. Significant values and intervals excluding zero are bolded. Location abbreviations are defined in Table 3.1.

	NCI	**CAT**	**MLPC**	**LA**	**GI**
NCI		**(0.033, 0.052)**	**(0.020, 0.028)**	**(0.054, 0.088)**	**(0.101, 0.148)**
CAT	**0.041**		**(0.027, 0.042)**	**(0.064, 0.101)**	**(0.109, 0.163)**
MLPC	**0.023**	**0.032**		**(0.025, 0.056)**	**(0.073, 0.116)**
LA	**0.067**	**0.079**	**0.034**		**(0.103, 0.165)**
GI	**0.119**	**0.131**	**0.090**	**0.128**	

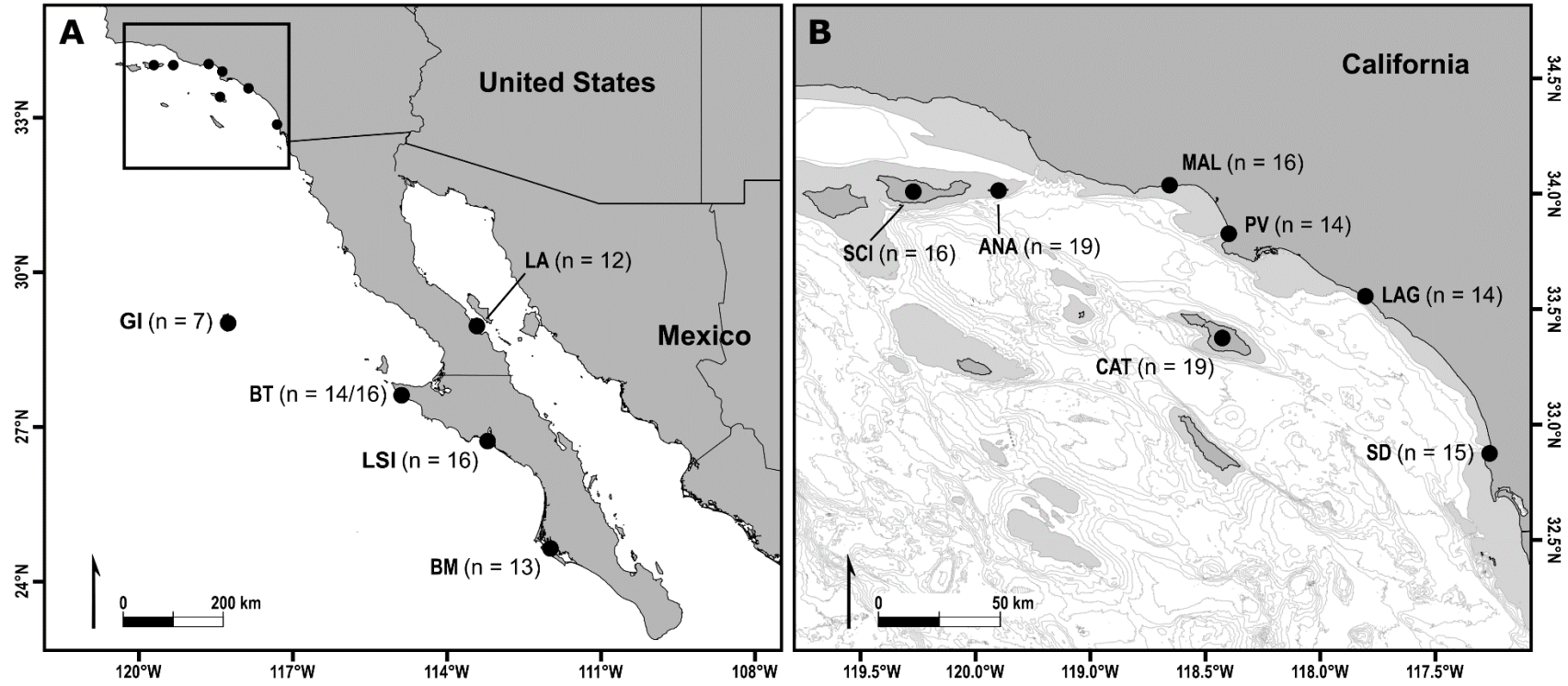

Figure 4.1. Sampling locations of *Heterodontus francisci* with sample sizes indicated in parentheses. (**A**) A large-scale view of sampling locations along the Baja California peninsula (including Isla Guadalupe). The sample size for BT indicates that two specimens were removed due to quality issues. (**B**) Expanded view of the inset box in (**A**) showing sampling locations within the Southern California Bight, including the California mainland as well as the California Channel Islands. Depth contour lines represent 200-meter increments, and the light-gray areas surrounding landmasses represent depths from 0 m to 200 m. **ANA** = Anacapa Island, **SCI** = Santa Cruz Island, **CAT** = Santa Catalina Island, **MAL** = Malibu, **PV** = Palos Verdes, **LAG** = Laguna, **SD** = San Diego, **GI** = Isla Guadalupe, **BT** = Bahia Tortugas, **LSI** = Laguna San Ignacio, **BM** = Bahia Magdalena, **LA** = Las Animas.

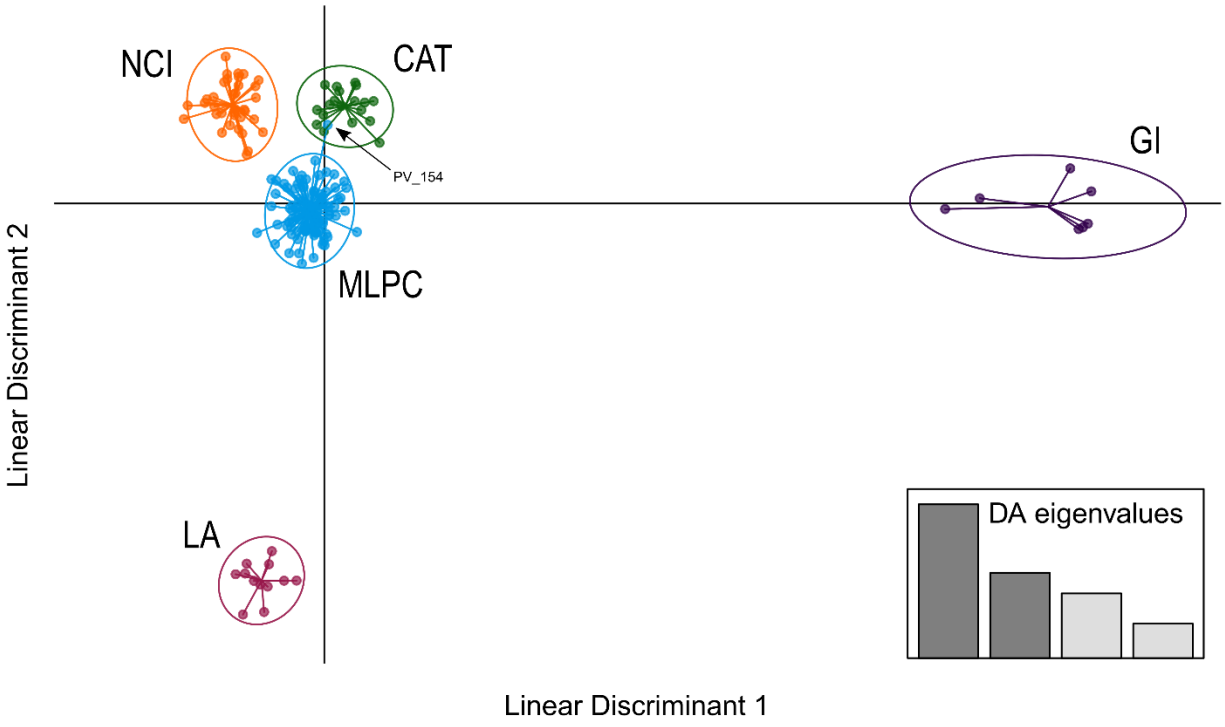

Figure 4.2. Discriminant Analysis of Principal Components (DAPC) results for 9,063 neutral SNP loci from *Heterodontus francisci*. One individual (PV_154) from the Mainland Pacific Coast (**MLPC**, in blue) was assigned to the cluster corresponding to Santa Catalina Island (**CAT**, in green). **NCI** = Northern Channel Islands, **CAT** = Santa Catalina Island, **GI** = Isla Guadalupe, and **LA** = Las Animas.

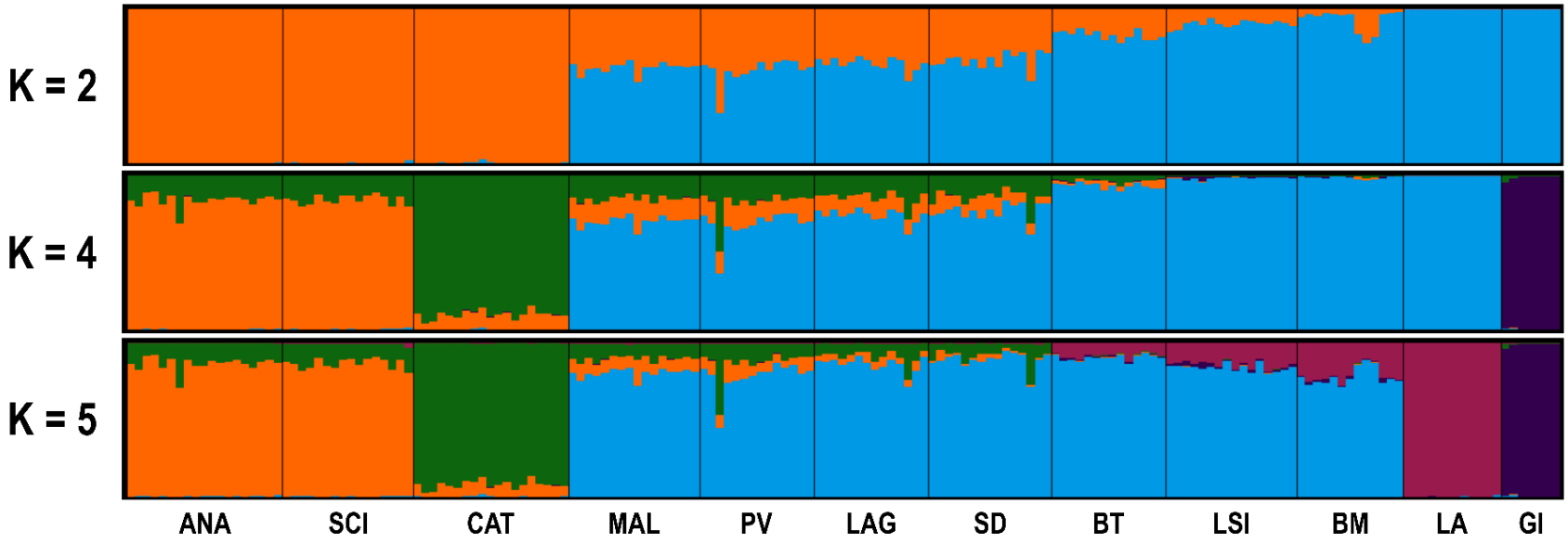

Figure 4.3. STRUCTURE results for 9,063 neutral SNP loci from *Heterodontus francisci*. Results for K=2, K=4, and K=5 are shown. Location abbreviations are defined in Figure 4.1.

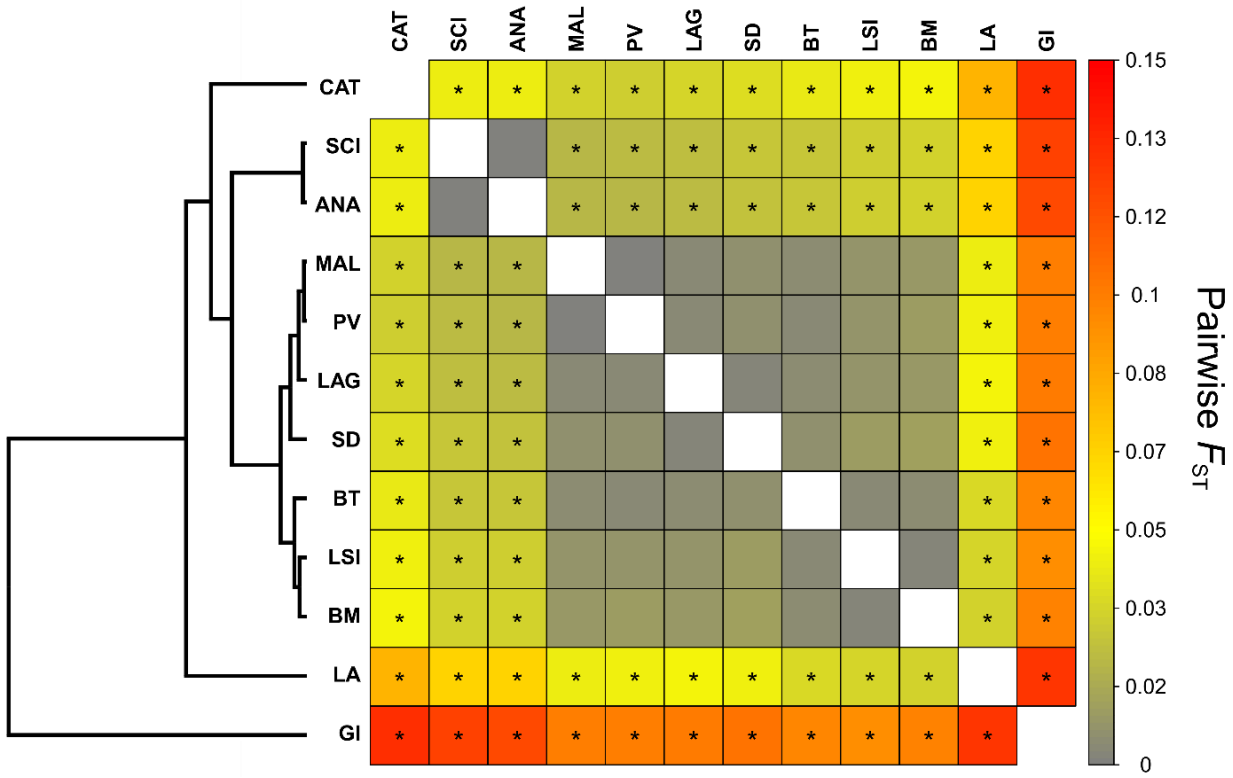

Figure 4.4. Heatmap of pairwise F_{ST} among sampling sites for *Heterodontus francisci*. The UPGMA dendrogram (left) was calculated using pairwise F_{ST} values. F_{ST} ranged from 0.000 to 0.131. Asterisks (*) inside squares denote F_{ST} values which remained significant after a Benjamini and Hochberg (1995) correction for false discovery rate ($P < 0.05$). Location abbreviations are defined in Figure 4.1.

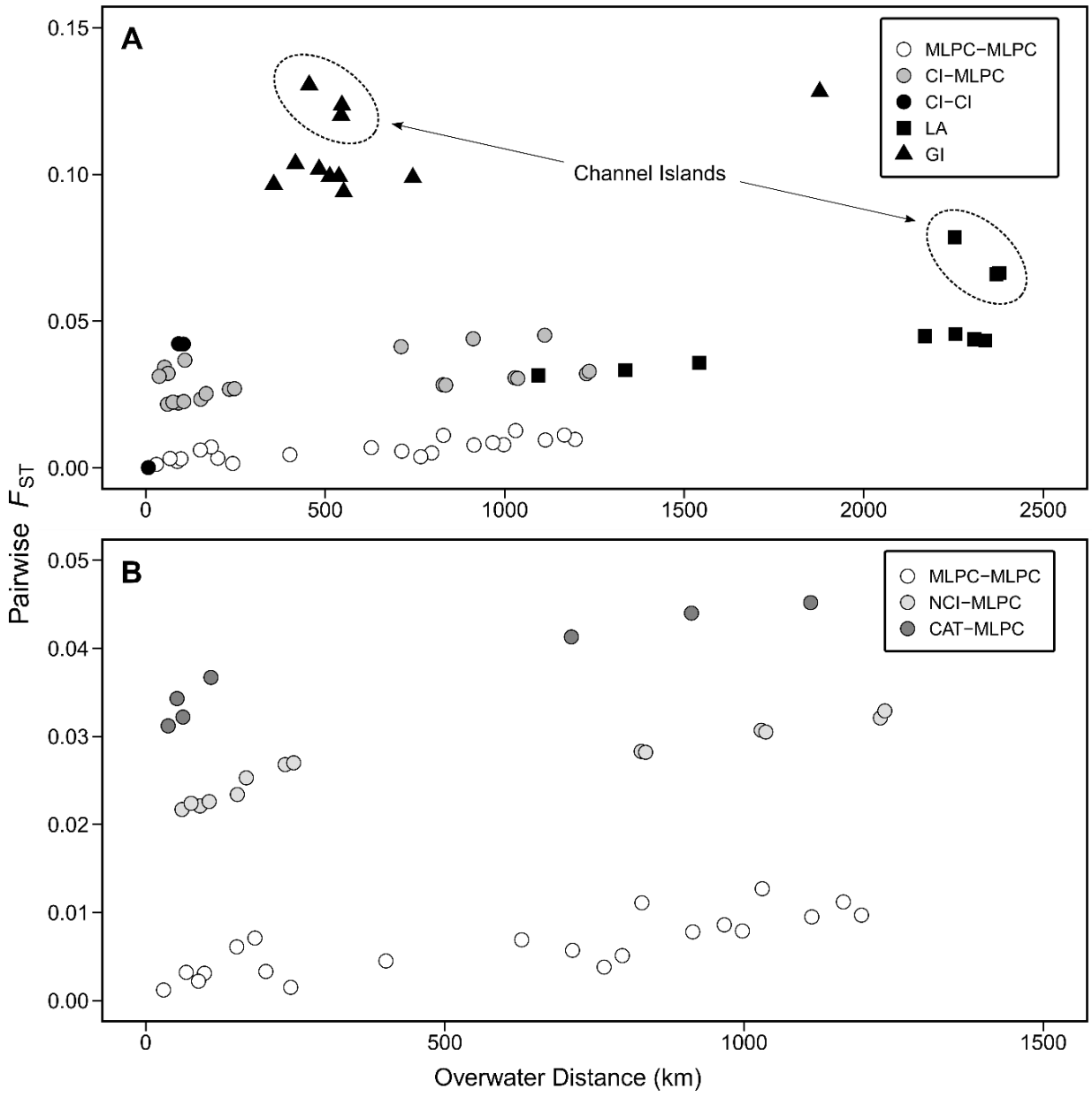

Figure 4.5. Plots of pairwise genetic distance (F_{ST}) vs overwater distance (km) among sampling sites for *Heterodontus francisci*. (A) All pairwise comparisons. Specific categories are indicated by shape and shading. Comparisons between Channel Island (CI) sites and Las Animas (LA) and Isla Guadalupe (GI) are indicated by dashed ovals and arrows. MLPC = Mainland Pacific Coast. (B) Pairwise comparisons among Mainland Pacific Coast sites (MLPC-MLPC), between Northern Channel Island sites and MLPC sites (NCI-MLPC), and between Santa Catalina Island and MLPC sites (CAT-MLPC).

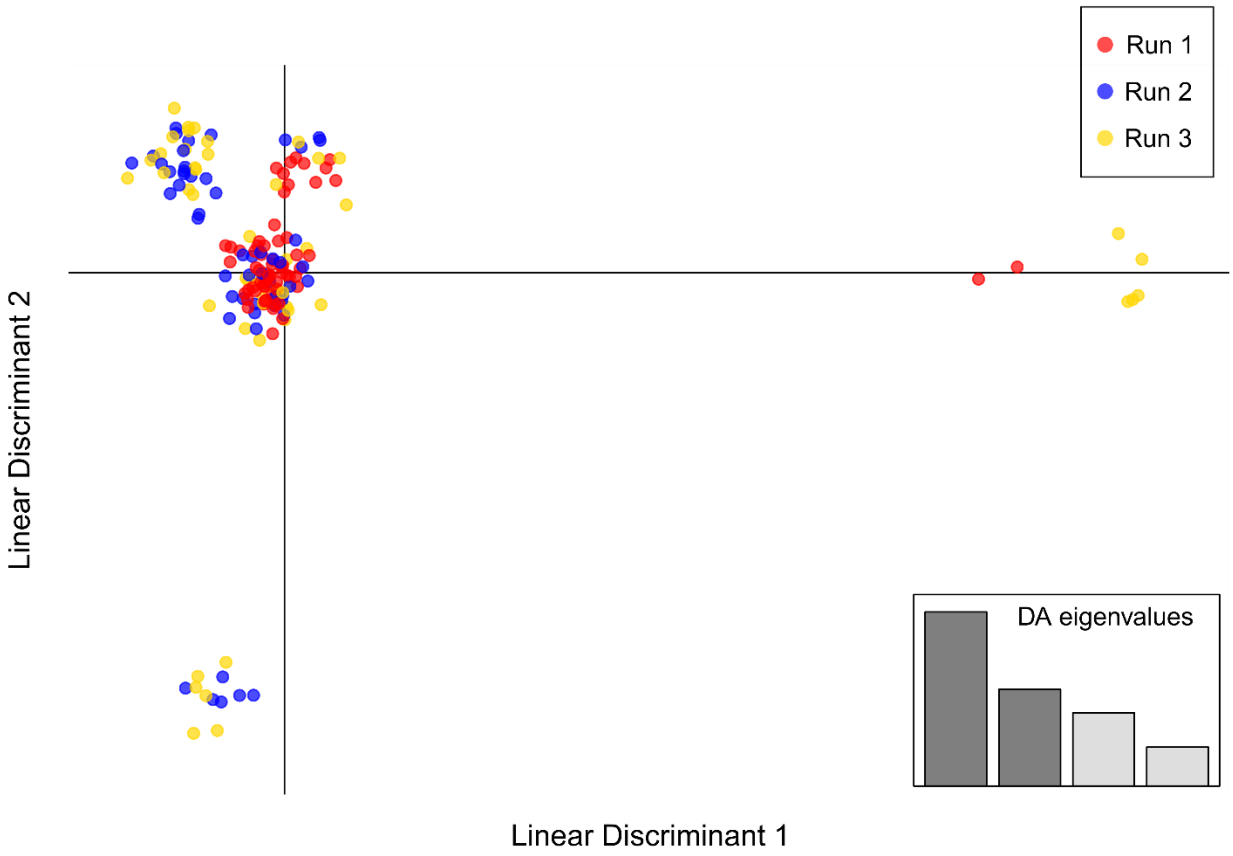

Figure S4.1. Discriminant Analysis of Principal Components (DAPC) results for 9,063 neutral SNP loci from *H. francisci*, with individuals grouped by sequencing runs. Individuals denoted in red were sequenced during Run 1, individuals denoted in blue were sequenced during Run 2, and individuals denoted in yellow were sequenced during Run 3.

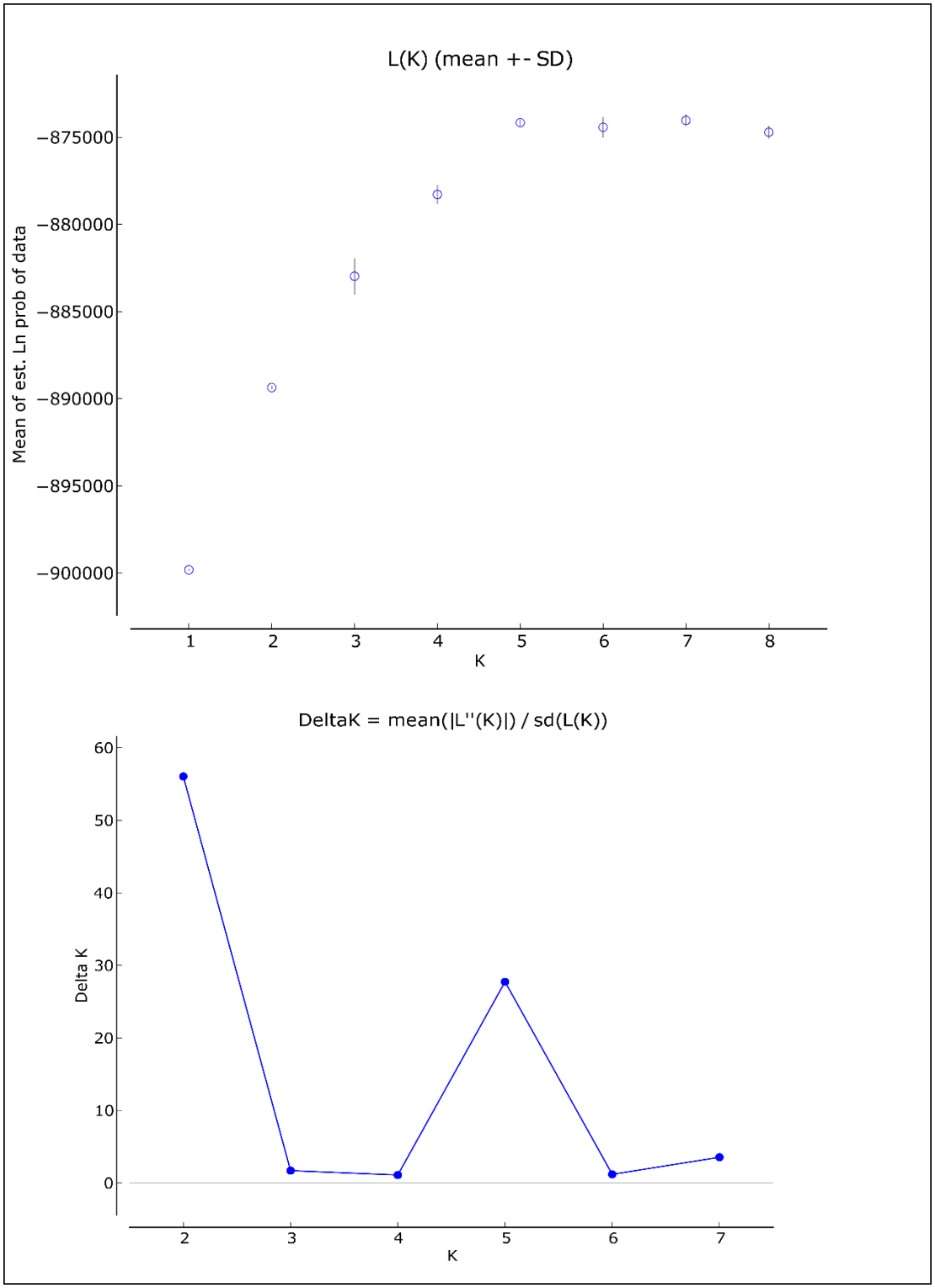

Figure S4.2. STRUCTURE HARVESTER outputs for log-likelihood estimates (top) and Evanno's Δ*K* (bottom) over increasing values of *K*.

CHAPTER 5. CONCLUSIONS

The overall goals of this dissertation were two-fold. First, I developed and presented a sequencing-free PCR-RFLP method for quick and reliable species identification of the eastern Pacific horn sharks (genus *Heterodontus*; Chapter 2). Second, I utilized two sets of genetic markers – one mitochondrial locus, and thousands of nuclear SNP loci – to detect and characterize population genetic structure across the range of the California horn shark, *Heterodontus francisci* (Chapters 3 and 4). Each of these pursuits has significant conservation implications, and the latter sets the stage for new areas of scientific exploration. In particular, the discovery of genetic structure over unprecedented small distances in *H. francisci* makes a strong case for re-examining our understanding of the spatial scale of population structure in marine elasmobranchs.

The PCR-RFLP assay as a practical, low-tech tool for shark conservation

Accurate species identification and delineation of species ranges are critical to the successful implementation of conservation measures, and inaccurate estimates of range sizes and species distributions can have serious negative impacts on conservation efforts (see Jetz et al. 2007). In the eastern Pacific, there are three species of *Heterodontus* with overlapping distributions: *H. francisci*, *H. mexicanus*, and *H. quoyi*. While there are reports of local population declines and indications that horn sharks are vulnerable to fishing pressures in some areas (Furlong-Estrada et al. 2017, S.J.C. pers. obs.), extremely little is known about catch rates and overall population status for all three species (Kyne et al. 2004; Garayzar 2006; Carlisle 2015). To complicate matters, these species can be difficult to distinguish in the field, and considerable uncertainty exists regarding species ranges and the overlap of distributions (Compagno et al. 2005; Garayzar 2006; Canfield and Bowen 2021).

To address this issue, I developed and tested a PCR-RFLP assay to distinguish between the three species of *Heterodontus* in the eastern Pacific, which achieved a 100% success rate (Chapter 2). The use of DNA to identify species is by no means a recent innovation (Hebert et al. 2003; Avise 2004), and the origins of restriction fragment length polymorphism (RFLP) techniques can be traced back more than four decades (Botstein et al. 1980). In this regard, the technique is certainly not novel. However, the technique is simple, fast, and (best of all) cheap,

leveraging DNA polymorphisms without the need for expensive sequencing. It is also highly parallelizable, such that researchers and managers are only limited in output volume by their access to reagents. Thus, Chapter 2 serves as a demonstration that older genetic techniques can have great utility in the modern age of genomics, and may even prove superior in some applications (Bowen et al. 2014). In this case, the PCR-RFLP assay is a cost-effective alternative to direct sequencing of DNA barcodes for shark identification, particularly for resource-limited research programs and management initiatives.

The California horn shark displays genetic structure pertinent to conservation

An examination of population structure in *H. francisci* reveals distinct genetic partitions across its range. The most consistent result of this study was structure among populations separated by stretches of deep, cold water, such as those between the California mainland and the California Channel Islands, which appear to limit dispersal over remarkably small distances (> 40 km). In contrast, horn sharks display widespread connectivity along the continental margin, and nuclear SNP data indicate that isolation-by-distance (IBD) acts weakly along continuous coastlines. Due to a large sampling gap between Bahia Magdalena (on the southwest coast of the Baja Peninsula) and Las Animas deep in the Gulf of California, it remains unclear whether the sharks of Las Animas appear genetically distinct due to IBD, or whether they represent a distinct evolutionary partition isolated from their Pacific coast counterparts. Finally, while nuclear SNP loci (Chapter 4) generally provided greater power for resolving population genetic structure than the mitochondrial control region (mtCR; Chapter 3), only the mtCR revealed a conspicuous genetic break between mainland populations to the north and south of Punta Eugenia, a known biogeographic barrier for marine fishes (Bernardi et al. 2003; Briggs and Bowen 2012).

This dissertation represents the first exploration of population genetic structure in *H. francisci*, and hopefully will prove highly informative with regard to the implementation of management strategies. As indicated in the previous section, there is good reason to believe that horn shark populations are vulnerable to fishing pressures in the southern portion of their range, and population declines have been reported in southern California as well (Carlisle 2015). My own conversations with fishers and divers on both sides of the Baja peninsula revealed a conspicuous decrease in sightings of *H. francisci* in recent years, notably at Ejido Valle Tranquilo (approximately 25 km north of El Rosario along the Pacific coast) and Bahia de Los

Angeles in the Gulf of California. Though horn sharks appear to display high levels of connectivity over thousands of kilometers of continuous coastline, they are still vulnerable to local population declines. More research is needed to assess population trends, as well as to shed light on the drivers behind these apparent declines.

Island populations of *H. francisci* represent distinct demographic units and demonstrate little to no connectivity with each other or the California mainland. The results of this dissertation reveal the existence of at least two distinct lineages occupying the California Channel Islands: a Northern Channel Island lineage (grouping Santa Cruz Island and Anacapa Island) and a Southern Channel Island lineage (occupying Santa Catalina Island), indicating that they should be treated as independent management units.

The IUCN Red List classifies this species as Data Deficient, citing a dearth of information regarding biology, ecology, and population structure (Carlisle 2015). Thus, one of my ambitions in designing and conducting this dissertation is to fill a critical knowledge gap to enable informed management of the California horn shark.

Re-Assessing the spatial scale of isolation in marine elasmobranchs: new strategies and a shifting focus

The population structure of most sharks is measured on the scale of hundreds or thousands of kilometers. In this regard, *H. francisci* is exceptional: the scale of population structure between the horn sharks of Anacapa Island and their California mainland brethren (approximately 20 km) is the smallest discovered in any species of elasmobranch to-date. This is made even more remarkable with the realization that these two landmasses are separated by only 10 km of waters deeper than 150 m, which is the approximate depth limit of *H. francisci* (Weigmann 2016). However, it is not my contention that this feature is unique to the California horn shark. On the contrary, this may be a common pattern among small, demersal elasmobranchs, which are woefully understudied in this context. There are at least three other species of demersal elasmobranchs in the Southern California Bight (SCB) alone which are worthy of study along these lines: the round stingray (*Urobatis halleri*), the California angel shark (*Squatina californica*), and the swell shark (*Cephaloscyllium ventriosum*). Previous population genetic studies on the round stingray and the California angel shark indicate that both species exhibit population genetic structure within the SCB, over distances of approximately 100

km and less than 50 km, respectively. In the case of the California angel shark (Gaida 1997), sampling was limited to two Northern Channel Islands (Santa Rosa Island and Santa Cruz Island) and one Southern Channel Island (San Clemente Island). In the case of the round stingray (Plank et al. 2010), Santa Catalina Island was the only island population from which samples were obtained. And while as of yet no population genetic studies have been performed for *C. ventriosum*, differences in egg-case morphology between Santa Catalina Island swell sharks and mainland swell sharks indicate population-level differences (Grover 1970). Thus, with a carefully considered and comprehensive sampling design (including multiple sites along the California mainland and several California Channel Islands), it may be possible to detect fine-scale population structure among the demersal elasmobranchs of the SCB that rivals that of the California horn shark.

In general, perspectives on the spatial scale of genetic structure in the Elasmobranchii have been influenced by two factors: opportunistic sampling schemes that are often inadequate for the detection of fine-scale structure (see examples above), and taxonomic bias towards large-bodied species with moderate to high dispersal potential (Hirschfeld et al. 2021). These are not trivial considerations, as they may lead to a general underestimation of population genetic structure in elasmobranchs (thereby resulting in an overestimation of the spatial scale of management units in this diverse group). Furthermore, our understanding of dispersal capability, as well as the nature and scale of dispersal barriers in the marine environment, directly informs our understanding of evolutionary processes – both in the short term (habitat disturbance on an ecological timescale) and in the long term (past and future diversification). My hope is that this dissertation will focus attention and future research on these issues, as well as promote an appreciation for the remarkable, albeit somewhat indolent, California horn shark.

LITERATURE CITED

Aceves-Medina G, Jiménez-Rosenberg SPA, Saldierna-Martínez RJ, et al (2018) Distribution and abundance of the ichthyoplankton assemblages and its relationships with the geostrophic flow along the southern region of the California Current. *Lat Am J Aquat Res* 46:104–119. https://doi.org/10.3856/vol46-issue1-fulltext-12

Alfaro-Shigueto J, Mangel JC, Pajuelo M, et al (2010) Where small can have a large impact: Structure and characterization of small-scale fisheries in Peru. *Fish Res* 106:8–17. https://doi.org/10.1016/j.fishres.2010.06.004

Allendorf FW, Hohenlohe PA, Luikart G (2010) Genomics and the future of conservation genetics. *Nat Rev Genet* 11:697–709. https://doi.org/10.1038/nrg2844

Andrews S (2017) FastQC: A quality control tool for high throughput sequence data. 2010.

Arenas M, Ray N, Currat M, Excoffier L (2012) Consequences of range contractions and range shifts on molecular diversity. *Mol Biol Evol* 29:207–218. https://doi.org/10.1093/molbev/msr187

Arnason U, Gullberg A, Janke A (2001) Molecular phylogenetics of gnathostomous (jawed) fishes: Old bones, new cartilage. *Zool Scr* 30:249–255. https://doi.org/10.1046/j.1463-6409.2001.00067.x

Ashe JL, Feldheim KA, Fields AT, et al (2015) Local population structure and context-dependent isolation by distance in a large coastal shark. *Mar Ecol Prog Ser* 520:203–216. https://doi.org/10.3354/meps11069

Avise JC (1994) Molecular Markers, Natural History and Evolution. Chapman & Hall, London

Avise JC (2004) Molecular Markers, Natural History, and Evolution, 2nd edn. Sinauer Associates, Sunderland

Bailleul D, Mackenzie A, Sacchi O, et al (2018) Large-scale genetic panmixia in the blue shark (*Prionace glauca*): A single worldwide population, or a genetic lag-time effect of the "grey zone" of differentiation? *Evol Appl* 11:614–630. https://doi.org/10.1111/eva.12591

Baird NA, Etter PD, Atwood TS, et al (2008) Rapid SNP discovery and genetic mapping using sequenced RAD markers. *PLoS One* 3:e3376. https://doi.org/10.1371/journal.pone.0003376

Ballard JWO, Whitlock MC (2004) The incomplete natural history of mitochondria. *Mol Ecol* 13:729–744. https://doi.org/10.1046/j.1365-294X.2003.02063.x

Bandelt H-J, Forster P, Röhl A (1999) Median-joining networks for inferring intraspecific phylogenies. *Mol Biol Evol* 16:37–48. https://doi.org/10.1111/j.1469-1795.2000.tb00107.x

Baum JK, Myers RA, Kehler DG, et al (2003) Collapse and conservation of shark populations in the Northwest Atlantic. *Science* 299:389–392. https://doi.org/10.1126/science.1079777

Benestan LM, Ferchaud AL, Hohenlohe PA, et al (2016) Conservation genomics of natural and managed populations: Building a conceptual and practical framework. *Mol Ecol* 25:2967–2977. https://doi.org/10.1111/mec.13647

Benjamini Y, Hochberg Y (1995) Controlling the false discovery rate: A practical and powerful approach to multiple testing. *J R Stat Soc Ser B* 57:289–300. https://doi.org/10.1111/j.2517-6161.1995.tb02031.x

Bernard AM, Feldheim KA, Heithaus MR, et al (2016) Global population genetic dynamics of a highly migratory, apex predator shark. *Mol Ecol* 25:5312–5329. https://doi.org/10.1111/mec.13845

Bernardi G (2000) Barriers to gene flow in *Embiotoca jacksoni*, a marine fish lacking a pelagic larval stage. *Evolution* 54:226–237. https://doi.org/https://doi.org/10.1111/j.0014-3820.2000.tb00023.x

Bernardi G, Findley L, Rocha-Olivares A (2003) Vicariance and dispersal across Baja California in disjunct marine fish populations. *Evolution* 57:1599–1609. https://doi.org/10.1111/j.0014-3820.2003.tb00367.x

Bonfil R, Meÿer M, Scholl MC, et al (2005) Transoceanic migration, spatial dynamics, and population linkages of white sharks. *Science* 310:100–103. https://doi.org/10.1126/science.1114898

Botstein D, White RL, Skolnick M, Davis RW (1980) Construction of a genetic linkage map in man using restriction fragment length polymorphisms. *Am J Hum Gen* 32:314–331

Bouckaert R, Vaughan TG, Barido-Sottani J, et al (2019) BEAST 2.5: An advanced software platform for Bayesian evolutionary analysis. *PLoS Comput Biol* 15:e1006650. https://doi.org/10.1371/journal.pcbi.1006650

Bowen BW, Shanker K, Yasuda N, et al (2014) Phylogeography unplugged: Comparative surveys in the genomic era. *Bull Mar Sci* 90:13–46. https://doi.org/https://doi.org/10.5343/bms.2013.1007

Bowen BW, Gaither MR, DiBattista JD, et al (2016) Comparative phylogeography of the ocean planet. *Proc Natl Acad Sci USA* 113:7962–7969. https://doi.org/10.1073/pnas.1602404113

Bowen BW, Forsman ZH, Whitney JL, et al (2020) Species radiations in the sea: What the flock? *J Hered* 111:70–83. https://doi.org/10.1093/jhered/esz075

Briggs JC, Bowen BW (2012) A realignment of marine biogeographic provinces with particular reference to fish distributions. *J Biogeogr* 39:12–30. https://doi.org/https://doi.org/10.1111/j.1365-2699.2011.02613.x

Canfield SJ, Bowen BW (2021) A rapid PCR-RFLP method for species identification of the eastern Pacific horn sharks (genus *Heterodontus*). *Conserv Genet Resour* 13:79–84. https://doi.org/10.1007/s12686-020-01172-6

Carlisle A (2015) *Heterodontus francisci*. IUCN Red List Threat Species 2015 e.T39333A80671300. https://doi.org/https://doi.org/10.2305/IUCN.UK.2015-4.RLTS.T39333A80671300.en

Castellanos-Vidal CM (2017) Reproductive biology of the horn shark *Heterodontus francisci* in Ojo de Liebre Lagoon, Baja California Sur, Mexico. Ensenada Center for Scientific Research and Higher Education (CICESE)

Castro ALF, Stewart BS, Wilson G, et al (2007) Population genetic structure of Earth's largest fish, the whale shark (*Rhincodon typus*). *Mol Ecol* 16:5183–5192. https://doi.org/10.1111/j.1365-294X.2007.03597.x

Castro JI (2010) The Sharks of North America. Oxford University Press, Oxford

Catchen JM, Amores A, Hohenlohe P, et al (2011) Stacks: Building and genotyping loci de novo from short-read sequences. *G3 Genes, Genomes, Genet* 1:171–182. https://doi.org/10.1534/g3.111.000240

Chang CC, Chow CC, Tellier LCAM, et al (2015) Second-generation PLINK: Rising to the challenge of larger and richer datasets. *Gigascience* 4:s13742-015. https://doi.org/10.1186/s13742-015-0047-8

Chen C, Huang S, Lee S (2001) Genetic variation between populations of starspotted dogfish *Mustelus manazo* in central Japan and northern Taiwan. *Fish Sci* 67:30–35

Chen X, Peng X, Huang X, Xiang D (2014) Complete mitochondrial genome of the Zebra bullhead shark *Heterodontus zebra* (Heterodontiformes: Heterodontidae). *Mitochondrial DNA* 25:280–281. https://doi.org/10.3109/19401736.2013.796514

Clark K, Karsch-Mizrachi I, Lipman DJ, et al (2016) GenBank. *Nucleic Acids Res* 44:D67–D72. https://doi.org/10.1093/nar/gkv1276

Clark PU, Clark PU, Dyke AS, et al (2009) The last glacial maximum. *Science* 325:710–714. https://doi.org/10.1126/science.1172873

Compagno L (2002) Sharks of the World: An Annotated and Illustrated Catalogue of Shark Species Known to Date (Volume 2). Rome

Compagno L, Dando M, Fowler S (2005) Sharks of the World. Princeton University Press, Princeton

Corrigan S, Huveneers C, Stow A, Beheregaray LB (2016) A multilocus comparative study of dispersal in three codistributed demersal sharks from eastern Australia. *Can J Fish Aquat Sci* 73:406–415. https://doi.org/https://doi.org/10.1139/cjfas-2015-0085

Daly-Engel TS, Seraphin KD, Holland KN, et al (2012) Global phylogeography with mixed-marker analysis reveals male-mediated dispersal in the endangered scalloped hammerhead shark (*Sphyrna lewini*). *PLoS One* 7:e29986. https://doi.org/10.1371/journal.pone.0029986

Danecek P, Auton A, Abecasis G, et al (2011) The variant call format and VCFtools. *Bioinformatics* 27:2156–2158. https://doi.org/10.1093/bioinformatics/btr330

Darriba D, Taboada GL, Doallo R, Posada D (2012) JModelTest 2: More models, new heuristics and parallel computing. *Nat Methods* 9:772. https://doi.org/10.1038/nmeth.2109

Day J, Clark JA, Williamson JE, et al (2019) Population genetic analyses reveal female reproductive philopatry in the oviparous Port Jackson shark. *Mar Freshw Res* 70:986–994. https://doi.org/10.1071/MF18255

de Vries A, Ripley BD (2020) ggdendro: Create Dendrograms and Tree Diagrams Using "ggplot2"

Domingues RR, Hilsdorf AWS, Gadig OBF (2018) The importance of considering genetic diversity in shark and ray conservation policies. *Conserv Genet* 19:501–525. https://doi.org/10.1007/s10592-017-1038-3

Domínguez-Reza RH (2017) Age and growth of the horn shark (*Heterodontus francisci*) in Ojo de Liebre Lagoon, Baja California Sur, Mexico. Ensenada Center for Scientific Research and Higher Education (CICESE)

Dudgeon CL, Broderick D, Ovenden JR (2009) IUCN classification zones concord with, but underestimate, the population genetic structure of the zebra shark *Stegostoma fasciatum* in the Indo-West Pacific. *Mol Ecol* 18:248–261. https://doi.org/10.1111/j.1365-294X.2008.04025.x

Dudgeon CL, Blower DC, Broderick D, et al (2012) A review of the application of molecular genetics for fisheries management and conservation of sharks and rays. *J Fish Biol* 80:1789–1843. https://doi.org/10.1111/j.1095-8649.2012.03265.x

Dulvy NK, Baum JK, Clarke S, et al (2008) You can swim but you can't hide: The global status and conservation of oceanic pelagic sharks and rays. *Aquat Conserv Mar Freshw Ecosyst* 18:459–482. https://doi.org/https://doi.org/10.1002/aqc.975

Dulvy NK, Fowler SL, Musick JA, et al (2014) Extinction risk and conservation of the world's sharks and rays. *Elife* 3:1–34. https://doi.org/10.7554/elife.00590

Dulvy NK, Simpfendorfer CA, Davidson LNK, et al (2017) Challenges and priorities in shark and ray conservation. *Curr Biol* 27:R565–R572. https://doi.org/10.1016/j.cub.2017.04.038

Dulvy NK, Pacoureau N, Rigby CL, et al (2021) Overfishing drives over one-third of all sharks and rays toward a global extinction crisis. *Curr Biol* 31:1–15. https://doi.org/10.1016/j.cub.2021.08.062

Earl DA, VonHoldt BM (2012) STRUCTURE HARVESTER: A website and program for visualizing STRUCTURE output and implementing the Evanno method. *Conserv Genet Resour* 4:359–361. https://doi.org/10.1007/s12686-011-9548-7

Ebert DA (2003) Sharks, Rays, and Chimaeras of California. University of California Press, Berkeley

Ebert DA, Fowler S, Compagno LJV (2013) Sharks of the World: A Fully Illustrated Guide. Wild Nature Press, Plymouth

Eggert LS, Mundy NI, Woodruff DS (2004) Population structure of loggerhead shrikes in the California Channel Islands. *Mol Ecol* 13:2121–2133. https://doi.org/10.1111/j.1365-294X.2004.02218.x

Evanno G, Regnaut S, Goudet J (2005) Detecting the number of clusters of individuals using the software STRUCTURE: A simulation study. *Mol Ecol* 14:2611–2620. https://doi.org/10.1111/j.1365-294X.2005.02553.x

Excoffier L, Smouse PE, Quattro JM (1992) Analysis of molecular variance inferred from Metric distances among DNA haplotypes: Application to human mitochondrial DNA restriction data. *Genetics* 131:479–491

Excoffier L, Lischer HEL (2010) Arlequin suite ver 3.5: A new series of programs to perform population genetics analyses under Linux and Windows. *Mol Ecol Resour* 10:564–567. https://doi.org/10.1111/j.1755-0998.2010.02847.x

Feldheim KA, Gruber SH, Dibattista JD, et al (2014) Two decades of genetic profiling yields first evidence of natal philopatry and long-term fidelity to parturition sites in sharks. *Mol Ecol* 23:110–117. https://doi.org/10.1111/mec.12583

Fischer MC, Foll M, Excoffier L, Heckel G (2011) Enhanced AFLP genome scans detect local adaptation in high-altitude populations of a small rodent (*Microtus arvalis*). *Mol Ecol* 20:1450–1462. https://doi.org/10.1111/j.1365-294X.2011.05015.x

Fogarty MJ, Botsford LW (2007) Population connectivity and spatial management of marine fisheries. *Oceanography* 20:112–123. https://doi.org/10.5670/oceanog.2007.34

Foll M, Gaggiotti O (2008) A genome-scan method to identify selected loci appropriate for both dominant and codominant markers: A Bayesian perspective. *Genetics* 180:977–993. https://doi.org/10.1534/genetics.108.092221

Foll M, Fischer MC, Heckel G, Excoffier L (2010) Estimating population structure from AFLP amplification intensity. *Mol Ecol* 19:4638–4647. https://doi.org/10.1111/j.1365-294X.2010.04820.x

Frankham R (1997) Do island populations have less genetic variation than mainland populations? *Heredity* 78:311–327. https://doi.org/10.1038/hdy.1997.46

Frankham R (2010) Challenges and opportunities of genetic approaches to biological conservation. *Biol Conserv* 143:1919–1927. https://doi.org/10.1016/j.biocon.2010.05.011

Frankham R, Briscoe DA, Ballou JD (2010) Introduction to Conservation Genetics, 2nd edn. Cambridge University Press, Cambridge

Frantz AC, Cellina S, Krier A, et al (2009) Using spatial Bayesian methods to determine the genetic structure of a continuously distributed population: Clusters or isolation by distance? *J Appl Ecol* 46:493–505. https://doi.org/10.1111/j.1365-2664.2008.01606.x

Fréminville CPP (1840) Notice sur une nouvelle espèce de poisson, appartenant au genre Cestracion de Cuvier. *Mag Zool d'anatomie comparée Palaeontol Guerin* 2:1–3

Fu Y-X (1997) Statistical tests of neutrality of mutations against population growth, hitchhiking and background selection. *Genetics* 147:915–925

Funk WC, McKay JK, Hohenlohe PA, Allendorf FW (2012) Harnessing genomics for delineating conservation units. *Trends Ecol Evol* 27:489–496. https://doi.org/10.1016/j.tree.2012.05.012

Furlong-Estrada E, Galván-Magaña F, Tovar-Ávila J (2017) Use of the productivity and susceptibility analysis and a rapid management-risk assessment to evaluate the vulnerability of sharks caught off the west coast of Baja California Sur, Mexico. *Fish Res* 194:197–208. https://doi.org/10.1016/j.fishres.2017.06.008

Gaida IH (1997) Population structure of the Pacific angel shark, *Squatina californica* (Squatiniformes: Squatinidae), around the California Channel Islands. *Copeia* 1997:738–744. https://doi.org/10.2307/1447291

Garayzar CV (2006) *Heterodontus mexicanus*. IUCN Red List Threat Species 2006 e.T60235A12331644. https://doi.org/http://dx.doi.org/10.2305/IUCN.UK.2006.RLTS.T60235A12331644.en

Gilbert DA, Lehman N, O'Brien SJ, Wayne RK (1990) Genetic fingerprinting reflects population differentiation in the California Channel Island fox. *Nature* 344:764–767. https://doi.org/https://doi.org/10.1038/344764a0

Giles JL, Ovenden JR, Dharmadi D, et al (2014) Extensive genetic population structure in the Indo-West Pacific spot-tail shark, *Carcharhinus sorrah*. *Bull Mar Sci* 90:427–454. https://doi.org/10.5343/bms.2013.1009

Girard C (1855) Characteristics of some cartilaginous fishes of the Pacific coast of North America. *Proc Acad Nat Sci Philadelphia* 7:196–197. https://doi.org/10.1093/nq/s5-vi.146.318i

Grant WS, Bowen BW (1998) Shallow population histories in deep evolutionary lineages of marine fishes: Insights from sardines and anchovies and lessons for conservation. *J Hered* 89:415–426. https://doi.org/https://doi.org/10.1093/jhered/89.5.415

Grover CA (1970) The egg-cases of the Swell shark, *Cephaloscyllium ventriosum*: Formation, function, and population differences. University of British Columbia

Gubili C, Sims DW, Veríssimo A, et al (2014) A tale of two seas: Contrasting patterns of population structure in the small-spotted catshark across Europe. *R Soc Open Sci* 1:140175. https://doi.org/10.1098/rsos.140175

Guindon S, Gascuel O (2003) A simple, fast, and accurate algorithm to estimate large phylogenies by maximum likelihood. *Syst Biol* 52:696–704. https://doi.org/10.1080/10635150390235520

Guzman HM, Gomez CG, Hearn A, Eckert SA (2018) Longest recorded trans-Pacific migration of a whale shark (*Rhincodon typus*). *Mar Biodivers Rec* 11:1–6. https://doi.org/10.1186/s41200-018-0143-4

Harpending HC (1994) Signature of ancient population growth in a low-resolution mitochondrial DNA mismatch distribution. *Hum Biol* 66:591–600

Hasegawa M, Kishino H, Yano T aki (1985) Dating of the human-ape splitting by a molecular clock of mitochondrial DNA. *J Mol Evol* 22:160–174. https://doi.org/10.1007/BF02101694

Hebert PDN, Cywinska A, Ball SL, deWaard JR (2003) Biological identifications through DNA barcodes. *Proc R Soc B Biol Sci* 270:313–321. https://doi.org/10.1098/rspb.2002.2218

Heupel MR, Simpfendorfer CA, Collins AB, Tyminski JP (2006) Residency and movement patterns of bonnethead sharks, *Sphyrna tiburo*, in a large Florida estuary. *Environ Biol Fishes* 76:47–67. https://doi.org/10.1007/s10641-006-9007-6

Hey J (2010) Isolation with migration models for more than two populations. *Mol Biol Evol* 27:905–920. https://doi.org/10.1093/molbev/msp296

Hey J, Chung Y, Sethuraman A, et al (2018) Phylogeny estimation by integration over isolation with migration models. *Mol Biol* Evol 35:2805–2818. https://doi.org/10.1093/molbev/msy162

Hilário A, Metaxas A, Gaudron SM, et al (2015) Estimating dispersal distance in the deep sea: Challenges and applications to marine reserves. *Front Mar Sci* 2:1–14. https://doi.org/10.3389/fmars.2015.00006

Hirschfeld M, Dudgeon C, Sheaves M, Barnett A (2021) Barriers in a sea of elasmobranchs: From fishing for populations to testing hypotheses in population genetics. *Glob Ecol Biogrography* 1–17. https://doi.org/10.1111/geb.13379

Hoelzel AR, Shivji MS, Magnussen J, Francis MP (2006) Low worldwide genetic diversity in the basking shark (*Cetorhinus maximus*). *Biol Lett* 2:639–642. https://doi.org/10.1098/rsbl.2006.0513

Hohenlohe PA, Hand BK, Andrews KR, Luikart G (2018) Population genomics provides key insights in ecology and evolution. In: Rajora O (ed) Population Genomics. Springer, pp 483–510

Holbrook NJ, Scannell HA, Sen Gupta A, et al (2019) A global assessment of marine heatwaves and their drivers. *Nat Commun* 10:1–13. https://doi.org/10.1038/s41467-019-10206-z

Hueter RE, Heupel MR, Heist EJ, Keeney DB (2005) Evidence of philopatry in sharks and implications for the management of shark fisheries. *J Northwest Atl Fish Sci* 35:239–247. https://doi.org/10.2960/j.v35.m493

Janes JK, Miller JM, Dupuis JR, et al (2017) The K=2 conundrum. *Mol Ecol* 26:3594–3602. https://doi.org/https://doi.org/10.1111/mec.14187

Jeffries DL, Copp GH, Handley LL, et al (2016) Comparing RADseq and microsatellites to infer complex phylogeographic patterns, an empirical perspective in the Crucian carp, *Carassius carassius*, L. *Mol Ecol* 25:2997–3018. https://doi.org/10.1111/mec.13613

Jetz W, Sekercioglu CH, Watson JEM (2007) Ecological correlates and conservation implications of overestimating species geographic ranges. *Conserv Biol* 22:110–119. https://doi.org/10.1111/j.1523-1739.2007.00847.x

Jirik KE, Lowe CG (2012) An elasmobranch maternity ward: Female round stingrays *Urobatis halleri* use warm, restored estuarine habitat during gestation. *J Fish Biol* 80:1227–1245. https://doi.org/10.1111/j.1095-8649.2011.03208.x

Jombart T (2008) Adegenet: A R package for the multivariate analysis of genetic markers. *Bioinformatics* 24:1403–1405. https://doi.org/10.1093/bioinformatics/btn129

Karl SA, Castro ALF, Garla RC (2012a) Population genetics of the nurse shark (*Ginglymostoma cirratum*) in the western Atlantic. *Mar Biol* 159:489–498. https://doi.org/10.1007/s00227-011-1828-y

Karl SA, Toonen RJ, Grant WS, Bowen BW (2012b) Common misconceptions in molecular ecology: Echoes of the modern synthesis. *Mol Ecol* 21:4171–4189. https://doi.org/10.1111/j.1365-294X.2012.05576.x

Keenan K, Mcginnity P, Cross TF, et al (2013) DiveRsity: An R package for the estimation and exploration of population genetics parameters and their associated errors. *Methods Ecol Evol* 4:782–788. https://doi.org/10.1111/2041-210X.12067

Keeney DB, Heist EJ (2006) Worldwide phylogeography of the blacktip shark (*Carcharhinus limbatus*) inferred from mitochondrial DNA reveals isolation of western Atlantic populations coupled with recent Pacific dispersal. *Mol Ecol* 15:3669–3679. https://doi.org/10.1111/j.1365-294X.2006.03036.x

Kopelman NM, Mayzel J, Jakobsson M, et al (2015) CLUMPAK: A program for identifying clustering modes and packaging population structure inferences across K. *Mol Ecol Resour* 15:1179–1191. https://doi.org/10.1111/1755-0998.12387

Kousteni V, Kasapidis P, Kotoulas G, Megalofonou P (2015) Strong population genetic structure and contrasting demographic histories for the small-spotted catshark (*Scyliorhinus canicula*) in the Mediterranean Sea. *Heredity* 114:333–343. https://doi.org/10.1038/hdy.2014.107

Kraft DW, Conklin EE, Barba EW, et al (2020) Genomics versus mtDNA for resolving stock structure in the silky shark (*Carcharhinus falciformis*). *PeerJ* 8:1–20. https://doi.org/10.7717/peerj.10186

Kress WJ, García-Robledo C, Uriarte M, Erickson DL (2015) DNA barcodes for ecology, evolution, and conservation. *Trends Ecol Evol* 30:25–35. https://doi.org/10.1016/j.tree.2014.10.008

Kyne P, Rivera F, Leandro L (2004) *Heterodontus quoyi*. IUCN Red List Threat Species 2004 e.T44579A10907948

Lande R (1995) Mutation and conservation. *Conserv Biol* 9:782–791. https://doi.org/https://doi.org/10.1046/j.1523-1739.1995.09040782.x

Leigh JW, Bryant D (2015) POPART: Full-feature software for haplotype network construction. *Methods Ecol Evol* 6:1110–1116. https://doi.org/10.1111/2041-210X.12410

Lepais O, Weir JT (2014) SimRAD: An R package for simulation-based prediction of the number of loci expected in RADseq and similar genotyping by sequencing approaches. *Mol Ecol Resour* 14:1314–1321. https://doi.org/10.1111/1755-0998.12273

Li H, Qu W, Obrycki JJ, et al (2020) Optimizing sample size for population genomic study in a global invasive lady beetle, *Harmonia axyridis*. *Insects* 11:290. https://doi.org/10.3390/insects11050290

Lim KC, Then AYH, Wee AKS, et al (2021) Brown banded bamboo shark (*Chiloscyllium punctatum*) shows high genetic diversity and differentiation in Malaysian waters. *Sci Rep* 11:1–15. https://doi.org/10.1038/s41598-021-94257-7

Lischer HEL, Excoffier L (2012) PGDSpider: An automated data conversion tool for connecting population genetics and genomics programs. *Bioinformatics* 28:298–299. https://doi.org/10.1093/bioinformatics/btr642

Love M (1996) Probably More Than You Want to Know About the Fishes of the Pacific Coast. Really Big Press, Santa Barbara

Malenfant RM, Coltman DW, Davis CS (2015) Design of a 9K Illumina BeadChip for polar bears (*Ursus maritimus*) from RAD and transcriptome sequencing. *Mol Ecol Resour* 15:587–600. https://doi.org/10.1111/1755-0998.12327

Martin AP, Naylor GJP, Palumbi SR (1992) Rates of mitochondrial DNA evolution in sharks are slow compared with mammals. *Nature* 357:153–155. https://doi.org/10.1038/357153a0

Martin AP (1999) Substitution rates of organelle and nuclear genes in sharks: Implicating metabolic rate (again). *Mol Biol Evol* 16:996–1002. https://doi.org/10.1093/oxfordjournals.molbev.a026189

McKinney GJ, Waples RK, Seeb LW, Seeb JE (2017) Paralogs are revealed by proportion of heterozygotes and deviations in read ratios in genotyping-by-sequencing data from natural populations. *Mol Ecol Resour* 17:656–669. https://doi.org/10.1111/1755-0998.12613

Meese EN, Lowe CG (2020) Environmental effects on daytime sheltering behaviors of California horn sharks (*Heterodontus francisci*). *Environ Biol Fishes* 103:703–717. https://doi.org/10.1007/s10641-020-00977-6

Meirmans PG (2012) The trouble with isolation by distance. *Mol Ecol* 21:2839–2846. https://doi.org/10.1111/j.1365-294X.2012.05578.x

Meirmans PG (2015) Seven common mistakes in population genetics and how to avoid them. *Mol Ecol* 24:3223–3231. https://doi.org/10.1111/mec.13243

Mejía-Falla PA, Navia AF (2019) Checklist of marine elasmobranchs of Colombia. *Univ Sci* 24:241–276. https://doi.org/10.11144/Javeriana.SC24-1.come

Michael SW (1993) Reef Sharks and Rays of the World. A Guide to Their Identification, Behavior and Ecology. Sea Challengers, Monterey, California

Miller MA, Pfeiffer W, Schwartz T (2010) Creating the CIPRES Science Gateway for inference of large phylogenetic trees. New Orleans

Miller MR, Dunham JP, Amores A, et al (2007) Rapid and cost-effective polymorphism identification and genotyping using restriction site associated DNA (RAD) markers. *Genome Res* 17:240–248. https://doi.org/10.1101/gr.5681207

Musick JA, Burgess G, Cailliet G, et al (2000) Management of Sharks and Their Relatives (Elasmobranchii). *Fisheries* 25:9–13. https://doi.org/10.1577/1548-8446(2000)025<0009:mosatr>2.0.co;2

Musick JA, Harbin MM, Compagno LJV (2004) Historical zoogeography of the Selachii. In: Carrier JC et al. (ed) Biology of Sharks and Their Relatives. CRC Marine Biology Series, CRC Press, Boca Raton, pp 33-78.

Nance HA, Klimley P, Galván-Magaña F, et al (2011) Demographic processes underlying subtle patterns of population structure in the scalloped hammerhead shark, *Sphyrna lewini*. *PLoS One* 6:e21459. https://doi.org/10.1371/journal.pone.0021459

Narum SR, Buerkle CA, Davey JW, et al (2013) Genotyping-by-sequencing in ecological and conservation genomics. *Mol Ecol* 22:2841–2847. https://doi.org/10.1111/mec.12350

Naylor G, Caira K, Jensen K, et al (2012) A DNA sequence-based approach to the identification of shark and ray species and its implications for global elasmobranch diversity and parasitology. *Bull Am museum Nat Hist* 2012:1–262. https://doi.org/https://doi.org/10.1206/754.1

Nazareno AG, Bemmels JB, Dick CW, Lohmann LG (2017) Minimum sample sizes for population genomics: An empirical study from an Amazonian plant species. *Mol Ecol Resour* 17:1136–1147. https://doi.org/10.1111/1755-0998.12654

Nelson DR, Johnson RH (1970) Diel activity rhythms in the nocturnal, bottom-dwelling sharks, *Heterodontus francisci* and *Cephaloscyllium ventriosum*. *Copeia* 1970:732–739. https://doi.org/10.2307/1442315

Nielsen R, Wakeley J (2001) Distinguishing migration from isolation: A Markov chain Monte Carlo approach. *Genetics* 158:885–896

O'Gower AK, Nash AR (1978) Dispersion of the Port Jackson shark in Australian waters. In: Hodgson ES, Mathewson RF (eds) Sensory Biology of Sharks, Skates, and Rays. Office of Naval Research, Washington, DC, pp 529–544

Oliver ECJ, Burrows MT, Donat MG, et al (2019) Projected marine heatwaves in the 21st century and the potential for ecological impact. *Front Mar Sci* 6:1–12. https://doi.org/10.3389/fmars.2019.00734

Orsini L, Mergeay J, Vanoverbeke J, Meester L de (2013) The role of selection in driving landscape genomic structure of the waterflea *Daphnia magna*. *Mol Ecol* 22:583–601. https://doi.org/10.1111/mec.12117

Palumbi SR (2003) Population genetics, demographic connectivity, and the design of marine reserves. *Ecol Appl* 13:146–158. https://doi.org/doi:10.1890/1051-0761(2003)013[0146:pgdcat]2.0.co;2

Paris JR, Stevens JR, Catchen JM (2017) Lost in parameter space: A road map for stacks. *Methods Ecol Evol* 8:1360–1373. https://doi.org/10.1111/2041-210X.12775

Perez MF, Franco FF, Bombonato JR, et al (2018) Assessing population structure in the face of isolation by distance: Are we neglecting the problem? *Divers Distrib* 24:1883–1889. https://doi.org/10.1111/ddi.12816

Peterson BK, Weber JN, Kay EH, et al (2012) Double digest RADseq: An inexpensive method for de novo SNP discovery and genotyping in model and non-model species. *PLoS One* 7:e37135. https://doi.org/10.1371/journal.pone.0037135

Phillips NM, Devloo-Delva F, McCall C, Daly-Engel TS (2021) Reviewing the genetic evidence for sex-biased dispersal in elasmobranchs. *Rev Fish Biol Fish* 9:1–21. https://doi.org/10.1007/s11160-021-09673-9

Plank SM, Lowe CG, Feldheim KA, et al (2010) Population genetic structure of the round stingray *Urobatis halleri* (Elasmobranchii: Rajiformes) in southern California and the Gulf of California. *J Fish Biol* 77:329–340. https://doi.org/10.1111/j.1095-8649.2010.02677.x

Portnoy DS, McDowell JR, Heist EJ, et al (2010) World phylogeography and male-mediated gene flow in the sandbar shark, *Carcharhinus plumbeus*. *Mol Ecol* 19:1994–2010. https://doi.org/10.1111/j.1365-294X.2010.04626.x

Portnoy DS, Hollenbeck M, Belcher CN, et al (2014) Contemporary population structure and post-glacial genetic demography in a migratory marine species, the blacknose shark, *Carcharhinus acronotus*. *Mol Ecol* 23:5480–5495. https://doi.org/10.1111/mec.12954

Pratt HL, Pratt TC, Morley D, et al (2018) Partial migration of the nurse shark, *Ginglymostoma cirratum* (Bonnaterre), from the Dry Tortugas Islands. *Environ Biol Fishes* 101:515–530. https://doi.org/10.1007/s10641-017-0711-1

Pritchard JK, Stephens M, Donnelly P (2000) Inference of population structure using multilocus genotype data. *Genetics* 155:945–959. https://doi.org/10.1093/genetics/155.2.945

Pritchard JK, Wen X, Falush D (2010) Documentation for structure software: Version 2.3

Purcell S, Neale B, Todd-Brown K, et al (2007) PLINK: A tool set for whole-genome association and population-based linkage analyses. *Am J Hum Genet* 81:559–575. https://doi.org/10.1086/519795

Puritz JB, Matz M V, Toonen RJ, et al (2014) Demystifying the RAD fad. *Mol Ecol* 23:5937–5942. https://doi.org/10.1111/mec.12965

R Core Team (2020) R: A language and environment for statistics computing

R Core Team (2015) R: A language and environment for statistical computing.

Ramírez-Amaro S, Ramírez-Macías D, Vázquez-Juárez R, et al (2017) Population structure of the Pacific angel shark (*Squatina californica*) along the northwestern coast of Mexico based on the mitochondrial DNA control region. *Ciencias Mar* 43:69–80. https://doi.org/10.7773/cm.v43i1.2692

Ramírez-Amaro S, Galván-Magaña F (2019) Effect of gillnet selectivity on elasmobranchs off the northwestern coast of Mexico. *Ocean Coast Manag* 172:105–116. https://doi.org/10.1016/j.ocecoaman.2019.02.001

Ramos-Onsins SE, Rozas J (2002) Statistical properties of new neutrality tests against population growth. *Mol Biol Evol* 19:2092–2100. https://doi.org/https://doi.org/10.1093/oxfordjournals.molbev.a004034

Ray N, Currat M, Excoffier L (2003) Intra-deme molecular diversity in spatially expanding populations. *Mol Biol Evol* 20:76–86. https://doi.org/10.1093/molbev/msg009

Read TD, Petit RA, Joseph SJ, et al (2017) Draft sequencing and assembly of the genome of the world's largest fish, the whale shark: *Rhincodon typus* Smith 1828. *BMC Genomics* 18:532. https://doi.org/10.1186/s12864-017-3926-9

Robertson DR, Cramer KL (2009) Shore fishes and biogeographic subdivisions of the Tropical Eastern Pacific. *Mar Ecol Prog Ser* 380:1–17. https://doi.org/10.3354/meps07925

Rochette NC, Rivera-Colón AG, Catchen JM (2019) Stacks 2: Analytical methods for paired-end sequencing improve RADseq-based population genomics. *Mol Ecol* 28:4737–4754. https://doi.org/10.1111/mec.15253

Rogers AR, Harpending H (1992) Population growth makes waves in the distribution of pairwise genetic differences. *Mol Biol Evol* 9:552–569. https://doi.org/https://doi.org/10.1093/oxfordjournals.molbev.a040727

Rozas J, Ferrer-Mata A, Sanchez-DelBarrio JC, et al (2017) DnaSP 6: DNA sequence polymorphism analysis of large data sets. *Mol Biol Evol* 34:3299–3302. https://doi.org/10.1093/molbev/msx248

Ryman N, Jorde PE (2001) Statistical power when testing for genetic differentiation. *Mol Ecol* 10:2361–2373. https://doi.org/10.1046/j.0962-1083.2001.01345.x

Schwartz MK, Luikart G, Waples RS (2007) Genetic monitoring as a promising tool for conservation and management. *Trends Ecol Evol* 22:25–33. https://doi.org/10.1016/j.tree.2006.08.009

Selkoe KA, Gaggiotti OE, Bowen BW, Toonen RJ (2014) Emergent patterns of population genetic structure for a coral reef community. *Mol Ecol* 23:3064–3079. https://doi.org/10.1111/mec.12804

Strong WR (1989) Behavioral ecology of horn sharks, *Heterodontus francisci*, at Santa Catalina Island, California, with emphasis on patterns of space utilization. California State University, Long Beach

Taguchi M, King JR, Wetklo M, et al (2015) Population genetic structure and demographic history of Pacific blue sharks (*Prionace glauca*) inferred from mitochondrial DNA analysis. *Mar Freshw Res* 66:267–275. https://doi.org/10.1071/MF14075

Taylor LR (1972) A revision of the shark family Heterodontidae (Heterodontiformes, Selachii). University of California San Diego

Taylor LR, Castro-Aguirre JL (1972) *Heterodontus mexicanus*, a new horn shark from the Golfo de California. *An la Esc Nac Ciencias Biol México* 19:123–143

Teske PR, Golla TR, Sandoval-Castillo J, et al (2018) Mitochondrial DNA is unsuitable to test for isolation by distance. *Sci Rep* 8:8488. https://doi.org/10.1038/s41598-018-25138-9

Toonen RJ, Bowen BW, Iacchei M, Briggs JC (2016) Biogeography, Marine. In: Kliman RM (ed) Encyclopedia of Evolutionary Biology. Academic Press, Oxford, pp 166–178

Untergasser A, Cutcutache I, Koressaar T, et al (2012) Primer3 - new capabilities and interfaces. *Nucleic Acids Res* 40:1–12. https://doi.org/10.1093/nar/gks596

Vandeperre F, Aires-da-Silva A, Fontes J, et al (2014) Movements of blue sharks (*Prionace glauca*) across their life history. *PLoS One* 9:. https://doi.org/10.1371/journal.pone.0103538

Vaudo JJ, Lowe CG (2006) Movement patterns of the round stingray *Urobatis halleri* (Cooper) near a thermal outfall. *J Fish Biol* 68:1756–1766. https://doi.org/10.1111/j.0022-1112.2006.01054.x

Vendrami DLJ, Telesca L, Weigand H, et al (2017) RAD sequencing resolves fine-scale population structure in a benthic invertebrate: Implications for understanding phenotypic plasticity. *R Soc Open Sci* 4:160548. https://doi.org/10.1098/rsos.160548

Veríssimo A, McDowell JR, Graves JE (2010) Global population structure of the spiny dogfish *Squalus acanthias*, a temperate shark with an antitropical distribution. *Mol Ecol* 19:1651–1662. https://doi.org/10.1111/j.1365-294X.2010.04598.x

Veríssimo A, Sampaio Í, McDowell JR, et al (2017) World without borders—genetic population structure of a highly migratory marine predator, the blue shark (*Prionace glauca*). *Ecol Evol* 7:4768–4781. https://doi.org/10.1002/ece3.2987

Wang IJ, Glor RE, Losos JB (2013) Quantifying the roles of ecology and geography in spatial genetic divergence. *Ecol Lett* 16:175–182. https://doi.org/10.1111/ele.12025

Wei T, Simko V (2017) R package "corrplot": Visualization of a Correlation Matrix (Version 0.84)

Weigmann S (2016) Annotated checklist of the living sharks, batoids and chimaeras (Chondrichthyes) of the world, with a focus on biogeographical diversity. *J Fish Biol* 88:837–1037. https://doi.org/10.1111/jfb.12874

Weir BS, Cockerham CC (1984) Estimating F-statistics for the analysis of population structure. *Evolution* 38:1358–1370. https://doi.org/10.1111/j.1558-5646.1984.tb05657.x

Whitney NM, Robbins WD, Schultz JK, et al (2012) Oceanic dispersal in a sedentary reef shark (*Triaenodon obesus*): Genetic evidence for extensive connectivity without a pelagic larval stage. *J Biogeogr* 39:1144–1156. https://doi.org/10.1111/j.1365-2699.2011.02660.x

Willing EM, Dreyer C, van Oosterhout C (2012) Estimates of genetic differentiation measured by Fst do not necessarily require large sample sizes when using many SNP markers. *PLoS*

One 7:e42649. https://doi.org/10.1371/journal.pone.0042649

Wood DE, Salzberg SL (2014) Kraken: Ultrafast metagenomic sequence classification using exact alignments. *Genome Biol* 15:R46. https://doi.org/10.1186/gb-2014-15-3-r46

Wood DE, Lu J, Langmead B (2019) Improved metagenomic analysis with Kraken 2. *Genome Biol* 20:257. https://doi.org/10.1186/s13059-019-1891-0

Wright S (1943) Isolation by distance. *Genetics* 28:114–138

Younger JL, Clucas G V., Kao D, et al (2017) The challenges of detecting subtle population structure and its importance for the conservation of emperor penguins. *Mol Ecol* 26:3883–3897. https://doi.org/10.1111/mec.14172